PGJ/F-131(82)

National Uranium Resource Evaluation

SILVER CITY QUADRANGLE NEW MEXICO AND ARIZONA

MASTER

Bendix Field Engineering Corporation
Grand Junction, Colorado

Issue Date
May 1982

PREPARED FOR THE U.S. DEPARTMENT OF ENERGY
Assistant Secretary for Nuclear Energy
Grand Junction Area Office, Colorado

DISCLAIMER

This report is a result of work performed by Bendix Field Engineering Corporation, Operating Contractor for the U.S. Department of Energy, as part of the National Uranium Resource Evaluation. NURE is a program of the U.S. Department of Energy's Grand Junction, Colorado, Office to acquire and compile geologic and other information with which to assess the magnitude and distribution of uranium resources and to determine areas favorable for the occurrence of uranium in the United States.

Available from: Technical Library
Bendix Field Engineering Corporation
P.O. Box 1569
Grand Junction, CO 81502-1569

Telephone: (303) 242-8621, Ext. 278

Price per Microfiche Copy: $7.00

PGJ/F--131-82

DE82 015723

PGJ/F-131(82)

NATIONAL URANIUM RESOURCE EVALUATION
SILVER CITY QUADRANGLE
NEW MEXICO AND ARIZONA

A. J. O'Neill and D. S. Thiede

BENDIX FIELD ENGINEERING CORPORATION
Grand Junction Operations
Grand Junction, Colorado 81502

May 1982

PREPARED FOR THE U.S. DEPARTMENT OF ENERGY
GRAND JUNCTION AREA OFFICE
UNDER CONTRACT NO. DE-AC07-76GJ01664

This is the final version of the subject-quadrangle evaluation report to be placed on open file. This report has not been edited. In some instances, reductions in the size of favorable areas on Plate 1 are not reflected in the text.

CONTENTS

CONTENTS (continued)

CONTENTS (continued)

CONTENTS (continued)

ILLUSTRATIONS

ABSTRACT

Reconnaissance and detailed geologic, geochemical, and radiometric studies were conducted throughout the Silver City Quadrangle, New Mexico and Arizona, to identify environments and delineate areas favorable for the occurrence of uranium deposits using National Uranium Resource Evaluation criteria. Surface and limited subsurface studies were augmented by aerial radiometric and hydrogeochemical and stream-sediment reconnaissance surveys.

Results of the investigations indicate several areas favorable for magmatic-hydrothermal uranium deposits. They include Precambrian granitic, gneissic, and diabasic rocks; the Cretaceous Beartooth Quartzite where it overlies Precambrian granite; certain Laramide to mid-Tertiary monzonitic rocks; and Tertiary volcanic rocks adjacent to a quartz monzonitic stock. Studies also indicate environments favorable for allogenic deposits in the Tyrone laccolith and for uranium deposits in upper Cenozoic volcaniclastic lacustrine rocks.

Formations judged unfavorable for magmatic-hydrothermal uranium deposits include large areas of Precambrian granitic and metamorphic rocks, almost all Laramide and mid-Tertiary intrusive rocks, and intruded Paleozoic and Cretaceous carbonate rocks. Precambrian metamorphic rocks are also considered unfavorable for contact metasomatic as well as for unconformity-related and vein-type uranium deposits. The entire Paleozoic and Cretaceous sedimentary section is considered unfavorable for sandstone and marine-black-shale uranium deposits. Moreover, mid-Tertiary rocks were judged unfavorable for volcanogenic uranium deposits, and upper Cenozoic basin-fill and surficial deposits are unfavorable for sandstone-type deposits and for uranium deposits associated with volcaniclastic lacustrine environments.

INTRODUCTION

PURPOSE AND SCOPE

The Silver City Quadrangle, New Mexico and Arizona (Fig. 1), was evaluated to identify geologic environments and delineate areas that could containg uranium deposits aggregating at least 100 tons U_3O_8 at an average grade not less than 100 ppm U_3O_8. Selection of a favorable environment was based on the similarity of its geologic characteristics to National Uranium Resource Evaluation (NURE) recognition criteria described in Mickle and Mathews (eds., 1978).

The study was conducted by Bendix Field Engineering Corporation (BFEC) for the NURE program, managed by the Grand Junction, Colorado, Office of the U.S. Department of Energy (DOE). The study began March 1, 1980, and ended March 31, 1981. Time spent in literature review, field work, data analysis and interpretation, and preparation of the final report totaled about 1.5 man-years.

ACKNOWLEDGMENTS

We thank W. E. Elston of the University of New Mexico Geology Department and R. B. Scarborough of the Arizona Bureau of Geology and Mineral Technology for their discussions and helpful contributions drawn from their experience in the area. We also acknowledge L. M. Fukui, Petrology Laboratory, BFEC, for performing thin-section analyses and mineral identifications.

We also thank personnel of Anaconda Co., Texasgulf, Inc., Uranerz U.S.A., Inc., and Western Nuclear, Inc., who provided us with subsurface data. We also acknowledge the cooperation of Asarco Co., Kennecott Corp., Phelps-Dodge Corp., McCauley Mining Co., and the Black Hawk Consolidated Mines Co. in permitting our access to their private lands.

PROCEDURES

During March and April of 1980, literature research was done, and a work plan was formulated. Field studies, conducted from May through December of 1980, included examination of uranium occurrences (App. A), detailed geologic investigations within possible favorable areas, reconnaissance studies in areas of relatively low favorability, and followup studies of aerial radiometric and magnetic (ARMS) and hydrogeochemical and stream-sediment reconnaissance (HSSR) surveys. The subsurface data available are inadequate for evaluating the uranium favorability of any geologic environment at depth. The sparse subsurface information was used to estimate the thickness of Cenozoic basin-fill deposits in some areas.

Specific field procedures involved reconnaissance geologic mapping and outcrop examination, radiometric surveys with scintillometer or gamma-ray spectrometer (App. D; Pl. 9), and rock sampling (App. B; Pl. 5). Laboratory data comprise chemical, gamma-ray spectroscopic, and petrographic analyses of rock samples. Selected rock samples were analyzed for chemical uranium (cU_3O_8), equivalent uranium (eU), equivalent thorium (eTh), percent

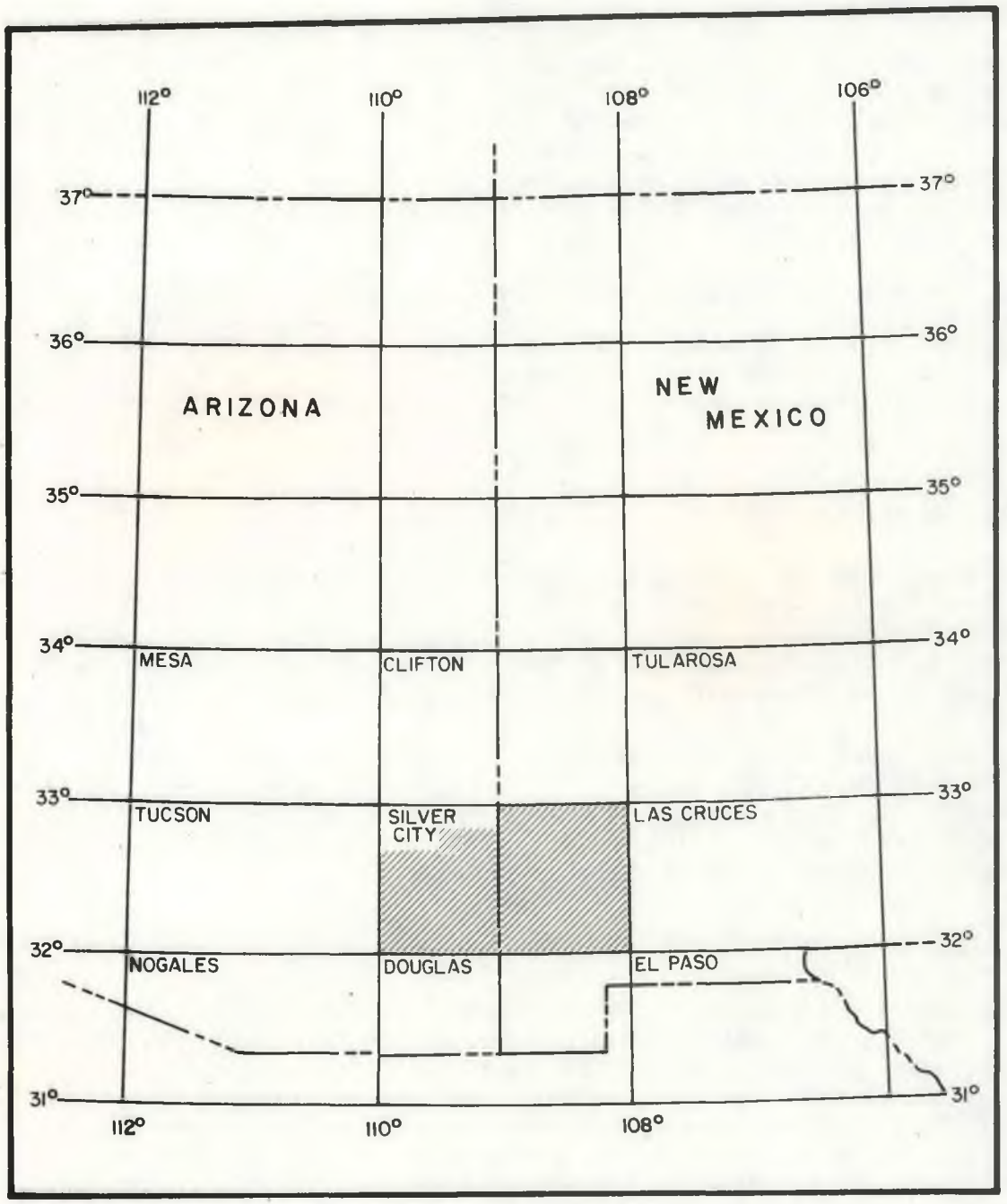

Figure 1. Quadrangle location map.

potassium (%K), major element oxides, and trace elements. Chemical-uranium contents were determined by fluorometric or colorimetric methods. Equivalent-uranium, equivalent-thorium, and percent-potassium determinations were made by laboratory gamma-ray spectrometric Ge(Li) or NaI detectors. Major oxide contents were determined by atomic absorption spectrometry; trace elements, by atomic absorption or emission spectrometry. Petrographic procedures are explained in Appendix E.

The ARMS survey was flown at a 3-mi (4.8-km) spacing by Texas Instruments Corporation (1978b). They statistically analyzed the data and identified apparent anomalies. Selected anomalies were field checked as part of the geologic investigations (Pl. 3).

In total, 755 stream-sediment and 474 water samples were collected in the New Mexico portion of the quadrangle during the HSSR survey. No samples were collected within the Arizona portion. Samples were analyzed and data reported by the Los Alamos Scientific Laboratory (Sharp and others, 1978). One area was found to contain anomalously high concentrations of uranium based on HSSR sampling (Pl. 4).

The final 3 months of the project involved the interpretation of field and analytical data and preparation of the final report.

GEOLOGIC SETTING

The Silver City Quadrangle, which includes approximately 20,700 km^2, is located between lat 31°00'00' N. and 32°00'00" N. and long 108°00'00" W. and 110°00'00" W. It lies largely within the Mexican Highland Section of the Basin and Range physiographic province (Fig. 2). However, part of the north-central and the northeastern areas of the quadrangle lie within the Transition Zone, a northwest-trending zone that is structurally and topographically intermediate between the Basin and Range and Colorado Plateau Provinces.

Southwestern New Mexico and southeastern Arizona are structurally complex. The Basin and Range portion of the quadrangle is characterized by at least three major tectonic elements (Drewes and Thorman, 1978). Northwest-trending complex faults, many of which record repeated and diverse direction of movement, are the most significant and widespread structures. Thrust faults, commonly low angle and Late Cretaceous or possibly Tertiary in age, are recognized in isolated areas in the quadrangle. Typically northwest-trending Cenozoic Basin and Range faults, probably reactivated segments of subparallel Precambrian basement structures, occur along many of the prominent range fronts. The area of the quadrangle lying within the Transition Zone is also characterized by northwest-trending fault systems and Basin and Range faults. However, northeast- and east-northeast-trending faults, fractures, and dikes are common, especially in the Big and Little Burro Mountains (Gillerman, 1964). These structures may be related in part to large regional structures or possibly be associated with regional warping and intrusion of igneous rocks (Trauger, 1972).

Rocks ranging in age from Precambrian to Quaternary are exposed in the quadrangle (Fig. 3). The geologic history, as recorded in these rocks, begins in the early Proterozoic, a time during which several thousand meters of

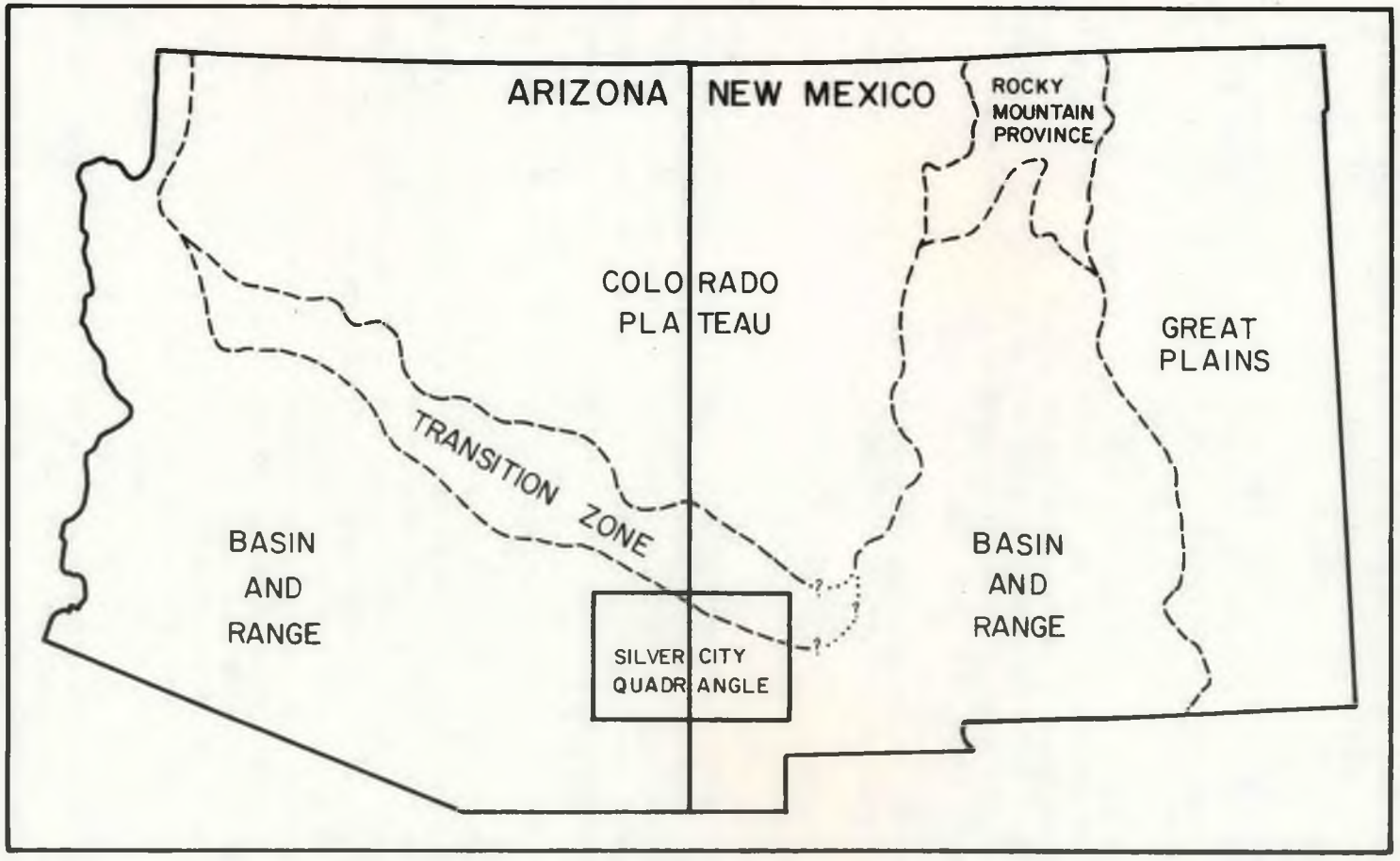

Figure 3. Location of Silver City Quadrangle in relation to the approximate boundries of major physiographic provinces (adapted, in part, from Scarborough and Peirce, and Trauger, 1972).

clastic sedimentary and volcanic rocks accumulated within a strongly subsiding eugeosyncline. At the same time, clastic sediments only were being deposited within an adjacent shelf area. Subsequent deep burial and dynamometamorphism, which occurred about 1,700 m.y.b.p., formed quartzite, schist, phyllite, amphibolite, and gneiss--the Pinal Schist in the western part of the quadrangle and the correlative(?) Bullard Peak and Ash Creek series rocks (Gillerman, 1964) in the eastern part. The Pinal and equivalent(?) rocks were deformed and extensively intruded by granitic stocks and batholiths about 1400 m.y.b.p., and, somewhat later, by diabasic dikes and sills.

During the latest Precambrian and Early Cambrian times, Precambrian rocks were uplifted and then peneplained. The Middle and Upper Cambrian Bolsa Quartzite, Coronado Sandstone, and Bliss Sandstone were deposited over the peneplain in beach and nearshore environments of a transgressing sea. The Abrigo and El Paso formations, predominantly carbonate units, record continued marine transgression through Early Ordovician. Repeated marine transgressive-regressive cycles occurred from Ordovician through Permian time. This thick marine assemblage comprises the Ordovician Montoya Group and Silurian Fusselman Dolomite, which consist mainly of carbonates, the largely dark-colored shales of the Devonian Martin Formation and Percha Shale, the predominantly carbonate Pennsylvanian Magdalena Group, and the limestones and minor siltstones of the Pennsylvanian-Permian Naco Group.

The region was emergent during Triassic and Jurassic time. There are no sedimentary rocks of Triassic or Jurassic age within the quadrangle, nor are there any Jurassic intrusive or extrusive rocks known in the quadrangle, although they are common in nearby areas.

Lower Cretaceous rocks are present only in the south-central and southwestern portions of the quadrangle. They are the continental Glance Conglomerate and other transgressive, shallow-marine units of the Bisbee Group. Continued marine transgression during Late Cretaceous time, mainly in the eastern part of the quadrangle, resulted in deposition of the Beartooth Quartzite and Colorado Shale. Local continental deposition toward the end of the Cretaceous is inferred from the Virden Formation and associated rocks in the north-central part of the quadrangle.

Renewed uplift and deformation of the area during Laramide time were accompanied by andesitic volcanism and intrusion of stocks of mainly intermediate composition. Although widespread erosion of uplifted areas produced thick continental deposits in parts of Arizona, no appreciable sedimentary deposits of early Tertiary age are known in the Silver City Quadrangle.

Evidence for early to middle Tertiary deformation and metamorphism is imprinted in Precambrian meta-igneous and metasedimentary rocks of the Pinaleno Mountains, in the western part of the quadrangle. Coney and Reynolds (1980) suggested that this localized, distinctive metamorphic terrane in the Pinalenos represents one of several isolated metamorphic core complexes found throughout the North American Cordillera. The evolution of these complexes is believed to have been related to regional extensional tectonism. This extension coincided in part with the eruption of voluminous volcanic and associated intrusive rocks in Oligocene to early Miocene time. Initially, a calc-alkalic suite of volcanic rocks erupted. Later, more silicic volcanics

and basaltic andesite formed. Large cauldron complexes formed during the later stages of calc-alkalic volcanism and during the more silicic volcanism; intermediate to silicic, composite stocks and felsic dikes were also emplaced during this middle Tertiary event.

In Miocene and Pliocene time, Basin and Range faulting produced the characteristic block-fault ranges and intermontane basins. Thick basin-fill deposits, consisting largely of unnamed and complexly interstratified conglomerates, mudstones, evaporites, and minor fresh-water limestones, accumulated in hydrologically closed basins through early Pleistocene time. Pliocene to Pleistocene alkali basalt and felsic tuff are commonly interlayered with basin-fill sediments.

Development of through-flowing drainage during later Pleistocene and Holocene times changed the sedimentologic regime of the basin from conditions of widespread aggradation to general degradation. Once-extensive pediment and interior basin deposits have been deeply incised. Holocene deposits of pediment-cap conglomerate, alluvial-fan deposits, terrace gravels, and inner-valley alluvial fill cover present-day valleys and adjacent piedmonts.

ENVIRONMENTS FAVORABLE FOR URANIUM DEPOSITS

In the Silver City Quadrangle, favorable environments include magmatic-hydrothermal deposits (Class 330, Mathews, 1978a) in Precambrian granitic and diabasic rocks (areas A and E, Pl. 1), in Precambrian quartz diorite gneiss and in Laramide to mid-Tertiary hornblende monzonite porphyry (area B), in Precambrian granite and overlying Cretaceous Beartooth Quartzite (area D), and in Tertiary volcanic rocks (area F); uranium deposits associated with volcaniclastic lacustrine environments of the hydroallogenic Class 540 (Pilcher, 1978) in late Cenozoic tuffaceous, lacustrine rocks (area C); and allogenic deposits (Class 370, Mathews, 1978a) in Laramide quartz monzonite of the Tyrone laccolith (area G).

AREA A: WHITE SIGNAL REGION

A portion of the White Signal structural block of the Precambrian Burro Mountains batholith (area A, Pl. 1) is favorable for uranium deposits of the magmatic-hydrothermal type (Class 330). The favorable host rocks are Precambrian Burro Mountains granite and mafic dikes, ranging in age from Precambrian to Tertiary, that intrude the granite. Area A is favorable because the host rock is both structurally and chemically favorable for uranium deposition. Structural favorability is indicated by the numerous faults and shear zones that transect the area. Chemical favorability is indicated because the host rocks are silicified, sericitized, argillized, and iron stained in a zonal relationship about veins present along shears. The uranium-bearing veins contain silica, carbonate, sulfides, anomalous thorium, fluorine, and anomalous amounts of heavy metals, including Ag, Au, Bi, Cu, Mo, Pb, Sb, Sn, W, Zn, and Zr, all of which characterize magmatic-hydrothermal uranium deposits. A source for the uranium-bearing magmatic-hydrothermal ore solutions is speculative, but several sources are available. An HSSR uranium anomaly is present over the entire Burro Mountains batholith (Pl. 4).

Area A contains 69 reported uranium occurrences (Pl. 2b, Pl. 11), 16 of which are described in uranium-occurrence reports (App. C). Uranium mineralization is characterized by secondary concentrations of uranyl phosphate minerals in mafic dikes where the dikes are intersected by fissure-filling, uranium-bearing vein systems. It is postulated that, during the Tertiary, uranium-bearing hydrothermal solutions were generated by a concealed intrusive body and entered an existing pervasive system of east-northeast- to east- and northwest-trending faults and shear zones. As the solutions moved through the fault system, fissure-filling veins were formed in fractures and brecciated zones cutting Precambrian granite and dikes ranging in age from Precambrian to Tertiary. The veins contained uranium, probably as uraninite, and variable amounts of base and precious metals. After deposition of the veins, a deep-weathering profile developed, which progressively oxidized the primary ore minerals of the veins. Within the oxidization zone, uranium became mobile and started to be dispersed from the near-surface portion of the veins. Where the veins had intersected, or were located adjacent to high-phosphate mafic dikes, uranium was precipitated as secondary concentrations of uranyl phosphate minerals.

Lithology

Area A consists primarily of granite, quartz monzonite, and associated rocks of the Precambrian Burro Mountains batholith. The Burro Mountains granite (Precambrian Y; Hedlund, 1978d) contains small, scattered xenoliths of metamorphic rocks (Bullard Peak Series, Hewitt, 1959) and is intruded by Precambrian diabase dikes. The Precambrian rocks are intruded by several plugs, sills, and numerous basaltic to rhyolitic dikes of Tertiary age. Volumetrically, the Tertiary intrusive rocks are a minor component of area A. Portions of area A are covered with a thin layer of Gila Conglomerate (Miocene to Pleistocene), Pleistocene to Holocene fan deposits and terrace gravels, and recent alluvium (Hedlund, 1978d, 1978e). The Burro Mountains granite, Precambrian diabase dikes, and Tertiary rhyolitic intrusive bodies are the dominant rock types.

The Burro Mountains granite, which constitutes more than 90% of area A, is characterized more by its heterogeneity than its homogeneity. The rock varies in texture, color, weathering response, and chemical and mineralogic composition. As yet, neither detailed field nor petrographic studies have been done to statistically analyze the different varieties (Gillerman, 1970). Hewitt (1959), Gillerman (1964, 1967, 1968, 1970), and Hedlund (1978d, 1978e) provided more detailed descriptions. The rock is leucocratic, typically light pinkish gray to tan, and medium to coarse grained. It has a hypidiomorphic-granular to xenomorphic-granular texture that is locally porphyritic; euhedral feldspar phenocrysts range up to 5 cm in length. Potassium feldspar and quartz are the dominant constituents; there are smaller amounts of plagioclase and mafic minerals. Quartz content ranges from 25% to 40% of the rocks. Potassium feldspar content ranges from 23% to 30% and is dominantly perthitic microcline, but variable amounts of orthoclase are present. Plagioclase constitutes 12% to 70% of the rock, is commonly sodic oligoclase, and occurs in microperthite and as anhedral grains. The mafic mineral contents range from less than 1% to 10% of the rock, the dominant mafic mineral being biotite. Accessory minerals are hornblende, sphene, zircon, tourmaline, apatite, magnetite, rutile, ilmenite, and allanite.

The diabase dikes are thought to be Precambrian (Hedlund, 1978d) and are as large as 3 km long and 100 m thick. More typically, they are less than 15 m thick. Most trend to the northwest. The diabase is dark greenish gray and has a subophitic to intergranular texture. The rock contains 60% to 65% andesine, 20% to 30% augite, and as much as 12% magnetite-ilmenite (Hedlund, 1976d). Biotite, chlorite, secondary quartz, and apatite are accessory minerals. The diabase alters readily to chlorite, hydrous iron oxides, epidote, and clay minerals.

Tertiary rhyolite plugs and associated dikes and apophyses in area A intrude east-northeast- to east-trending faults and zones of weakness (Pl. 11). The Precambrian granite is also intruded by the Saddle Mountain rhyolite (Pl. 2b), a sill that covers an area of 2.6 km^2. Tullock Peak, a small hill in the area, is composed of a rhyolitic, welded, ash-flow tuff. The rhyolite plugs are commonly elongate and show alignment along a N. 70° to 90° E. direction, parallel to the rhyolite dike swarms. The plugs are commonly less than 30 m wide, but a few are as wide as 60 m. The dike swarms commonly contain as many as 13 to 20 dikes per kilometer. Petrographically, the plugs, dikes, and the sill are similar. The rhyolite ranges in texture from felsic to porphyritic and generally contains less than 10% phenocrysts. Occasionally, phenocrysts will constitute up to 50% of the rock. Most of the rhyolite is a fine-grained, dense, hard, light-gray rock with a few bipyramidal quartz grains, sanidine, biotite phenocrysts, and local disseminations of pyrite. The intrusive rhyolite is commonly flow banded; banding in the dikes is parallel to the dike walls, and banding in the plugs is contorted. Specular hematite is common, both as thin fracture fillings in the plugs and as anastomosing veinlets that are locally pervasive along the intrusive contacts of the rhyolite sill. Rhyolite breccia is common along borders of dikes, plugs, and the sill. In places, the rhyolite is slightly vesicular (Gillerman, 1970). Many of the sanidine phenocrysts are argillized, and the biotite is usually sericitized. Limonite stains and limonite-filled cavities are abundant in all the intrusive rhyolite. The extrusive rhyolite of Tullock Peak is a very light gray, devitrified, welded ash-flow tuff that contains flattened pumice lapilli and a few percent of lithic fragments of quartzite and latite. The welded tuff has a pronounced eutaxitic texture and contains about 4% phenocrysts of bipyramidal quartz and sanidine. Biotite and iron oxides are accessory minerals (Hedlund, 1978e). The age of the rhyolite in area A is uncertain. Gillerman (1970) believed that it is pre-Tyrone laccolith intrusion in age. The Tyrone laccolith has a radiometric age of 56.2 $\pm$ 1.7 m.y. (McDowell, 1971). However, Hedlund (1978a, 1978c, 1978e) contended that the rhyolite is post-Tyrone laccolith in age. The presence of rhyolite dikes within the Tyrone laccolith supports the theory of Hedlund, who assigned an age of late Paleocene and (or) Eocene to the rhyolitic intrusive activity in area A.

Structure

The Burro batholith is the major portion of a complex, northwest-trending fault block that, in part at least, is tilted to the northeast. The Burro batholith is divided by a northwest-trending graben into the Big Burro Mountain block on the east and the Gold Hill block on the west (Pl. 7). The Big Burro Mountain block is subdivided into three subsidiary blocks by a series of northeast-trending faults (Pl. 11). Subsidiary structural blocks

are the Willow Creek block, the Burro Peak-Tyrone block, and the White Signal block (Gillerman, 1967, 1970). Area A is located within the White Signal block. Within and bounding area A, faulting and fracturing were concentrated in three directions--northwesterly, northeasterly, and east-northeasterly to easterly (Pl. 11).

The fault-filling, northwest-trending Precambrian dikes provide the earliest evidence of faulting. Gillerman (1970) stated that the dikes were emplaced along pre-existing faults and fractures. The northwest-trending Walnut Creek-Uncle Sam fault (Pl. 11) is apparently post-Tyrone-stock intrusion in age, but pre-lead-silver mineralization. The fault is believed to be older than late Tertiary (Gillerman, 1970). The northwest-trending bounding faults of the Big Burro Mountain block, which includes the subsidiary White Signal block, are the Taylor fault on the west and the Mangas fault on the east. The latest movement of the faults was in the late Pliocene or Pleistocene. The time of the earliest movement is not known but could have been as early as early Tertiary.

The east-northeast to east set of fractures is prominent within area A in the White Signal block (Pl. 11). The fractures are filled with numerous dikes, primarily of rhyolitic composition, but also of latitic, dacitic, and quartz monzonitic compositions. The alignment of rhyolite plugs in an east-northeast to east trend (Pl. 11) is probably also controlled by these fractures. The minimum age of the fractures is indicated by the ages of the oldest dike rocks intruding along them. Thus, faults and fractures filled by the dikes were formed prior to the Eocene.

Northeast structures are represented in area A by the northeast-trending Sprouse-Copeland fault, which acts as the boundary between the White Signal block, which contains area A, and the upthrown Burro Peak-Tyrone block to the north. The age of earliest activity of this fault is unknown, but repeated movement is indicated, and the most recent movement was post-Miocene.

Description of Uranium Occurrences

Area A encloses the well-known White Signal district, a sporadic producer of gold, silver, and uranium. Uranium was first identified at the Merry Widow Mine in 1920. Small-scale mining of torbernite for its radium content occurred in the 1920's in the district. Torbernite was mined at the Merry Widow, California, Acme Shamrock, and other properties (App. A) for use in "radioactive face powder," "radioactive water," medicinal radium salts, and for the extraction of radium (Gillerman, 1964). Total amount of production during the radium boom of the 1920's is unknown. Renewed activity in the district occurred between 1948 and 1955 with extensive prospecting and limited development. Cumulative production from this later period was four carloads of uranium ore averaging between 0.1% and 0.2% U_3O_8 (Gillerman, 1964). The four carloads of ore were supplied by two mines, the Inez (Occurrence 108) and the Floyd Collins (Occurrence 71). Since 1955, no uranium production has occurred, but exploration has continued intermittently to 1981.

Area A contains 69 uranium occurrences, 16 of which are described in Appendix C. The rocks of area A are host to two classes of uranium deposits, pegmatitic (Class 320) and magmatic-hydrothermal (Class 330).

The pegmatitic uranium occurrences are small and scattered; only two are known in area A (Occurrences 114 and Y63). The pegmatites, which are Precambrian in age and are in Burro Mountains granite, contain only limited amounts of uranium.

Most of the uranium in area A is associated with weathered magmatic-hydrothermal uranium deposits. Uranium, principally in secondary uranium phosphates, occurs at the surface in oxidized uranium-bearing hydrothermal veins and in fractures in the Precambrian granite associated with the veins. Concentrations of secondary uranium minerals also occur in fractures and as disseminations in altered mafic (primarily diabasic) dikes where the dikes intersect or are adjacent to oxidized veins. Many of the secondary concentrations consist of closely spaced fractures filled or coated with uranium phosphate minerals. The fillings are rarely more than 1 mm thick, but, where numerous, can result in high uranium contents (Gillerman, 1968). In places, the hydrothermal solutions rose along fractures already occupied by dikes. The ore solutions impregnated and altered the dikes to such an extent that the veins are unrecognizable, and only extremely altered linear zones within the dikes indicate the presence of hydrothermal veins. Such situations have occurred at the Floyd Collins (Occurrence 71) and the Inez Uranium Mine (Occurrence 108). Gillerman (1964, 1968) grouped the uranium-bearing hydrothermal veins mineralogically into four categories: quartz-pyrite, quartz-specularite, high-silver and lead-silver, and turquoise deposits. Secondary uranium occurrences are associated with all four types, but the vast majority are associated with the quartz-pyrite veins. Some significant occurrences are associated with the quartz-specularite and lead-silver veins. The radioactive turquoise veins are minor occurrences. As all veins, outcrops, and subsurface workings are in the oxidized zone, no information is available on the hypogene mineral assemblage except what can be extrapolated from the supergene assemblage and from a few reports of primary hypogene minerals.

It is not unusual to find more than one of the four types of veins at a single uranium occurrence. However, a single vein type predominates at each occurrence. For example, at the Merry Widow Mine (Occurrence Y72), the veins are predominantly quartz pyrite, but minor quartz-specularite veins are present. At the Chapman Turquoise Mine (Occurrence 113), minor quartz-pyrite and quartz-specularite veins are present with the predominant turquoise veins. At the Apache Trail (Occurrence 46Y), the predominant veins type is quartz specularite, but minor quartz-pyrite veins are present.

Quartz-pyrite veins. The quartz-pyrite veins contain gold, chalcopyrite, sphalerite, galena, bismuth, silver, and uranium in a gangue of quartz, pyrite, hematite, siderite, limonite, and magnetite (Gillerman, 1964). Most of the pyrite has been completely oxidized to limonite. Gold is present in all uranium occurrences that have quartz-pyrite veins except the Floyd Collins (Occurrence 71), the Blue Jay (Occurrence 100), and the Inez Uranium Mine (Occurrence 108). Uranium-occurrence reports 80, 95, 99, 102, 103, 105, 106, and 115 (App. C) describe occurrences associated with quartz-pyrite veins.

Anomalous amounts of Au, Bi, Cu, Mo, Pb, Sn, W, Zn, and Zr seem to be characteristically associated with the veins and the surrounding mineralized country rocks (Table 1). Anomalous amounts of Ag, Co, Cr, Li, Ni, Sc, Sn, and Y are also common (Table 1).

TABLE 1. TRACE-ELEMENT ANALYSES OF SELECTED SAMPLES FROM THE WHITE SIGNAL REGION

Sample no.	Analyses
MLM 034	377 ppb Au, 99 ppm Bi, 574 ppm Cu, 79 ppm Mo, 357 ppm Pb, 776 ppm Sb, 176 ppm Sn, 460 ppm W, 239 ppm Zn, 203 ppm Zr
MLM 037	387 ppb Au, 30 ppm Ag, 231 ppm Bi, 1520 ppm Cu, 25 ppm Mo, 226 ppm Pb, 65 ppm Sn, 355 ppm W, 347 ppm Zn, 502 ppm Zr
MLM 041	257 ppb Au, 92 ppm Bi, 1540 ppm Cu, 33 ppm Mo, 384 ppm Pb, 75 ppm Sc, 100 ppm Sn, 198 ppm W, 122 ppm Y, 2630 ppm Zn
MLM 042	3100 ppb Au, 1250 ppm Bi, 7230 ppm Cu, 83 ppm Mo, 314 ppm Pb, 133 ppm Sn, 394 ppm W, 691 ppm Zn
MLM 046	15300 ppb Au, 54 ppm Ag, 1400 ppm Bi, 1190 ppm Cu, 75 ppm Mo, 804 ppm Pb, 79 ppm Sn

In outcrop, the highest uranium analyses are from secondary uranium concentrations in latite, diabase, or basalt dikes that are cut by or adjacent to radioactive quartz-pyrite veins. The highest uranium value obtained is 0.541% cU_3O_8 (sample MLM 033), and median values range from 0.2% to 0.3% cU_3O_8. The highest uranium content in an oxidized quartz-pyrite vein is 0.1% cU_3O_8 (MLM 041). Gillerman (1964) reported values approaching 1% cU_3O_8. Thorium contents are quite variable--maximum values occur in the quartz-pyrite veins (MLM 039, 547 ppm eTh; MLM 049, 582 ppm eTh; MLM 067, 702 ppm eTh), and much lower values are found in the secondary uranium concentrations. Uranium is almost always out of equilibrium with its daughter products. The secondary uranium concentrations almost always contain more chemical uranium than radiometric equivalent uranium. In contrast, the oxidized veins usually contain much more equivalent uranium than chemical uranium (MLM 039: 33 ppm cU_3O_8, 542 ppm eU). Uranium minerals identified are secondary uranyl phosphate minerals, such as meta-autunite and hydrogen-autunite (MLM 051). The uranyl phosphates torbernite and metatorbernite and the iron-uranyl phosphate bassetite have also been identified (Gillerman, 1964). Uraninite was identified in one place at the Blue Jay (Occurrence 100; Gillerman, 1968). Gillerman (1968) reported that, at the Merry Widow Mine (Occurrence Y72), there is a zonation of uranyl phosphate minerals with depth. Autunite is abundant at the surface but is not present below a depth of 30 ft. Torbernite is present from the surface down to a depth of 184 ft. Bassetite is known only at depths greater than 100 ft.

Alteration of uranium occurrences is extensive, and oxidation of pyrite in the veins is pervasive. At only one location (MLM 060) was pyrite observed in a quartz vein in outcrop. At the Merry Widow Mine, pyrite is completely oxidized to a depth of 80 ft and is partially oxidized from 80 to 150 ft. Below 150 ft, pyrite is oxidized only in the large veins. However, Granger and Bauer (1951) stated that the main quartz-pyrite vein at the Merry Widow was still completely oxidized at a depth of 550 ft, the greatest depth at which the vein was sampled. In granite adjacent to veins, the plagioclase is almost completely sericitized, the potassium feldspar is variably argillized and sericitized, the biotite is replaced by muscovite, and the rock is moderately to strongly iron stained and silicified and is cut by an anastomosing network of limonitic veinlets. Diabase dikes, where cut by veins or where the hydrothermal solutions were disseminated throughout the dike (Floyd Collins, Occurrence 71; Inez Uranium Mine, Occurrence 108), are completely altered to a mixture of hydrous iron oxides, sericite, clay minerals, and epidote (MLM 051, MLM 052, MLM 055).

Quartz-specularite veins. The quartz-specularite veins consist of 75% to 90% specular hematite. Magnetite is locally abundant, and minor amounts of gold and bismutite are reported (Gillerman, 1964). Few of the many quartz-specularite veins are uranium occurrences. The Apache Trail occurrence (Occurrence Y47, App. A) is the best example. Granger and others (1952) and Gillerman (1964) provided extensive descriptions of the occurrence, so only a brief summary will be given here. The vein has the characteristic east-northeasterly trend common to most of the hydrothermal veins in area A, and it cuts Precambrian Burro Mountains granite and a Precambrian diabase dike. The vein ranges from 3.5 to 8 ft wide and consists of specular hematite, quartz, magnetite, and hematite. It has local concentrations of gold, bismuth, copper carbonates, oxidized pyrite, fluorite, lead minerals, and torbernite. Uranium

is present largely as concentrations of secondary uranyl phosphate minerals where the vein intersects altered diabase. Granger and others (1952) reported uranium values as high as 0.041% cU_3O_8. The quartz-specularite vein is also anomalously radioactive throughout its length; cU_3O_8 values are as high as 0.012% (Granger and others, 1952). Samples from the Alhambra Bluebell No. 2 (Occurrence 69) and the Hope No. 1 (Occurrence 49--outside area A) show that the heavy-metal, trace-element suite of the quartz-specularite veins is similar to that of quartz-pyrite veins. Alteration of Burro Mountains granite and diabase dikes adjacent to the quartz-specularite veins is also similar to the alteration patterns of the quartz-pyrite veins.

High-silver and lead-silver veins. The Uncle Sam Silver Mine (Occurrence 120) is the only example of high-silver or lead-silver hydrothermal veins in area A known to contain uranium mineralization (Gillerman, 1968). In general, this type of vein is characterized by the absence of gold. The underground workings are all inaccessible, but from an examination of dumps and old records Gillerman (1964) postulated that the primary minerals were galena and argentite in a gangue of quartz, pyrite, and minor barite and variable amounts of bismuth and chalcopyrite. In the oxidized zone, cerargyrite was the primary ore mineral. Like other types of hydrothermal veins in the area, the lead-silver veins fill open spaces and fractures, with little replacement of country rock. The veins are in Burro Mountains granite. There are no nearby diabase dikes exposed.

Unlike most other veins in the area, the Uncle Sam vein was not formed in an east-northeast-trending structure, but in the N. 40° to 45° W.-trending Uncle Sam-Walnut Creek fault. Quartz and sulfides fill fractures in a 6-m-wide shear zone along the Uncle Sam fault. The main vein varies in width from less than 1 ft to more than 8 ft (Gillerman, 1964). No uranium minerals have been identified, and uranium content of the vein at depth is unknown. Outcrop samples of the vein along 1220 m of strike length vary from a low of 25 ppm cU_3O_8 (MLM 074) to a high of 49 ppm cU_3O_8 (MLM 073). Except for one sample, uranium is essentially in equilibrium with its decay products. The anomalous sample, MLM 073, contains 49 ppm cU_3O_8 and 151 ppm eU. Thorium levels are moderate (MLM 074, 35 ppm eTh). Fluorine is moderate, but still anomalous (MLM 075, 2177 ppm F) compared to the country rock (MLM 077, 290 ppm F). Trace-element contents of the samples demonstrate the silver-lead nature of the vein (MLM 076: 97 ppm Ag, 302 ppm Cu, 13 ppm Mo, 12,900 ppm Pb, and 507 ppm Zn).

Alteration at the Uncle Sam occurrence is similar to alteration at the quartz-pyrite and quartz-specularite types of uranium occurrences in area A. Alteration is characterized by pervasive oxidization of the vein material and sericitization, argillization, silicification, and iron staining of the country rock.

Turquoise veins. The fourth type of anomalously radioactive hydrothermal veins within area A is represented by turquoise deposits. Only two examples (Red Hill Turquoise Mine, Occurrence 62; Chapman, Occurrence 113) are known within area A. As a contributing factor to the uranium potential of the area, this type of hydrothermal mineralization is insignificant. The Chapman occurrence (Pl. 2b) is hosted by the Saddle Mountain Rhyolite Sill along a N.

12° W.-trending shear zone. Parallel to subparallel quartz-pyrite veinlets are present, and they may have provided the uranium. Uranium values are low (MLM 063, 63 ppm cU_3O_8), and the major heavy-metal trace element present is copper. Alteration is characterized by intense sericitization, kaolinization, and oxidation of pyrite of the rhyolite. Adjacent Burro Mountains granite is variably sericitized and iron stained.

The Red Hill Turquoise Mine (Pl. 2) is located in a 30-m-wide shear zone along a northeast-trending fault that cuts Burro Mountains granite. Pervasive veinlets of turquoise are present along the shear in granite that is so altered that the rock is composed of sericite, clay minerals, and quartz grains. No uranium minerals were identified. A selected sample (MLM 005) contained 121 ppm cU_3O_8, 125 ppm eU, 18 ppm eTh, 546 ppm Cu, 100 ppm Mo, 28 ppm Sn, and 741 ppm Zr.

Size of deposits. Most surficial expressions of the deposits are small, and few veins have been followed for more than 500 ft. An exception is the Apache Trail vein (Occurrence Y47), which Gillerman (1964) stated can be traced for more than 7,500 ft. Although individual veins appear rather short on the surface, many individual veins occur along strike lengths of several miles within single faults. An example of multiple veins along a fault is the east-northeast-trending Blue Jay fault where, from west to east, the Banner (Occurrence 80), Blue Jay (Occurrence 100), Calamity (Occurrence 99), possibly the Inez Uranium Mine (Occurrence 108), and many individual prospects occur along a fault-strike length of approximately 2.4 km. The radioactive vein of the Uncle Sam Silver Mines (Occurrence 120) is traceable for at least 1.2 km along the northwest-trending Uncle Sam fault. The occurrence of multiple veins along the strike of a fault raises the possibility that the deposits at depth may be more continuous along the fault. Such a situation occurs in favorable area B, where intermittent veins at the surface become a continuous network at depth.

Width of the individual radioactive veins is commonly less than 30 cm, but is reported (Gillerman, 1964) to be as much as 3 m at the Apache Trail vein (Occurrence Y47). However, the veins seldom occur singly across the width of a fault or fault zone but occur in swarms of parallel to subparallel veins and veinlets that are difficult to trace individually on the surface for more than 25 m. At the Blue Jay (Occurrence 100), individual radioactive veins have been mapped (Granger and Bauer, 1951) as occurring over a width of 55 m along the trend of the Blue Jay fault. Individual veins are surrounded by a zone of altered country rock, usually Burro Mountains granite, that is intensely sericitized, argillized, variably mineralized, and cut by an an anastomosing network of oxidized, siliceous, limonitic veinlets up to several millimeters thick. The weakly mineralized halo can extend for tens of meters away from an individual vein and fills the area between parallel or subparallel veins in a vein system. The surficial lateral extent of uranium mineralization is further enhanced by secondary concentrations of uranium phosphate minerals in weathered, commonly diabasic rocks cut by, or adjacent to, the radioactive veins. Secondary uranium minerals are also variably disseminated in altered granite. Total width of anomalous surficial mineralization, including the extent of individual veins and associated mineralized country rock, has been observed to be as great as 60 m (Blue Jay, Occurrence 100). Widths of vein zones below the oxidization zone are unknown.

The depth of mineralized zones in area A is unknown. The deepest workings in the district reach a depth of 260 ft at the Tullock shaft (Occurrence 105), but most workings are less than 100 ft deep (Gillerman, 1964). Except for the Floyd Collins and Inez occurrences, the workings were originally exploited for gold, silver, or copper. That depth marked the limits of high-grade supergene ore along the veins; when the grade of gold, silver, and copper dropped as the workings approached the hypogene zone of mineralization, mining ceased. Shallow drilling at the Merry Widow Mine (Occurrence Y72) intersected the main zone at a depth of 550 ft (Granger and Bauer, 1951).

Origin of Uranium Mineralization

Granger and Bauer (1952), Granger and others (1952), Gillerman (1968), and this writer believe that the origin of the uranyl phosphate concentrations in the diabase and other mafic dikes of area A is secondary and that they are locally derived from hypogene uranium minerals contained in the various types of magmatic-hydrothermal veins present in area A.

Evidence that the uranium in the mafic dikes is secondary is provided by uranium mineralogy, habit, and trace-element chemistry. The uranium minerals present are all uranyl phosphates, which are widely recognized as being secondary uranium minerals. The habit of uranyl phosphates in the host rock, fracture fillings, surficial coatings, and disseminations in highly altered rock, is also characteristic of secondary deposition. Thorium values are low, and the uranium is not in equilibrium with its daughter products; the chemical uranium-to-equivalent uranium (cU/eU) ratio is greater than 1. Both the low thorium and high cU/eU values are consistent with a secondary origin.

As mentioned previously, the nature of the uranium-bearing veins is obscured by the fact that no unoxidized vein material is available. However, substantial evidence supports the contention that magmatic-hydrothermal veins containing hypogene uranium minerals were the source of uranium for the secondary uranium mineralization in area A. A genetic relationship between the veins and mineralized mafic dikes is suggested by their spatial relationship. Secondary uranyl phosphate concentrations in mafic dikes are present only where the veins intersect dikes (Eugenie, Occurrence 102), where the veins have formed in a fracture already intruded by a dike (Floyd Collins, Occurrence 71), or where a vein is near a dike (Inez Uranium Mine, Occurrence 108). Throughout area A, mafic dikes contain only background levels of uranium, except where they are cut by or are near radioactive hydrothermal veins. Where, for example, a diabase dike is cut by a single vein, the diabase contains progressively less uranium away from the vein intercept (Inez Uranium Mine). Intensive alteration of the mafic dikes to hydrated iron oxides, sericite, and clay minerals occurs only where they are intersected by veins. This empirical relationship indicates that presence of the veins was necessary for development of secondary uranium concentrations. That the veins were the source of the uranium is suggested by the fact that the hydrothermal veins are themselves anomalously radioactive and in many places have a higher chemical uranium content than the adjacent country rock, which is either granite or mafic dikes. In occurrences such as the Banner (Occurrence 80), where an oxidized quartz-pyrite vein cuts granite, the progressive increase in uranium from unaltered country rock to altered granite in the alteration halo

surrounding the vein to the vein itself is characteristic of a uranium-bearing magmatic-hydrothermal vein. The thorium values and the cU/eU ratios of the veins are also characteristic of a primary origin. Thorium values are higher in the veins than in the country rock and are as high as 702 ppm eTh (MLM 67, Occurrence 105). The cU/eU ratios are often much less than 1 (33 ppm cU_3O_8, 542 ppm eU; MLM 039, Occurrence 80). Both sets of data are diagnostic of an oxidized magmatic-hydrothermal vein that contained hypogene uranium. As described earlier, the veins contain anomalous amounts of Ag, Au, Bi, Cu, Mo, Pb, Sb, Sn, W, Zn, and Zr--elements common in uranium-bearing hydrothermal veins. Fluorine contents of the veins are not high, but they are anomalous compared to those of the country rock. Burro Mountains granite in area A contains little fluorine (MLM 061, <200 ppm; MLM 077, 290 ppm). Fluorite was reported (Gillerman, 1964) in the vein at the Apache Trail (Occurrence Y47). Anomalous fluorine is common in uranium-bearing hydrothermal veins.

Age of magmatic-hydrothermal mineralization. The age of the vein-type uranium mineralization is uncertain, primarily because unoxidized portions of the mineralized veins have not been observed. Therefore, paragenesis, mineral associations, and detailed geologic relationships cannot be determined with certainty. However, an approximation of the time of vein formation can be gained from known structural and lithologic relationships of veins with the country rocks. The veins are present in east-northeast- to east-trending and northwest-trending faults and fractures. Gillerman (1970) believed that the veins are younger than the faults because of the open-space and fracture-filling nature of the veins. Some east-northeast to east fractures are filled with dike material compositionally identical to the Tyrone laccolith, indicating that these fractures are probably not younger than the intrusion of the Tyrone laccolith (late Paleocene). However, the northwest-trending Walnut Creek-Uncle Sam fault is younger than the Tyrone laccolith (Gillerman, 1970), and the Uncle Sam vein (Occurrence 120) is younger than the fault. The youngest rocks cut by the veins are the rhyolite dikes, which Hedlund (1978e) mapped as being younger than the Tyrone laccolith. The dikes are probably Eocene in age. At the Tullock shaft (Occurrence 105), field relationships seem to show a radioactive quartz-pyrite vein cutting a rhyolite dike, and the vein, in turn, being cut by a second rhyolite dike. The relationships are obscure because of the intense surficial weathering of the area, but they seem to indicate that the veins are late stage and contemporaneous with the rhyolitic intrusive activity of the area. Therefore, field relationships appear to indicate that the mineralization that formed the uranium-bearing veins was probably post-Paleocene in age.

Determination of the age of primary uranium mineralization is complicated by regional patterns of mineralization. Gillerman (1964, 1968, 1970) recognized two primary episodes of post-Precambrian mineralization in the Burro Mountains batholith. The first is post-Tyrone laccolith intrusion, but pre-late Tertiary volcanic activity, dominantly characterized by base-metal mineralization. The second period is a post-volcanic episode in the late Tertiary that was characterized by fluorite-gold mineralization. Gillerman (1968) believed that uranium mineralization may have been associated with the latter period of mineralization because of the association of uranium and fluorite in the Redrock district (area D) to the north of area A.

Field relationships seem to indicate an early to mid-Tertiary, pre-volcanism age for the uranium-bearing veins in area A, whereas Gillerman (1968) indicated that regional patterns of mineralization suggest a late Tertiary, post-volcanic period of uranium mineralization. At present, data are insufficient to discriminate between the hypotheses. A further possibility, that of several episodes of mineralization within the faults and fractures of area A, ranging from early to late Tertiary, cannot be ruled out without detailed determination of ore paragenesis of unoxidized, hypogene vein mineralization. The age of the secondary uranium mineralization associated with the veins of the area is, of course, post-vein to Holocene in age.

Source of uranium. With the data available, discussion of the source of uranium-bearing solutions is highly speculative. However, as determination of the uranium source has strong implications regarding the eventual delineation of favorable areas, even a speculative discussion has worth. Constraints on the age of hydrothermal uranium mineralization limits consideration of potential uranium sources to three possibilities.

The first possible source is the Paleocene Tyrone laccolith. However, the laccolith is quartz dioritic to quartz monzonitic and does not meet the chemical criteria listed by Mathews (1978a) as indicating a highly differentiated pluton capable of generating uraniferous solutions. In addition, the chemical-uranium contents of rock samples from the laccolith are low (MLM 023, 024, <1 ppm cU_3O_8), and none of the Laramide intrusive bodies that have undergone porphyry copper mineralization in the Silver City Quadrangle have any associated hydrothermal uranium minerals.

The second potential uranium source is related to the mid- to late Tertiary episode of volcanism. Gillerman (1968) associated this period with fluorite-uranium mineralization of the northern Burro Mountains. The problem with invoking such an origin for the uranium within area A is that the known volcanic eruptive centers are either to the north in the Schoolhouse Mountain area or to the south in the Lordsburg area. Invoking a mid- to late Tertiary intrusive body beneath area A, inasmuch as there is no surficial evidence of such a body, is speculative.

The third alternative source, a buried pluton, is also speculative, but at this time it is the most likely of the three possibilities. The pluton as inferred by Hedlund (1978d, 1978e) would have the subsurface extent of the numerous rhyolite dikes, several plugs, and the sill in area A. It is unknown if the rhyolite in outcrop is representative of the buried pluton or if the rhyolite is a differentiate. The subsurface intrusive body, as represented by the rhyolite, has several features that indicate it might be the source of uranium-bearing hydrothermal solutions. The first is the spatial relationship of the uraniferous veins with the rhyolite. Not only do a great number of uranium occurrences cluster about the intrusive rhyolite plugs and the rhyolite sill, but it is common to find a rhyolite dike intruding the same faults as a uraniferous vein (Blue Jay, Occurrence 100). There is also the correct temporal relationship. Although some veins do cut the rhyolite, in at least one case it appears that the rhyolite cuts a vein (Tullock shaft, Occurrence 105), indicating that uranium mineralization was post-intrusive and perhaps even contemporaneous. Petrographically, the rhyolite has features consistent with its being the uranium source. Where radioactive veins do cut

the rhyolite, they are always at the outer margins of the intrusive bodies. Specularite, the major component of the quartz-specularite type of vein, is present in the rhyolite, both as anastomosing veinlets at the margins of the rhyolite sill and as minute fracture filling in the dikes and plugs. Pyrite is present locally in the rhyolite as disseminations. The rhyolite is also locally vesicular. There are iron staining and argillization of feldspars, and the sericitization of biotite is pervasive. Uranium (8 ppm cU_3O_8, MLM 062) and fluorine (1,500 ppm, MLM 109) contents of the rhyolite are also consistent with the possibility that an unexposed intrusive body, of which the rhyolitic intrusives are an expression, was the source of uranium-bearing hydrothermal solutions.

Transport and deposition of hypogene uranium. Whatever the source of hydrothermal solutions, it is clear that they migrated along the pervasive system of east-northeast- to east- and northwest-trending fractures that cut area A, because that is where uranium has been deposited.

The hypogene suite of uranium minerals is speculative, but Gillerman (1968) postulated uraninite as the primary uranium mineral in the veins. That conclusion is based on three factors: 1) Sulfide-bearing veins are the source of secondary uranium. Uranium in sulfide veins is characteristically present as uraninite (Mathews, 1978a). 2) Uraninite has been identified at the Blue Jay occurrence. 3) The occurrences within area A are similar to the deposits of Urgeirica, Portugal (Bain, 1950). At Urgeirica, a high-phosphate diabase dike with concentrations of secondary uranium minerals is associated with oxidized veins. The uranium phosphates of the oxidized zone grade downward along the veins into primary uraninite. Gillerman (1968) cited several other analogs where secondary uranyl phosphates are present in the oxidized portion of the vein and primary uraninite is in the deeper, unoxidized portion of the vein. For these reasons, Gillerman postulated that within area A, primary uraninite is present within the veins below the level of oxidation. Evidence from the Merry Widow Mine (Granger and Bauer, 1951) indicates that oxidation of the primary veins extends to a depth of at least 500 ft.

Deposition of uraninite from hydrothermal solutions was probably caused by one of two mechanisms. The first is a pressure-temperature-related drop of oxidation potential of the hydrothermal solutions as they ascended. As the oxygen fugacity of the solutions decreased, hexavalent uranium in complexes, perhaps of fluorine, was reduced and deposited as uraninite. The second possibility is that there were several mineralization pulses from the source. The sulfide minerals might have been deposited first. Subsequent uranium-bearing solutions encountering sulfides already within the vein could then have deposited uraninite. The data available do not permit discrimination between the two mechanisms. It is not known if the sulfides and uranium represent separate episodes of mineralization, or even if the four classes of uranium-bearing veins (quartz-pyrite, quartz-specularite, lead- silver, and turquoise) were formed contemporaneously in a zoned relationship, or if they represent successive pulses of mineralizing solutions of slightly differing composition from the same source.

Deposition of supergene uranium. It has been proposed (Gillerman, 1968) that primary uranium minerals in the veins were oxidized, the uranium

transported and then deposited as secondary uranyl phosphates in adjacent, high-phosphate, mafic dikes. Such a process would account for the observed secondary minerals that are present in many occurrences within area A. Such an explanation is consistent with all field relationships observed and with all geochemical data available.

Exposure of the uraninite- and sulfide-bearing veins in the weathering zone could have caused oxidization of the sulfides, resulting in an acidic, oxidizing environment in which tetravalent uranium minerals would no longer be stable. The uranium would be oxidized to the hexavalent state, in which state it is mobile in aqueous solution. In an arid to semiarid environment, such as that in area A, uranium could be dispersed from the veins into the country rock during periods when water was available. The oxidized veins from which uranium was derived would contain relatively high levels of thorium and more equivalent uranium than chemical uranium because of the selective removal of uranium relative to its decay products and thorium (De Voto, 1978). As discussed before, the oxidized veins display such relationships.

Several groups of hexavalent uranium minerals are stable and relatively insoluble in an oxidizing environment. One such group is the uranyl phosphate minerals. If dissolved uranium from the veins encountered environments that contained high levels of phosphate, various secondary uranyl phosphate minerals could have formed. Within area A, Precambrian diabase and early Tertiary latite dikes provided such environments. Gillerman (1968) stated that both diabasic and latitic dikes contain abnormal phosphate levels: an average 1.60% P_2O_5 in the diabase and 0.37% P_2O_5 in the latite of the Merry Widow Mine. The high-phosphate mafic dikes would first have been differentially altered by the hydrothermal solutions and then affected by acidic solutions from the oxidizing sulfides of the nearby veins. Both alteration and oxidation could have decomposed apatite in the mafic dikes and released quantities of phosphate ions. Hexavalent uranium released from the oxidizing veins could have precipitated as uranyl phosphate minerals upon encountering the mafic dikes and their available phosphate ions. Such mechanisms could have resulted in concentrations of uranyl phosphate minerals in mafic dikes where the dikes are cut by adjacent, oxidized, anomalously radioactive, hydrothermal veins. Uranyl phosphate minerals are found in area A where veins and mafic dikes are in proximity.

An additional factor to consider in the case of the secondary uranium minerals is that, although the uranyl phosphate minerals are stable in an oxidizing environment, they are somewhat soluble in aqueous solutions. This is because in a near-surface, slightly acidic environment, the dominant uranium-transporting complex is the $UO_2(HPO_4)_2^{-2}$ complex (Langmuir, 1978). Phosphate ions would be available both from the high phosphate mafic dikes and from weathering of the granite, which also contains phosphate (2,800 ppm P_2O_5, MLM 111). Therefore, every time water becomes available in the semiarid climate, uranium not only leaves the veins and is deposited as secondary uranyl phosphate minerals, but a minute amount of the secondary uranyl phosphate goes into solution and is transported away and dispersed. The secondary concentrations of uranium are, on a geologic time scale, only temporary time stoppages of the dispersion of uranium in the oxidizing zone from the hydrothermal veins. Langmuir (1978) also indicated that uranyl phosphate minerals are more insoluble in a more acidic environment. Because the most acidic environment in the area is where the sulfides of the veins are

being oxidized, the dispersion process becomes more effective as uranium gradually is transported from the vicinity of the veins.

The preceding discussion on the localization and size of the supergene uranium occurrences that are associated with the primary magmatic-hydrothermal occurrences has several implications. First, the only place secondary uranium concentrations can be expected is where high-phosphate mafic dikes are adjacent to the acidic, high-uranium environment of an oxidizing primary-uranium vein. Second, all the uranium present in secondary deposits was derived from the veins. Third, and most importantly, the amount of secondary minerals is not an accurate reflection of the amount of primary hydrothermal uranium once present in the oxidized portions of the veins. An unknown, but probably large, percentage of the uranium has been dispersed. Therefore, the uranium grades of the unoxidized portions of the hydrothermal veins are much higher than that indicated by the present grade of veins in the oxidized zone or the calculated grade of the veins derived by adding the amount of secondary uranium surrounding each vein to uranium remaining in each vein.

Delineation of Favorable Area

Primary controls on the extent of an area favorable for uranium deposition of the magmatic-hydrothermal type are related to the genesis of the uranium. In the case of magmatic-hydrothermal minerals and related secondary uranium minerals in area A, some conclusions regarding specific points of ore genesis are necessarily tentative. Therefore, some of the hypothetical controls in area A are also tentative.

One of the major ore controls, and, unfortunately, the most speculative, is the source of magmatic-hydrothermal ore solutions. As a working hypothesis, it is assumed that the rhyolitic intrusive bodies (dikes, plugs, and sills) that crop out in the region are genetically related to the uranium-source pluton. It is also assumed that dike and plug abundance decreases progressively away from the inferred pluton. As the greatest number of uranium occurrences cluster in the area of greatest dike and plug abundance, it is assumed that there is some positive correlation between outcrop frequency of rhyolite and intensity of magmatic-hydrothermal uranium minerals. Therefore, one guide to favorability is the abundance of rhyolite dikes. An area of abundant dikes is outline on Plate 11. The favorable area contains, and is adjacent to, the outlined area of abundant rhyolite dikes (Pl. 11).

The White Signal structural block of the Burro batholith has been structurally dropped a considerable distance along the generally northeast-trending Neglected-Sprouse-Copeland Fault (Pl. 11) relative to the Burro Peak-Tyrone block to the north (Gillerman, 1970). Displacement is uncertain, but topographic differences indicate that movement of thousands of feet is probable. Gillerman further stated that erosion of the upthrown block was severe, with an unknown, but probably great, thickness of rock removed. Therefore, it is suggested that the Neglected-Sprouse-Copeland Fault is the northern boundary of area A. It is suggested that the few scattered occurrences north of the Neglected-Sprouse-Copeland Fault (Hope No. 1, Occurrence 59) represent erosional remnants of occurrences and thus are likely to contain insufficient amounts of uranium to justify extending the boundary of area A.

The western boundary of area A is marked by the northwest-trending Taylor Fault, which forms the western boundary of the Big Burro Mountain block of the Burro batholith (Pl. 11). To the west of the fault is the Knights Peak graben. The eastern boundary of the White Signal structural block dips beneath a cover of Pleistocene to Holocene fan, terrace, and alluvial deposits. The eastern boundary of the block cannot therefore be determined, and the eastern boundary of area A is arbitrarily placed.

In summary, area A is bounded by faults on its north and west sides. Its southern boundary is drawn 3 km south of the southern extent of the area of abundant favorable structures (faults and dikes, Pl. 11). The eastern boundary of area A is under a cover of Tertiary basin fill, and the boundary is arbitrary. Area A has a surface area of 113.3 km^2. Depth from the surface to the favorable environment (surface of Precambrian bed rock) ranges from 0 m to approximately 100 m. The thickness of the favorable environment is the projected depth of the veins in the Precambrian country rock. Because there is an observed vein depth in excess of 150 m, and because there are several veins with lateral continuities greater than 1200 m, a projected vertical extent of veins in the favorable environment of 500 m is not unreasonable. Part of the land in area A is private, part is in the national forest, and part is state land.

AREA B: BLACK HAWK REGION

Area B is a roughly circular area in the northern part of the Burro Mountains batholith (Pl. 1). It is favorable for uranium deposits of the magmatic-hydrothermal type (Class 330). The host rocks are various Precambrian silicic intrusive rocks that are adjacent to a Laramide to post-Laramide hornblende monzonite porphyry intrusive. A Precambrian quartz diorite gneiss is particularly favorable. The outer rim of the hornblende monzonite porphyry intrusive is also favorable.

Area B is favorable because the host rock is structurally and chemically favorable for uranium deposition. Structural favorability is indicated by the numerous faults and shear zones that transect the area. Chemical favorability is indicated by silicification, sericitization, argillization, and iron staining, mainly near veins in the shear zones. The veins contain silica, carbonate, sulfides, anomalous fluorine, and anomalous amounts of heavy metals, all of which characterize magmatic-hydrothermal uranium deposits. Moreover, an HSSR uranium anomaly is present over the entire Burro Mountains batholith.

Area B contains seven uranium occurrences, two of which are described in uranium-occurrence reports (App. C). The occurrences are steeply dipping, imbricated, fissure veins, in which the most abundant metals are native silver, cobalt and nickel arsenides, and uraninite in a gangue of carbonates and silica. This type of uranium deposit, although rare in the United States, is similar to those at Great Bear Lake, Canada, and Joachimsthal, Czechoslavakia. Uranium mineralization occurred after Laramide time, but the source of ore solutions is unknown.

Geology of Favorable Area

Area B is structurally a part of the Willow Creek block (Pl. 10) of the Burro Mountains batholith (Gillerman, 1970). The batholith in the Willow Creek block is composed chiefly of the Burro Mountains granite, which contains inclusions and roof pendants of metamorphic rocks assigned (Hewitt, 1959) to the Bullard Peak and Ash Creek series (Fig. 3). The Precambrian rocks are intruded by numerous Laramide and post-Laramide intrusive bodies that range in composition from basaltic to rhyolitic. At the northern end of the Willow Creek block, the Precambrian rocks disappear beneath north-dipping Cretaceous sedimentary rocks and Tertiary volcanic rocks. Located in the volcanic rocks north of the northern boundary of the Precambrian rocks is the Schoolhouse Mountain Caldera (Pl. 10), a possible source of much of the Tertiary volcanic rocks of the area (Wahl, 1980).

The geology of area B has been discussed by Gillerman and Whitebread (1956), Hewitt (1959), and Gillerman (1964, 1968). Only factors relevant to uranium evaluation will be discussed in any detail here. The rocks are mainly quartz diorite gneiss of Precambrian age intruded by a stocklike mass of monzonite porphyry of Late Cretaceous to early Tertiary age (Pl. 7, 10).

The quartz diorite gneiss is a widespread phase of the Burro Mountains batholith and is believed to be somewhat older than the Burro Mountains granite (Gillerman, 1964). The gneiss is composed of 40% to 45% plagioclase (possibly andesine; Gillerman and Whitebread, 1956), 40% to 45% biotite, 5% to 10% quartz, and 2% to 3% hornblende. Traces of orthoclase, zircon, magnetite, and epidote are present. Phenocrysts of plagioclase and hornblende are present, and their long axes approximately parallel foliation of the rock. Biotite grains also parallel the foliation. The gneissic structure, which is believed to be a primary flow structure (Gillerman and Whitebread, 1956), strikes northeast and dips from 60° to the northwest to vertical. In places, feldspar is slightly altered to sericite, and biotite is altered to chlorite.

The monzonite porphyry intrudes the quartz diorite gneiss as a stocklike mass, as dikes, and as irregular apophyses throughout area B. In general, the monzonite porphyry consists of a grayish-white, fine-grained groundmass with abundant white, anhedral to subhedral feldspar crystals up to 0.5 cm in diameter. Black hornblende needles as much as 1 cm in length are common. Biotite is present in small variable amounts, and quartz is rare. In dikes, the rock has conspicuous feldspar phenocrysts in an aphanitic groundmass. The monzonite porphyry is variably altered. Where it is altered, the groundmass is aphanitic, the feldspars are soft and earthy, and the hornblende is argillized, chloritized, and epidotized (Gillerman and Whitebread, 1956). Pyrite, moderately to strongly oxidized to limonite, is present in altered areas of the porphyry. Gillerman and Whitebread (1956) assigned a Late Cretaceous to early Tertiary age to the intrusive body on the basis of comparisons with other intrusive bodies of that age in the region.

Area B is cut by four major fault systems, which trend northwest, northeast, west, and north. The regional structural trend is discussed more fully by Hewitt (1959) and in the discussion of area D, which is north of area B. Gillerman and Whitebread (1956) mapped the structure in the eastern part of area B, where most of the faults trend north, northeast, and east, and only a few trend to the northwest. The faults dip from 70° to 90°, with no

consistent direction of dip. In the eastern part of area B are two conspicuous, persistent, subparallel fault systems, which trend slightly east of north. Each system consists of a single, rather persistent fault, from which northeast- to east-trending faults branch.

Evidence of Favorability

Evidence for uranium mineralization in magmatic-hydrothermal-type systems within area B exists in seven reported uranium occurrences (Y29, Y30, 31, Y32, 33, Y34, Y35; Pl. 10). Uranium in area B occurs within uranium-bearing, nickel-cobalt-silver veins that are fracture fillings in Precambrian quartz diorite gneiss near intrusive monzonite porphyry. The uranium mineralization was magmatic-hydrothermal (Gillerman and Whitebread, 1956; Hewitt, 1959; Gillerman, 1964; Gillerman, 1968; Wahl, 1980). At the time of this investigation, all subsurface workings were inaccessible except for the upper part of the shaft at the Black Hawk Mine (Occurrence 31). However, Gillerman and Whitebread (1956) and Gillerman (1964, 1968) provided excellent descriptions of vein morphology, ore mineralogy, and ore paragenesis. A brief summary will be given here.

The veins occupy faults and fractures that have two major trends: north to north-northeast and northeast to east. The veins, which occur as fissure fillings along the faults, demonstrate only minor wall-rock replacement. Mineralization also occurred along open-fracture systems that are parallel to subparallel to the main fault zone. The subsidiary veins are horizontally and vertically discontinuous and pinch and join in an imbricating network. Most of the veins are 0.3 to 1 m wide in outcrop, but Gillerman and Whitebread (1956) reported that vein widths of 1 to 4 m in the subsurface are not uncommon. The maximum vein width reported (Gillerman, 1968) was 4.6 m in the Alhambra Mine (Occurrence 33). On the surface, individual veins range in length from 70 m to in excess of 300 m. At the Black Hawk Mine (Occurrence 31) at a depth of 236 m, the vein still contained excellent ore values (Gillerman and Whitebread, 1956) and showed no signs of pinching out. The ultimate depth to which mineralized veins extend is not known.

The veins are spatially associated with the monzonite porphyry that intrudes the Precambrian rocks of area B. The known veins (Gillerman and Whitebread, 1965) occur in a northeast- to southwest-trending belt within the Precambrian rocks adjacent to the intrusive contact. Some veins cut the outer margins of the monzonite porphyry, but they are small and weakly mineralized. Away from its margins the monzonite porphyry intrusive body seems barren of veins and therefore, except for its outer edges, is not considered a favorable environment. The veins cut all the various Precambrian rock types surrounding the porphyry, but the preferred host rock is the quartz diorite gneiss (Gillerman and Whitebread, 1956; Gillerman, 1968).

The veins contain native silver, argentite, nickel and cobalt sulfides and arsenides, uraninite, and minor amounts of other sulfides such as chalcopyrite, galena, stannite, and bismuthinite. Gangue minerals of the veins are dominantly carbonates (calcite, siderite, dolomite, rhodochrosite, manganocalcite, ankerite), quartz, chert, barite, and pyrite. Minor amounts of fluorite and hematite are also present. The ore occurs both as high-grade segregations and as disseminations of native silver and subsidiary nickel and

cobalt arsenides, as well as uraninite in the veins. In addition to Ag, As, Bi, Co, Cu, Ni, Pb, Sn, and Zn, which are present in the veins as identifiable minerals, anomalous amounts of Au, Cd, Li, Mo, Sc, W, and Zr have also been detected (Table 2). Fluorine contents of samples are low (Table 2). Gillerman (1968) reported that the Ni-Co arsenides form an outer zone within the veins, whereas silver is predominant in the core of the vein. Silver also seems more abundant in the upper parts of the veins, and nickel and cobalt increase with depth.

Uraninite was the only hypogene uranium mineral identified both in this study (MLM 127, MLM 132) and by other investigators. Uraninite occurs as disseminations (MLM 127, MLM 132), and Gillerman (1968) reported it occurring in the subsurface also as small masses, fracture coatings, and as distinct veinlets up to 2 in. wide. Gillerman reported that uranium is most prevalent where the ore is rich in Ni-Co arsenides and relatively scarce where silver is abundant. The positive correlation between increased cobalt and nickel contents and increased uranium values is illustrated by samples from the Black Hawk Mine (MLM 126, MLM 031, and MLM 132; Table 2). Given the observed association of uranium with cobalt and nickel, and the observed increase of cobalt and nickel with depth of the veins, Gillerman (1964) concluded that uranium content of the veins probably also increases with depth.

Supporting evidence for the proposed increase in uranium with depth is provided by uranium values at the Black Hawk Mine (Occurrence 31). The Black Hawk is the only occurrence in area B where even limited subsurface sampling of a vein is possible. In outcrop, the Black Hawk vein contains only 13 ppm cU_3O_8 (MLM 030). Radioactivity within the vein progressively increases with depth. At the deepest level accessible (50 m) the vein contained 640 ppm cU_3O_8 (MLM 126). The following evidence indicates that the increase of uranium with depth is a function of primary deposition and zonation rather than an apparent increase caused by oxidation and removal of uranium from the vein at the surface by weathering processes. Gillerman and Whitebread (1956) reported that oxidation of the veins occurs only in the near-surface environment; primary minerals are found within a few feet of the surface. Secondary uranium minerals do not occur where the veins crop out. Secondary uranium minerals would be present if the veins at the surface had contained primary uranium minerals. Unidentified secondary uranium minerals have been reported on the mine dumps where subsurface vein material has been oxidized.

Lack of significant amounts of uranium in the near-surface parts of the veins and limited subsurface information cause problems in the evaluation of the deeper veins. A primary source of data on the uranium content of the veins has been the old mine dumps. Gillerman and Whitebread (1965) reported a maximum of 0.24% cU_3O_8 from the Black Hawk Mine dump (Occurrence 31) and 0.15% cU_3O_8 from the Alhambra Mine dump (Occurrence 33). Data gained during this study include a water sample taken during the dewatering of the Black Hawk shaft (40 ppb cU_3O_8; MLM 103). A sample (MLM 031) from a dump along the main vein at the Black Hawk Mine contained 0.22% U_3O_8. Two samples taken from the Black Hawk shaft at a depth of 50 m contained 640 ppm cU_3O_8 (MLM 126) and 404 ppm cU_3O_8 (MLM 127). A dump sample from the Alhambra Mine, probably from the 150-ft level, contained the maximum value obtained in area B, 0.353% cU_3O_8 (MLM 132). Although Gillerman (1964, 1968) did not provide any analytical data, his descriptions of the abundance and habit of uraninite in the deeper levels of the Alhambra Mine indicated

TABLE 2. SELECTED ANALYSES OF ROCK SAMPLES FROM THE BLACK HAWK REGION

Sample no.	Analyses
MLM 030	369 ppm W, 899 ppm Zn, 13 ppm cU_3O_8
MLM 031	14 ppb Au, 583 ppm Ag, 5760 ppm As, 261 ppm Cd, 139 ppm Co, 151 ppm Cu, 182 ppm Li, 637 ppm Ni, 5160 ppm Pb, 107 ppm W, 9220 ppm Zn, 534 ppm Zr, 2200 ppm cU_3O_8
MLM 126	53 ppm Co, 92 ppm Cr, 259 ppm Cu, 27 ppm Mo, 69 ppm Ni, 7980 ppm Pb, 78 ppm Sc, 24 ppm Sn, 9230 ppm Zn, 185 ppm Zr, 551 ppm F, 640 ppm cU_3O_8
MLM 127	81 ppm Co, 109 ppm Cr, 15 ppm Mo, 266 ppm Ni, 1970 ppm Pb, 26 ppm Sc, 2790 ppm Zn, 150 ppm Zr, 935 ppm F, 404 ppm cU_3O_8
MLM 132	758 ppm Ag, 10300 ppm As, 1190 ppm Cd, 616 ppm Co, 279 ppm Cr, 82 ppm Mo, 733 ppm Ni, 2600 ppm Pb, 479ppm Sb, 3640 ppm Zr, 710 ppm F, 3530 ppm cU_3O_8

that uranium values exceeding several percent are not unlikely at depth. Thorium values are slightly elevated over background levels but commonly are low (maximum 42 ppm eTh, MLM 132). The dump samples, as would be expected, have a cU/eU ratio of >1. A sample from the Black Hawk shaft which had been exposed to mine water for years contained 404 ppm cU_3O_8 and 584 ppm eU (MLM 127).

The source and age of the uranium are uncertain. The time of magmatic-hydrothermal uranium mineralization within area B is unknown. It could have taken place during either of the two major periods of metallization in the region--the Laramide and the mid- to late Tertiary. Uranium is spatially associated with an intrusive body of monzonite porphyry that does not seem to be an adequate source for the hydrothermal solutions. No further conclusions than that are possible with the present data. It can be speculated that the margins of the intrusive body of monzonite porphyry could have acted as physical barriers or guides to ascending uranium-bearing hydrothermal solutions derived from some unknown intrusive body at depth.

The age of the monzonite porphyry is uncertain. On the basis of indirect geologic correlations and because of the presence of numerous Laramide intrusive bodies in the region, Gillerman and Whitebread (1956) assigned a Laramide age to the porphyry. Conversely, Wahl (1980) noted that the porphyry is chemically dissimilar to other Laramide intrusives in the area and is spatially located in the correct area (outer rim of Schoolhouse Mountain ring-fracture zone, Pl. 10) to be generally related to the mid-Tertiary episode of volcanism that formed the Schoolhouse Mountain Caldera (Pl. 10). In addition, Wahl (1980) pointed out that the porphyry is petrographically equivalent to an altered subvolcanic intrusive.

As the outer margin of the monzonite porphyry intrusive body is cut by a few veins, some of the veins, at least, are post-monzonite porphyry. Many workers, including Gillerman and Whitebread (1956) and Wahl (1980), have been impressed with the spatial association of the veins with the monzonite porphyry and have postulated a genetic association. Therefore, if the porphyry is mid-Tertiary in age and genetically associated with the Schoolhouse Mountain Caldera as Wahl (1980) suggested, then the uranium in area B would be genetically related to the mid-Tertiary episode of uranium mineralization which formed the magmatic-hydrothermal uranium deposits to the north (see discussion of favorable area D, Northern Big Burro and Little Burro Mountains).

However, chemical data regarding the porphyry do not indicate that the porphyry was the source of the hydrothermal solutions which formed the uranium occurrences of area B. The porphyry has low chemical-uranium, equivalent-uranium, and thorium contents--1 ppm eU, 3 ppm eTh, and less than 1 ppm cU_3O_8 (MLM 026). The Th/U ratio is low (3), and the cU/eU ratio is close to 1. A radiometric traverse of the porphyry indicates that these values are typical. Fluorine is low (<200 ppm), the Fe_2O_3-to-FeO ratio is low (0.53), and the index of igneous differentiation ($Na_2O + K_2O/Al_2O_3$) is low (0.58). These data do not meet the criteria that Mathews (1978a) listed as characteristic of intrusive bodies that have generated uranium-bearing hydrothermal solutions. Mathews (1978a) indicated that high uranium, thorium, and fluorine contents, a high Th/U ratio, a $Na_2O + K_2O/Al_2O_3$ ratio of greater than 1, and a high Fe_2O_3-to-FeO ratio are the characteristics of

an intrusive body which may have generated uranium-bearing magmatic-hydrothermal solutions. A cU/eU ratio of close to 1 indicates that the low uranium content of the porphyry is not due to loss of uranium caused by weather processes. Despite the spatial relationship between the uranium-bearing veins of area B and the intrusive porphyry, it seems that the porphyry was not the source of ore solutions.

Ore paragenesis (Gillerman, 1968), although uncertain, seems to indicate that uranium deposition followed deposition of silver, nickel, and cobalt arsenides and preceded sulfide deposition. Depositional mechanisms were probably related to decreasing oxygen fugacity of the solutions caused by decreases of temperature and pressure, or by destruction of uranium-transporting complexes by pH changes or by reactions between solutions and wall rocks. Gillerman (1968) suggested that both physical and chemical properties of the quartz diorite gneiss made it the preferred host rock. A favorable physical property of the gneiss was its response to fracturing, which resulted in larger open spaces along the faults than along faults in other rock types. Although replacement of wall rocks by the vein solutions was minor (Gillerman, 1968), the chemical effect of the gneiss on the ore depositional process is suggested by the alteration patterns. The gneiss, where cut by veins, is intensely argillized, sericitized, and, where uraninite is present, iron stained and cut by hematite veinlets. Wall-rock alteration is much less intense where the veins cut other rock types.

Favorable Area

The main guide on the extent of area B is the empirical spatial relationship between the veins and the monzonite porphyry intrusive. Although uranium-bearing veins are known to be present primarily on the southeastern side of the porphyry, there is no known genetic reason why similar veins could not occur on the other sides. The distance outward from the porphyry into the Precambrian country rock that is favorable was estimated from the mapped vein density on the southeast side of the intrusion (Gillerman and Whitebread, 1956). Gillerman and Whitebread (1956) indicated that the greatest number of veins and the veins with the greatest amount of ore minerals are located within approximately 1000 m of the intrusive contact. The outer margin of area B is arbitrarily drawn 2000 m from the intrusive contact. The bulk of the porphyry is unfavorable for uranium deposition, but some veins are known to occur along the outer margin of the porphyry. The inner boundary of area B is arbitrarily drawn approximately 300 m on the porphyry side of the porphyry intrusive contact. The doughnut shape of area B around the porphyry is further modified by three factors: First, the Precambrian metamorphic rocks of the Bullard Peak series are unfavorable. Second, north- to northeast-trending favorable structures are more likely to occur on the east and west sides of the porphyry than on the north and south sides. Third, there is a block of Precambrian quartz diorite gneiss (perhaps a xenolith) within the porphyry that is also considered favorable (Pl. 10).

Area B covers 10.9 km^2, and the favorable environment is at the surface. Thickness of the favorable environment is the projected depth of the veins. A vein (Occurrence 31) is known to reach a depth of 200 m with no indications of decrease in vein size or intensity of mineralization. Projected vein depth is estimated at 500 m. Land status of area B is national forest and patented land.

AREA C: LATE CENOZOIC LACUSTRINE ROCKS OF THE UPPER SAFFORD BASIN

Area C (Pl. 1), which is in the southeastern part of the upper Safford Basin, is favorable for uranium deposits in volcaniclastic lacustrine rocks (Class 540). There, favorable mudstone and carbonate host rocks have, because of included organic material and complex interfingering relationships among permeable beds and impervious strata, a capacity to trap, reduce, and preserve uranium. Uranium may have been derived from tuffaceous material in the host sediments, from interbedded vitric tuffs, or from the predominantly felsic and intermediate volcanic rocks of the adjacent mountains. Complex stratigraphic relationships among host sediments and transmissive beds, numerous local depressions in the bedrock surface, and the presence of vanadium in the host sediments favor a preservation of significant amounts of uranium in the near-surface, largely oxidized environment.

Geology of the Upper Safford Basin

The upper Safford Basin is a depositional subbasin of the extensive San Simon Valley (Harbour, 1966), a major northwest-trending structural trough formed during the late Cenozoic Basin and Range disturbance. The upper Safford Basin is bounded on the north and east by the Peloncillo and Whitlock Mountains, which are composed mainly of intermediate- to felsic-composition volcanic rocks of Tertiary age. On the west, the basin is flanked by the Pinaleno Mountains, a range consisting predominantly of Precambrian metasedimentary and meta-igneous rocks. The basin, open to the northwest and south, merges with a series of poorly connected basins that are aligned roughly parallel to the Basin and Range-Colorado Plateau boundary. Feth and Hem (1963) pointed out that this series of basins, whose overall distribution extends northwestward about 800 km from Chihuahua, Mexico, to the mouth of the Grand Canyon, are in part filled with thick lacustrine deposits.

The upper Safford Basin contains relatively flat-lying basin-fill deposits, more than 1200 m thick, which range in age from late Miocene to early Pleistocene. The lower part of the basin fill, which is largely unexposed, consists of basal conglomerate that grades both upward and laterally into nonmarine evaporites and green, red, and yellow claystone and siltstone (Harbour, 1966). The upper portion of the basin fill consists of extensive conglomerate to sandy-silt deposits of fluvial, alluvial-fan, and mudflow origins. Occurring near the top of the upper basin-fill sequence is an areally restricted sequence of light-colored, fine-grained tuffaceous rocks (Harbour, 1966). In addition to being quite distinctive lithologically, these tuffaceous rocks are also uranium bearing.

Stratigraphy and Lithology of Favorable Tuffaceous Lacustrine Rocks

An interstratified sequence of tuffaceous mudstone, carbonate, and diatomite and minor sandstone and vitric tuff extends throughout the northern and western piedmont of the Whitlock Mountain range (Harbour, 1966). This Blancan (late Pliocene) age (Lindsay, 1978) tuffaceous assemblage is particularly well exposed in the Dry Mountain-Ill Ranch area, at the northwestern end of the Whitlock range (Clay, 1960; Seff, 1962). There, the tuffaceous beds rest directly on Tertiary rhyolitic and minor andesitic bed

rock, which is widely exposed in the adjacent Whitlock range (Wynn, 1981). Considerable relief of this bedrock surface (Pl. 12) accounts for rapid thickness changes in the overlying tuffaceous strata; surface exposures vary from a few meters thick in the vicinity of partially buried bedrock knobs to more than 50 m thick in areas a short distance away from the protuberances. Maximum thickness of the tuffaceous sequence is estimated at about 100 m.

The petrology and stratigraphy of the tuffaceous sediments have been discussed at length by Clay (1960) and Seff (1962). Overall, the tuffaceous assemblage is dominated by green, brown, and reddish-brown mudstone units. These relatively impervious mudstones commonly grade into, and are complexly interstratified with, more permeable, commonly highly fractured, grayish-white micritic carbonates and highly porous and permeable diatomite beds. Thick-bedded or nodular chert occurs throughout the stratigraphic section. All rock types are characterized by a significant tuffaceous component, which is partially devitrified and commonly altered to montmorillonite or zeolites. Moreover, all rock types also contain angular silt- to fine-sand-sized grains of quartz, sanidine, plagioclase, and altered volcanic rock fragments that reflect the nearby volcanic provenance. Carbonaceous material is preserved in small amounts in the mudstone units, but impressions of plant detritus and silicified root and stem casts are commonly found throughout the mudstone, carbonate, and diatomite beds. The tuffaceous mudstone-carbonate-diatomite assemblage grades laterally (basinward) into mostly light-brown to light-reddish-brown siltstone, fine-grained sandstone, and pebbly sandstone, a rock association that characterizes the exposed basin fill throughout much of upper Safford Basin. Near the range front, the tuffaceous rocks grade downward into relatively darker colored, coarse- to fine-grained, angular, poorly sorted, locally derived volcaniclastic rocks.

The light-colored tuffaceous rocks were deposited within an areally restricted lacustrine environment under relatively cool and humid paleo-climatic conditions (Harbour, 1966; Seff, 1962). The thick (up to 6 m), laterally persistent carbonate beds with abundant aquatic and minor terrestrial invertebrate fossils, in conjunction with the thick (10 m) diatomites, provide good evidence for a well-developed lacustrine environment. The presence of interfingering and interbedded mudstones, with abundant evidence of plant material, indicates that paludal (or marsh) environments co-existed or alternated with the lacustrine setting.

Evidence of Uranium Favorability

Possible uranium source rocks for the lacustrine-paludal rocks of the upper Safford Basin include rhyolitic and minor intermediate volcanic rocks in the adjacent Whitlock Mountains, vitric air-fall tuffs interbedded in the host section, and tuffaceous material within the host and associated sediments. Rhyolite, which is exposed as bedrock knobs and in the adjacent range, is theoretically a good source of uranium. However, on the basis of calculated cU_3O_8/eU_3O_8 ratios (MLM 332, MLM 335, Table 3), the rhyolite does not appear to have been depleted of much of its original uranium. Interbedded air-fall tuffs of relatively minor volume appear fresh and probably also still contain most of their original uranium (MLM 330, Table 3). A more plausible uranium source is the tuffaceous detritus within the host and associated sedimentary rocks. Petrographic studies of the lacustrine and associated

TABLE 3. SELECTED ANALYTICAL AND PETROGRAPHIC DATA FOR UPPER SAFFORD BASIN LACUSTRINE-PALUDAL ROCKS SAMPLES AND ASSOCIATED VOLCANIC BEDROCK SAMPLES

Sample no.	Rock name	Chemical U_3O_8 (ppm)	Radiometric eU (ppm)	cU_3O_8/eU_3O_8	Organic carbon (%)	Significant Associated elements (ppm)
MLM 201	fossiliferous micritic carbonate	34	13	2.30	0.18	Li(1620), P(854), V(648),W(352)
MLM 203	diatomite	140	105	1.10		Mo(13, V(586)
MLM 204	fossiliferous micritic carbonate	443	236	1.10		Li(5700), V(573)
MLM 205	claystone	750	476	1.30	0.04	V(643)
MLM 206	mudstone	45	51	0.80		V(416)
MLM 207	mudstone	95	108	0.70	0.31	Mo(70, V(562)
MLM 208	diatomite	72	38	1.60		V(483)
MLM 329	chert	130	144	0.80	0.10	V(185)
MLM 330	water laid(?) tuff	4	3	1.10		Li(793)
MLM 331	tuffaceous, diatomaceous arkosic aranite	9	25	0.30		V(155)
MLM 332	vitric crystal tuff (vitrophyre)	6	7	0.80		
MLM 333	fossiliferous micritic carbonate	910	566	1.40	0.10	V(135)
MLM 334	mudstone	7	8	0.80	0.08	Li(3230)
MLM 335	rhyolite	6	7	0.80		
MLM 342	micritic carbonate	152	170	0.80	0.18	Li(5300), W(296)

rocks show that altered tuffaceous material is a major constituent of all rocks within the assemblage. Furthermore, the presence in most sediments of large amounts of montmorillonite, which is commonly derived from the alteration of volcanic material, is indicative of extensive alteration of the detrital tuffaceous component. Moreover, the widespread occurrence of chert suggests a once-plentiful supply of silica and provides yet further evidence for extensive devitrification and alteration of the tuffaceous detritus.

Devitrification during diagenesis of the sediments may have, in addition to releasing large amounts of silica, released large amounts of uranium. Interstitial water expelled by the compaction and dewatering of the largely calcareous sediments was probably alkaline, which would have made it a good transfer medium for hexavalent uranium (DeVoto, 1978). Uranium in solution could have been readily transported through porous and permeable diatomite, tuff, sandstone, and brecciated carbonate units that are interbedded with, and interfinger with, host mudstone and carbonate units. Differential permeability, resulting from the interfingering of relatively porous permeable units with less pervious mudstone and, in some cases, carbonate beds, may impede solution flow, thereby favoring the concentration and precipitation of uranium where a suitable reductant is encountered.

The presence of carbonaceous material in some mudstone beds and the common and widespread occurrence of leaf and root impressions and silicified plant casts in all surface rock types indicate an abundance of plant material in the paleolacustrine and paludal settings. Moreover, organic-carbon analyses of the various exposed rock types confirm the presence of minor amounts (0.04% to 0.31%) of organic carbon (Table 3) in the oxidized, near-surface environment. Limited drilling by private industry in the area encountered minor amounts of organic material in the subsurface. Pyrite and pyrite-replaced plant stems were also encountered at depth in greenish- to brownish-gray mudstone units. This suggests that reduced environments exist, at least locally, in the subsurface.

Uranium would be quite mobile in the highly oxidized, near-surface environment. However, appreciable amounts of vanadium in the host sediments (Table 3) effectively stabilize some of the uranium as carnotite in the oxidized zone. It is interesting to note, however, that studies to determine the relationship between chemical and equivalent U_3O_8 (Table 3) reveal that uranium has undergone appreciable remobilization. Remobilization may favor a sort of "multiple migration-accretion" situation (Gruner, 1956), with uranium becoming concentrated and ultimately preserved within favorable stratigraphic or structural settings.

As discussed, rapid facies changes characterize the tuffaceous lacustrine-paludal rock assemblage. The complex interfingering of permeable strata and impervious beds may provide stratigraphic "traps" favoring both uranium precipitation and preservation. The highly irregular bedrock surface (as diagrammatically shown in Pl. 12) may also increase the likelihood of uranium concentration and preservation. Uranium, possibly remobilized from surrounding areas, could become impounded in favorable host sediments within local bedrock depressions. There, the uranium might be less exposed to oxygenated ground waters and less likely to be dispersed after precipitation. Structural control of mineralization may also have been important in areas of small-scale, nontectonic folds and slump features, such as those developed at

the White Bluffs uranium prospect (Occurrence 16). Such structures may have enhanced transmissivity and provided sites for uranium precipitation among associated fractures.

There is, in the Dry Mountain-111 Ranch area, good evidence for widespread infiltration of uranium-bearing solutions into the lacustrine-paludal rock assemblage. Anomalous amounts of uranium occur in a wide variety of the exposed fine-grained or finely crystalline rocks: Uranium contents of sampled mudstones and associated claystones range from 45 to 750 ppm U_3O_8 (average of three samples: 297 ppm U_3O_8); those of the micritic carbonates, 34 to 910 ppm U_3O_8 (average of thre samples: 79 ppm U_3O_8); and that of a single sample of chert, 130 ppm U_3O_8. Anomalously radioactive beds, which are well exposed at the White Bluffs, Flat Tire, and other unnamed occurrences (Occurrences 16, 17, 18, and 19), average about 0.5 to 1.0 m thick. In and adjacent to these uranium occurrences, the radioactive strata may be traced laterally for as much as 25 m. Anomalous zones may have even greater lateral extents, but extensive slope debris, which can effectively attenuate radioactivity, commonly covers the interval of interest.

In the subsurface, low-grade (less than 0.01% equivalent U_3O_8) anomalous radioactivity, over 0.5- to 1-m-thick intervals, was encountered in greenish-gray mudstone units at various depths. In view of the high uranium mobility observed in the surface rocks, significant amounts of uranium may have been transported downdip. Widespread evidence of disequilibrium in surface rocks, the relative youth of uraniferous sediments, and thus the relatively late mineralization may indicate that uranium in the subsurface may be highly out of equilibrium with its daughter products in favor of chemical U_3O_8. Because of the relatively wide spacing of drill holes, the lateral extent of the anomalous radioactivity in the subsurface is not known.

Carnotite is the only uranium mineral observed in the tuffaceous lacustrine assemblage. It is commonly associated with limonite and (or) manganese oxide and is found as efflorescent coatings on outcrop and fracture surfaces. Petrographic study shows that the carnotite may be disseminated throughout the rock matrix and may coat clasts and fill fossil shells as well. In addition to vanadium, uraniferous samples are commonly enriched in lithium (Table 3). Other elements are also enriched in anomalously uraniferous samples (Table 3), but no characteristic elemental association is apparent.

Favorable Area

An area favorable for uranium associated with volcaniclastic lacustrine environments is defined as the combined surface distribution of the tuffaceous lacustrine-paludal rocks (Harbour, 1966) and the estimated subsurface extent of the rocks (Pl. 1, area C). The favorable environment is estimated to extend over a combined surface and subsurface area totaling about 139 km^2; composite thickness of the favorable beds is about 12 m. Volume of the favorable environment is therefore estimated to be 1.7 km^3. The subsurface portion of the favorable environment is estimated to extend to depths no greater than 100 m. Most of the land in the favorable area is public domain administered by the Bureau of Land Management.

AREA D: NORTHERN BIG BURRO AND LITTLE BURRO MOUNTAINS

An east-west-trending strip at the northern edge of the Burro Mountains batholith (area D1, Pl. 1) and the fault block of the Burro Mountains batholith in the adjacent Little Burro Mountains (area D2, Pl. 1) are favorable for uranium deposits of the magmatic-hydrothermal type (Class 330). The favorable host rocks are Burro Mountains granite and Beartooth Quartzite of Late Cretaceous age, which in area D unconformably overlies the granite.

Area D is favorable because the host rock is structurally and chemically favorable for uranium deposition. Structural favorability is indicated by numerous faults and shear zones that transect the area. Chemical favorability is indicated by silicification, sericitization, argillization, and iron staining, mainly near veins in shear zones. The veins contain silica, sulfides, anomalous fluorine, and anomalous amounts of heavy metals, all of which are characteristic of magmatic-hydrothermal uranium deposits. Moreover, an HSSR uranium anomaly is present over the entire Burro Mountains batholith. The processes of uranium concentration and deposition demonstrably occurred, as area D contains 10 uranium occurrences (App. C).

The uranium occurrences are characterized by primary uranium minerals hosted by shear zones in granite. Where the shears cut areas where Beartooth Quartzite overlies the granite, mineralization occurred along the shear in the granite, along the shear a short distance up into the overlying Beartooth Quartzite, and along the unconformity between the granite and the quartzite. The uranium mineralization is posulated to have occurred during mid- to late Tertiary time, during volcanism and concomitant caldera development, which occurred just to the north of area D.

Geology of Favorable Area

The northern Burro Mountains are structurally part of the Willow Creek block, which is the northern block of the larger Big Burro Mountains batholith (Gillerman, 1970). The northern Willow Creek block consists mainly of Burro Mountains granite, which intrudes the Bullard Peak and Ash Creek series, and is intruded by numerous Laramide and post-Laramide intrusive bodies that range in composition from basaltic to rhyolitic. At the north end of the range (Pl. 10), the Precambrian rocks disappear beneath north-dipping Cretaceous rocks and Tertiary volcanic rocks. Located in the volcanic rocks north of the northern boundary of the Precambrian rocks is the Schoolhouse Mountain Caldera (Pl. 10), the suggested source of the Tertiary volcanics of the area (Wahl, 1980). To the east, the Big Burro Mountain block dips below a southeast-trending valley filled with Pleistocene gravels. Approximately 5 km to the east is the southeast-trending Mangas fault that dips 60° to 80° southwest and has an estimated vertical displacement of at least 1,500 ft (Gillerman, 1964). Uplift along the fault caused the Little Burro Mountains (Pl. 10).

The Little Burro Mountains are a north-northeast- to south-southwest-trending, tilted fault block of Precambrian Burro Mountains granite and Bullard Peak metamorphic rocks overlain by Cretaceous sedimentary rocks and a thick sequence of Tertiary volcanic rocks. The sediments and volcanics dip 10° to 25° to the northeast and reflect the tilting of the fault block. At

the southern end of the Little Burros is an intrusive mass of altered quartz monzonite that is probably genetically related to the Tyrone stock (Gillerman, 1964).

The host rocks of the favorable environment in both areas D1 and D2 (Pl. 1) are undifferentiated Precambrian Burro Mountains granite and, where present, Upper Cretaceous Beartooth Quartzite. The Burro Mountains granite was described in detail by Hewitt (1959), Gillerman (1964, 1967, 1968, 1970), Hedlund (1978c, 1978d, 1978e), and elsewhere in this text (area A, White Signal region). In general, the Burro Mountains granite is a composite rock unit; although granite is the major rock type, tonalite, granodiorite, pegmatite, and aplite occur locally as separate intrusions and gradational facies. The granite is typically leucocratic, light pinkish gray to tan, medium to coarse grained, and has a hypidiomorphic-granular to xenomorphic-granular texture that is locally porphyritic.

The Upper Cretaceous Beartooth Quartzite unconformably overlies the Precambrian Burro Mountains granite and is exposed in a discontinuous band trending west to east across the northern Burro batholith and the Little Burro Mountains just south of the southerly extent of the younger Tertiary volcanic rocks (Pl. 10). The Beartooth forms dip slopes, caps hills, and outlines tilted fault blocks. The formation is mainly a fine- to medium-grained, gray, thick-bedded, well-sorted orthoquartzite. The quartzite is typically well stratified and locally contains small-scale cross-bedding. A basal arkose or arkosic conglomerate is present locally, and 5- to 30-cm-thick, sandy shale beds and thicker sandstone beds are interbedded with 0.3- to 4-m-thick quartzite beds. Although carbonaceous material has not been reported in the literature, it has been identified in the basal portion of the Beartooth in areas D1 and D2 (Occurrences 27 and 36). Gillerman (1964) reported a maximum measured thickness of the Beartooth in area D of 36 m. The formation was deposited in a trangressive, epicontinental sea. The Beartooth is conformably overlain by the Upper Cretaceous Colorado Shale. The Cretaceous rock units within and north of area D are overlain by Tertiary volcanic rocks.

Area D is cut by four major fault systems which trend northwest, northeast, west, and north. The most abundant faults are the northwest-trending faults, which range in strike from N. 15° W. to N. 60° W. Most strike N. 40° W. to N. 55° W., and most dips range from 41° to 85° to the southwest (Hewitt, 1959). The northeast-trending faults are the next most abundant faults. They generally strike from N. 20° E. to N. 75° E. Some dip up to 65° SE. and some dip up to 68° NW. The north- and west-trending faults are much less abundant, and they commonly dip steeply. The west-trending faults dip steeply to the north, and the north-trending faults dip almost vertically. Brecciation and (or) development of shear zones along the faults is common in faults of all four orientations. Movement of the faults has tilted the large blocks that lie between them. Cretaceous sediments often cap such fault blocks. Displacement along the faults has been measured in excess of 215 m (Hewitt, 1959). Hewitt (1959) interpreted the faults as having originated in the Laramide, perhaps following the prevailing structural grain of the Precambrian rocks, and having undergone later movements during the mid- to late Tertiary. The fault sets range in age, from oldest to youngest, as follows: northeast-, northwest-, west-, and north-trending (Hewitt, 1959).

Evidence of Favorability

That a mechanism for the concentration and deposition of uranium in magmatic-hydrothermal-type systems within area D exists is shown by the 10 reported uranium occurrences (Pl. 10), 8 of which are described in Appendix C (Occurrence 20, 22, 23, 24, 27, 28, 36, and 37). Occurrences 20, Y21, 22, 23, 24, Y26, 27, and 28 are located in area D1, and Occurrences 36 and 27 are located in area D2.

Morphology of the uranium occurrences is threefold: tabular vein (Sandy Group, Occurrence Y21; Springfield Claims, Occurrence 22; and May Day No. 1 and No. 2, Occurrence 24), stratiform (Prince Albert No. 2, Occurrence 28, and Tunoco Mining Company Claims, Occurrence 37), and a combination of tabular vein and stratiform (Purple Rock Mine, Occurrence 20; Union Hill Claim, Occurrence 23; and Oil Center Tool Co. Claims, Occurrence 36). Uranium present in the tabular-vein habit is hosted by fault and shear zones of all four fault orientations discussed earlier. Occurrences 27 and 36 are within northwest-trending faults; Occurrences 24 and 20 are within northeast-trending fault systems. Occurrence 23 is hosted by a west-trending fault zone, and Occurrence 22 is hosted by a north-trending shear. The tabular-vein habit occurs by itself only in those parts of area D where the Precambrian rocks are exposed and not covered by Cenozoic sediments. Host rocks of the tabular-vein occurrences are both Precambrian Burro Mountains granite and Precambrian Bullard Peak series metamorphic rocks. However, the preferred host is the granite; occurrences in the metamorphic rocks are minor, and the metamorphic rocks are not considered a favorable depositional environment.

The combination tabular-vein and stratiform occurrences are found where the Beartooth Quartzite and Colorado Shale unconformably overlie Precambrian granite or are brought into fault contact with the granite. Mineralization occurred along the shear, extended a short distance (usually less than 15 m) into the Beartooth along the shear, and spread laterally along the unconformity between the granite and overlying Beartooth. Lateral mineralization along the contact occurred primarily within the Beartooth above the contact, but mineralization also occurred in the granite below the contact. Mineralization also occurred in some places where the Cenozoic sediments were brought into fault contact with the granite. Mineralization occurred along the shear and spread laterally through the Cenozoic sediments in fault contact.

The stratiform occurrences are found along the unconformity between Burro Mountains granite and overlying Beartooth Quartzite. Anomalous radioactivity extends up from the contact into the Beartooth usually less than 5 m and extends below into the granite usually less than 3 m. Field relationships indicate that the stratiform occurrences are, or once were, part of the combination type of occurrences. The mineralized shear is either hidden or is located a short distance away. Uranium mineralization in the stratiform portions of the occurrences hosted by Beartooth Quartzite occurred preferentially in beds of sandstone, rather than in quartzite, and in shaly beds (Occurrence 27).

Field relationships indicate that all three habits of uranium mineralization in area D are genetically related. The most fully developed deposit morphology is where a mineralized shear cuts granite overlain by the

Beartooth Quartzite. A combination tabular-vein and stratiform deposit is then developed. Where the Beartooth is not present, mineralization occurred as tabular-vein deposits in the granite. At the two stratiform occurrences, field investigations showed in each case that, although a mineralized shear in the underlying granite did not actually intersect the stratiform occurrence, the veins were nearby.

The deposits were formed by ascending hydrothermal solutions rather than by descending supergene solutions. A hydrothermal origin is indicated by deposit morphology, heavy-metal trace-element associations and zonation patterns, alteration patterns, and ore mineralogy. These factors are discussed below. As described earlier, uranium along a shear zone cutting granite and overlying Beartooth Quartzite was not observed to extend along the shear more than 10 to 50 m into the Beartooth. The Colorado Shale, which overlies the Beartooth, was never observed to have been mineralized along such a shear zone. Descending, supergene solutions would have mineralized the Colorado Shale. Only ascending, magmatic-hydrothermal solutions could have resulted in the mineralization pattern observed.

Alteration is variable. Granite in and immediately adjacent to mineralized shears is variably silicified, iron stained, and intensely sericitized (Occurrences 20, 23). Granite along the unconformity of stratiform portions of the deposits is sericitized and iron stained for a depth of several meters (Occurrences 28, 37). The Beartooth Quartzite, in both shears and stratiform portions of the deposits, is less altered than the granite. Silicification and iron staining (Occurrences 27, 36) are the only alterations.

Vein development in the occurrences ranges from poor to excellent. Often, no megascopic vein is observable in the altered, mineralized, shear zone (Occurrences 23, 27), and the trace of the vein is identified only by a linear zone of intense alteration. A network of limonite-hematite and silica veinlets have been identified in portions of some shears (Occurrence 22). Only at the Purple Rock Mine (Occurrence 30) have well-defined veins been observed. No vein development except limonite veinlets (Occurrence 27) has been observed in the stratiform portions of the deposits.

The primary uranium mineral of the area D occurrences appears to be uraninite, which was identified at two locations (MLM 083, Occurrence 23; MLM 116, Occurrence 20). Uraninite is associated with pyrite at both locations. Uranyl phosphates, uranyl silicates (MLM 116, Occurrence 20), and kasolite (lead uranyl silicate hydroxide; MLM 141, Occurrence 37) were identified. The highest grade of uranium found in area D is in a shear zone where granite and quartzite are in fault contact (0.783% cU_3O_8, MLM 083). The composite tabular-vein/stratiform deposit morphology contains four potential environments of deposition. They are sheared granite, sheared quartzite, quartzite above the unconformity, and granite below the unconformity. Three of the potential depositional sites are known to contain close to or more than 0.1% uranium. A shear zone in granite contained a vein with 950 ppm cU_3O_8 (MLM 116). A shear zone in Beartooth Quartzite contain 1,140 ppm cU_3O_8 (MLM 141). Beartooth Quartzite in a stratabound portion of a deposit contained 1,240 ppm cU_3O_8 (MLM 142). However, the maximum amount of uranium detected in Precambrian granite below the unconformity in the stratiform portion of an occurrence was 163 ppm cU_3O_8 (MLM 082). The

variability of disequilibrium is indicated by cU/eU ratios. The ratios range from less than 1 to 1 to greater than 1. Thorium values are low (58 ppm eTh, MLM 083) but elevated over background levels (21 ppm eTh, MLM 092). The presence of primary uraninite and the fact that thorium levels are elevated above background levels support a magmatic-hydrothermal origin. The variation of cU/eU ratios is consistent with variable oxidization of primary hydrothermal mineralization and the formation of limited amounts of secondary uranium minerals.

The heavy-metal trace-element suite present in the occurrences is also consistent with a magmatic-hydrothermal origin. Anomalous amounts of Ag, Au, Bi, Cr, Cu, Mo, Ni, Pb, Sb, Sc, Sn, W, Y, Z, and Zr have been detected (MLM 083, 090, 114, 115, 117, 141, 142; App. B). There appears to be a crude zonation of precious metals from east to west across area D, although the significance is not known. Silver was detected only in the east (49 ppm Ag, MLM 142; Occurrence 36). Gold, although anomalous in the central portion of area D (56 ppm Au, MLM 117, Occurrence 22), has the highest values in the far western portion of area D (1,180 ppb Au, MLM 116, Occurrence 20).

Fluorine, another favorable criterion for uranium occurrences of the magmatic-hydrothermal type, is associated with the uranium of area D. Although fluorite was megascopically observed only in the uranium occurrences of the western part of area D (Occurrence 20), anomalous amounts of fluorine were present in the other occurrences. The levels of fluorine, although moderate (600 to 1,200 ppm F), are anomalous when compared to background levels of fluorine in the Precambrian rocks of the Burro batholith, which contain from less than 200 to 300 ppm fluorine. In addition to having anomalous fluorine contents, all occurrences are near vein-type fluorite occurrences that are in the same types of faults as are the uranium occurrences. From east to west across area D, uranium Occurrences 36 and 37 in the Little Burro Mountains (area D2) are closely associated with the Ace High fluorite occurrence (Gillerman, 1964). Occurrences 22, 23, 24, 27, and 28 (Pl. 10) are closely associated with the Purple Heart, Reed Mine, and Rambling Rudy fluorite occurrences (Gillerman, 1964). In the far west of area D, Occurrence 29 is not only hosted by veins with observable fluorite, but is closely associated with numerous fluorite occurrences, including the Great Eagle fluorspar mine (Gillerman, 1964). These fluorite occurrences commonly contain white and light-green fluorite that in outcrop is not anomalously radioactive, but there are several indications that the fluorite and uranium mineralization are genetically related.

The most important indication of a genetic relationship is the association of uranium and fluorite in the same veins at the Purple Rock Mine (Occurrence 20) and the surrounding region in the western part of area D. Petrographic studies by Hewitt (1959) of the fluorite veins demonstrated at least two successive episodes of fluorite mineralization. The first episode deposited clear to light-green fluorite devoid of associated uranium. The second episode deposited substantially less fluorine than the first. In the area of Occurrence 20, Hewitt (1959) described veins that contain only nonradioactive green fluorite, veins that contain only radioactive purple fluorite, and veins that contain both. It seems clear that there were two nearly contemporaneous episodes of fluorite mineralization, the latter of which deposited uranium. Age of the fluorite mineralization is interpreted to be mid- to late Tertiary (Hewitt, 1959; Gillerman, 1964; Gillerman, 1968). It

seems reasonable to postulate that the uranium in the central (Occurrences 22, 23, 24, 27, 28) and eastern (Occurrences 36 and 37) parts of area D was also derived from the later period of fluorine mineralization. Although all the uranium occurrences contain anomalous fluorine, only in the western region of area D is radioactive purple fluorite megascopically visible. Information from surface exposures indicates that only in the western region did the two episodes of fluorine mineralization occasionally occur within the same veins.

Uranium mineralization within area D was of the magmatic-hydrothermal type and occurred nearly contemporaneously with, and was probably genetically associated with, a major episode of fluorite mineralization. The time of uranium mineralization was probably mid- to late Tertiary. The nature and presumed time of the mineralization, together with its spatial relationship to the mid-Tertiary volcanic rocks to the north, suggest a genetic relationship between the mid-Tertiary vulcanism and the nearby magmatic-hydrothermal uranium mineralization.

In recent years, the mechanisms by which uranium-bearing hydrothermal solutions can be generated by the process of silicic igneous differentiation in volcanic sequences with caldera development has been extensively investigated and documented (see Steven and others, 1974; Elston, 1978; Rytuba and others, 1979; Burt and Sheridan, 1980). Typically, the magmatic-hydrothermal mineralization occurred in broad ring-fracture zones surrounding calderas. Wahl (1980) mapped the Schoolhouse Mountain Caldera as being just north of area D1, and he indicated that the faults in which uranium is present are part of the ring-fracture zone of the caldera (Pl. 10).

Wahl (1980) further postulated that the uranium- and fluorine-bearing solutions that formed the occurrences in area D1 were derived from caldera-related silicic magmatic differentiation. The uranium-bearing hydrothermal solutions traveled outward from the caldera region and ascended through the four pervasive sets of fractures within area D1. As the solutions ascended, cooling and pressure loss probably resulted in a gradual decrease in the oxygen fugacity of the transporting solutions, causing reduction of soluble hexavalent uranium to insoluble tetravalent uranium in uraninite. Given the indicated fluorine content of the hydrothermal solutions, an alternative precipitation mechanism would be the destruction of uranium fluoride complexes because of pH or temperature changes or solution/wall-rock reactions (DeVoto, 1978). In either case, uranium would be deposited as uraninite in the shear zones. If the shear zones in which the ore solutions were traveling cut granite that was overlain by Beartooth Quartzite, the solutions would have moved up into the shear and laterally away from the shear into the Beartooth along the unconformity between the granite and quartzite. The solutions would also have moved preferentially into the Beartooth where the shear intersected sandstone beds that had greater relative permeability than quartzite.

Two depositional mechanisms may have operated to deposit uranium in the Beartooth. First, as the Beartooth is a much more brittle unit than the underlying granite, shearing would have severely shattered and brecciated the quartzite. When the hydrothermal solutions moved upward along the shear in the granite, pressure loss would probably have been gradual, and uranium deposition would have been progressive, as was discussed earlier. However, when the solutions encountered the highly fractured and brecciated environment where the shear intersected the base of the Beartooth, pressure loss was

probably rapid, and there was probably a consequent rapid deposition of the uranium remaining in the hydrothermal solutions. As the solutions moved farther upward into the Beartooth along the shear, available uranium in the ore solutions was depleted and uranium deposition ceased. Such a process would account for the observed lack of uranium minerals within the shear zone for any distance up into the Beartooth.

Pressure, temperature, and probably pH remained relatively constant in the ore solutions that moved laterally into the Beartooth away from the shear, and so a second depositional mechanism is proposed for this case. This mechanism is reduction by organic matter within the Beartooth. As discussed in the section on the general geology of area D, the basal portion of the Beartooth contains both identifiable organic material (MLM 141) and interbeds of dark, clay-rich quartz wacke (MLM 096). The relatively organic-rich beds at the base of the Beartooth have been preferentially mineralized (Occurrences 27, 28, 36, 37). The depositional mechanism cited is consistent with known geochemical processes, geochemical data from the occurrences within area D, and field relationships between the occurrences and surrounding rocks.

Projected size of the individual occurrences is somewhat dependent on the depositional mechanism. The exposed occurrences are commonly small, but they potentially, especially the stratabound portions of the deposits, are large. Width of the mineralized shears is variable, but in one case (Occurrence 37) the mineralized shear is 12 m wide. Depth of mineralization along a shear is speculative, but anomalous radioactivity has been traced intermittently for at least 100 m where a shear was exposed in a canyon (Occurrence 37). The lateral extent of anomalous radioactivity along the mineralized shears in outcrop is usually continuous for less than 50 m. However, at the Prince Albert No. 2 (Occurrence 28), the mineralized shear was traced for 150 m. Thickness of the stratabound portions of anomalous radioactivity has been observed to be as great as 5 m (Occurrence 36), but may in places be greater. The horizontal extents of the stratiform occurrences may be large. At the Oil Center Tool Co. claims (Occurrence 36) in area D2, a stratiform occurrence covers an area of 180 m by 200 m. Moreover, that area is limited by erosion. There is no indication of the lateral extent of the occurrence in the Beartooth away from a single shear, but several hundred meters does not seem unreasonable. It is entirely possible in such areas as the Wild Horse Mesa area (central part of area D1, Pl. 10), where there is a substantial area of Beartooth Quartzite and several anomalously radioactive shear zones (Occurrences 22, 23, 24, 27), that several square kilometers of Beartooth Quartzite were mineralized above the unconformity.

Favorable Area

The boundaries of area D are determined by the areas where favorable host rocks (Precambrian Burro Mountains granite and Cretaceous Beartooth Quartzite) are intersected by caldera-related ring-fracture zones. The extent of the ring-fracture zone indicates the area where the uranium-bearing hydrothermal solutions derived from an associated caldera complex were likely to travel. The ring-fracture zone also is the most favorable area structurally. Area D1 is delineated by the coincidence of the Schoolhouse Mountain Caldera ring-fracture zone (Pl. 10) and favorable host rocks. The northern boundary of area D1 is extrapolated to extend under the Tertiary volcanic cover for an

unknown distance. The northern boundary is therefore somewhat arbitrary because the depth of the volcanic cover is unknown and probably exceeds the 5,000-ft depth limit for NURE evaluation.

Area D2 is located south of the Schoolhouse Mountain ring-fracture zone delineating area D1. However, multiple calderas and ring-fracture zones are common in this region. Therefore, because of the similarities of host rocks and geology, and geochemistry of the occurrences in area D2 compared to area D1, a ring-fracture zone is postulated in area D2 also. For these reasons, areas D1 and D2 are considered similar enough to be designated a single area favorable for magmatic-hydrothermal (Class 330) uranium deposits.

Area D has a surface area of 120.2 km^2, of which 108.1 km^2 are in area D1 and 12.1 km^2 are in area D2. Depth from the surface to the favorable environment ranges from 0 to 5,000 ft. Thickness of the favorable environment is the projected vertical extent of vein mineralization within the favorable environment. The vertical extent is unknown, but an estimate can be made between a minimum of 1000 m observed (Occurrence 37) and a tentative maximum of approximately 500 m, which is the difference in elevation of Occurrences 20 and 23 in the Precambrian granite of the Willow Creek structural block (area D1), uncorrected for any fault displacement. The depth of mineralization is arbitrarily placed at 300 m. Land status of area D is national forest, private, state-administered lands, and land administered by the Bureau of Land Management.

AREA E: STOCKTON PASS REGION--SOUTHERN PINALENO MOUNTAINS

Precambrian granitic rocks adjacent to a mid-Tertiary quartz monzonite intrusive body in the Stockton Pass area of the southern Pinaleno Mountains are favorable for uranium deposits of the magmatic-hydrothermal type (Class 330). The host rocks are Precambrian quartz monzonites and granites intruded by Precambrian diabasic dikes and sills. Area E is favorable because the host rock is structurally and chemically favorable for uranium deposition. Structural favorability is indicated by the numerous faults and shear zones that transect the area. Chemical favorability is indicated by silicification, sericitization, argillization, and iron staining, mainly near veins in shear zones. The veins contain silica, sulfides, anomalous fluorine, and anomalous heavy metals, all of which characterize magmatic-hydrothermal uranium deposits. Also, a possible source for uranium-bearing magmatic-hydrothermal solutions was identified. The presence of uranium occurrences demonstrates that uranium concentration and deposition occurred within the favorable area.

It is proposed that uranium-bearing hydrothermal solutions were generated in the mid-Tertiary Gillespie Quartz Monzonite stock and moved outward from the stock into surrounding Precambrian granitic rocks through a pervasive system of faults and shear zones. Uranium deposition occurred within the shear zones in the granitic rocks.

Geology of Favorable Area

The Stockton Pass region is located in the southern Pinaleno Mountains. The Pinaleno Mountains are a northwest-trending fault-block range that

consists predominantly of Precambrian granitic, metasedimentary, and metavolcanic rocks. Within the Stockton Pass area, the rocks are predominantly Precambrian granite intruded by northwest-trending Precambrian diabase dikes and sills and the mid-Tertiary Gillespie Quartz Monzonite. Also in the region is a small area of Pinaleno banded gneiss, a local equivalent of the Pinal Schist (Swan, 1976). In the southern portion of the Stockton Pass region, the intrusive rocks are overlain by Cretaceous-Tertiary andesites and intermediate to felsic Tertiary volcanic rocks. A further description of the volcanic rocks is provided in the discussion of area F. Intermediate to felsic, north- to northeast-trending Tertiary dikes, sills, and plugs intrude nearly all other rocks.

The favorable rocks in area E are the Precambrian granitic rocks and the Precambrian diabase that intrudes them. Swan (1976) mapped and provided radiometric ages for three granitic rock types in a limited portion of area E. They are the Stockton Pass granite (1,405 m.y.), the Pinaleno granite (1,384 m.y.), and the white gneissic granite (1,362 m.y.). All Precambrian granitic intrusive rocks of area E are sufficiently similar to merit treatment as a single rock type in this discussion. The granitic rocks are nonfoliated to weakly foliated, medium- to coarse-grained, allotriomorphic-granular rocks that are locally porphyritic. They consist primarily of microcline, plagioclase, quartz, biotite, and muscovite. They contain traces of epidote, apatite, zircon, and opaque minerals (MLM 118, 120). Compositionally, the rocks range from quartz monzonite to granite. The granite contains scattered pegmatites, some of which contain rare-earth minerals (Occurrence X13, Pl. 2A). However, the pegmatites are too small and scattered to be a potential uranium resource.

The mid-Tertiary (35 m.y., Swan, 1976) Gillespie Quartz Monzonite stock (Pl. 7) intrudes the Precambrian granitic rocks. The stock consists of a medium- to coarse-grained equigranular quartz monzonite and contains approximately equal amounts of quartz, alkali feldspar, and sodic plagioclase and lesser amounts of biotite and sphene. As the contact of the stock with the country rock is sharp and the quartz monzonite at the contact has an aphanitic texture, the stock is considered to be an epizonal intrusive body.

Intense faulting and shearing of the Precambrian rocks of area E resulted in widespread development of shear zones, breccias and microbreccias, mylonites, and fault gouge. The faults are oriented in an intense, west-northwest-trending zone cutting area E, and subsidiary north- and northeast-trending faults that also cut area E. Swan (1976) concluded that the northwest- and perhaps the north-trending faults and shears are elements of the Texas Lineament. All the faults have had repeated movement. Swan (1976) discerned at least three episodes of fault movement, which range in age from the Precambrian to post-Gillespie Quartz Monzonite intrusions.

Evidence of Favorability

The fact that mechanisms for the concentration and deposition of uranium within area E exists is evidenced by the presence of six uranium occurrences (Occurrences 6, 7, 8, 10, 11, 12, App. C; Pl. 2A). Uranium is present in northwest-, northeast-, and north-trending faults and shear zones in Precambrian granitic rocks. Uranium is also present in northwest-trending

mafic dikes (Occurrence 7). In Occurrences 6 and 7 discrete veins are present in the shear zones. In the other occurrences, disseminated anomalous radioactivity is present throughout the shear zone; however, detected levels of uranium were low in outcrop. The maximum value obtained was 286 ppm cU_3O_8 (Occurrence 8, MLM 133). However, previously reported values have been as high as 0.27% eU_3O_8 (Occurrence 11). The only uranium minerals observed in outcrop are secondary. Meta-autunite and potassium uranyl phosphate minerals were identified at Occurrence 8 (MLM 133). Uranophane and autunite are reported as being present at Occurrence 11. The cU/eU ratios are characteristically close to or less than 1, indicating that the anomalous radioactivity within the shears is probably not the result of recent secondary uranium deposition. Analytical data do not show thorium contents in the radioactive shear zones to be significantly greater than background levels. However, a thorium-silica-phosphate mineral was petrographically identified in sample MLM 133. The presence of uranium in shear zones, the presence of thorium minerals, and cU/eU ratios of close to or less than 1 are consistent with uranium mineralization of the magmatic-hydrothermal type.

Elements associated with uranium in the shear zones are variable. Fluorine is the most common. Fluorite was identified at Occurrences 6 and 11. Low-level, but anomalously high, fluorine contents were detected at Occurrences 7 (1,860 ppm F, MLM 129) and 12 (1,346 ppm F, MLM 118). At Occurrence 8 the single sample taken did not contain anomalous levels of fluorine. The heavy-metal trace-element suite in the shear zones is variable, and some samples contain no anomalous amounts of heavy metals. Anomalous amounts of Cu, Li, Mo, Pb, W, Y, and Zr have been detected in some samples (MLM 118, 128, 129, 130, 131). The presence of anomalous fluorine and heavy metals characterizes magmatic-hydrothermal uranium deposits (Mathews, 1978).

Alteration of the country rock within and adjacent to the uranium-bearing shear zones is variable but is of the magmatic-hydrothermal type. The granite is moderately to strongly sericitized, argillized, silicified, and iron stained. In some instances, the granite for a distance of tens of meters (Occurrences 7, 8) from the vein (when present) or central shear has been bleached, sericitized, and variably iron stained in a clear-cut zonal relationship. Diabase was completely altered to clay, limonite, and hematite where it was mineralized (130 ppm cU_3O_8, MLM 128).

The mid-Tertiary Gillespie Quartz Monzonite is proposed as the source of the uranium-bearing hydrothermal solutions that deposited the uranium of area E. The uranium occurrences in area E show a close spatial relationship to the intrusive monzonite (Pl. 2A and 7). The Gillespie Quartz Monzonite is a leucocratic epizonal intrusive body with anomalous fluorine (943 ppm F, MLM 124), a high uranium content (6 ppm cU_3O_8), a high Th/U ratio (5.5), and a calculated agpaitic coefficient of 0.88. The chemical characteristics of the intrusive body are similar to those listed by Mathews (1978a) as being common to source plutons for uranium-bearing hydrothermal solutions. The Gillespie Quartz Monzonite is also suggested as the source of the hydrothermal solutions that formed the uranium occurrence in the nearby volcanic rocks of area F.

Uranium-bearing solutions that left the intrusive body would have moved into the adjacent Precambrian granitic rocks along the extremely pervasive faults and shear-zone systems of the area. The faults and shear zones also provided favorable depositional sites for uranium. Uranium transported in the

ore solutions as hexavalent complexes may have been reduced and deposited as tetravalent uranium minerals as a result of mechanically induced decrease in oxygen fugacity as the solutions cooled and moved outward through the fracture zones (Mathews, 1978a). Uranium deposition may also have been induced by solution/wall-rock reactions. Postdepositional weathering processes would have removed most of the hypogene uranium from surficial outcrops.

Favorable Area

Factors controlling favorability of area E are extent of the host rock (Precambrian granitic rocks), extent of intense faulting and shearing (both ore-solution transport mechanisms and depositional sites), and proximity to the Gillespie Quartz Monzonite (ore-solution source). In area E (Pl. 1), all three factors are judged to be coincident.

Area E has a surface area of 145.2 km^2. Depth from the surface to the environment ranges from 0 m, where area E crops out, to 200 m, where area E is overlain by favorable area F. The thickness of the favorable environment is arbitrarily determined to be 500 m. Land status of area E is national forest, private, state-administered lands, and land administered by the Bureau of Land Management.

AREA F: MID-TERTIARY VOLCANIC ROCKS IN THE WILLOW SPRING CANYON AREA

Area F (Pl. 1), which is near Willow Spring Canyon in the southern Pinaleno Mountains, is favorable for magmatic-hydrothermal uranium deposits (Class 330). In this area, intermediate to felsic mid-Tertiary volcanic rocks and associated agglomeratic clastic units are widely faulted and brecciated and strongly altered. The volcanic assemblage is intruded by felsic to intermediate porphyritic dikes, which are believed to be related to a large mid-Tertiary quartz monzonite stock located just north of the favorable area.

At the Golondrina uranium prospect (Occurrence 9, App. A1; Pl. 2A), uranium is locally concentrated within a major north-trending fault. Uranium of grades as high as 0.6% U_3O_8 (Granger and Raup, 1956) is associated with mimetite, a supergene lead chloroarsenate. Zinc, copper, and iron are also found in sulfide and secondary minerals associated with the uranium. It is possible that uranium and the base metals are preserved under reducing conditions, at depth, along fractures and faults.

It is important to note here that the volcanic assemblage in the Willow Spring Canyon area does not derive its uranium favorability from volcanogenic processes. Rather, the presence of abundant faults and fractures, widespread evidence of hydrothermal alteration, and an inferred spatially related uranium source, the Gillespie Quartz Monzonite, support the hypothesis of a magmatic-hydrothermal uranium system.

Regional Geology of the Pinaleno Mountains

The Pinaleno Mountains are a rugged, northwest-trending fault-block range within the Basin and Range Province. The range consists predominantly of

Proterozoic metasedimentary and meta-igneous rocks, but a large, mid-Tertiary quartz monzonite stock and intermediate to mafic and felsic volcanic rocks occur in the southern part of the range. Also at the southern end, the range is traversed by a broad system of west-northwest-trending faults and shear zones. Swan (1976) proposed that these faults and shears are elements of the Texas Lineament, a broad, diffuse geomorphic and structural zone that trends west-northwest across the southern Cordillera of North America.

General Geology of the Willow Spring Canyon Area

Major rock types within and around the Willow Spring Canyon area include intermediate and felsic Tertiary volcanics, andesitic units of Tertiary-Cretaceous age, Precambrian granitic rocks, and abundant Tertiary-age dikes (Cooper, 1960). The dikes transect all the volcanic and granitic units. Immediately north of the Willow Spring Canyon area, there is a large stock of Tertiary quartz monzonite (Swan, 1976).

The Tertiary volcanic assemblage comprises welded rhyolitic tuff, porphyritic ("turkey track") andesite, and interlayered volcanic breccia and volcaniclastic and epiclastic rocks. Although there are no radiometric age dates available for the volcanic rocks in the southern Pinalenos, the volcanics are presumed, on the basis of similarity to other dated volcanic rocks in the region, to be mostly of mid-Tertiary age. Similar lava-flow and ash-flow tuff units in the adjacent Galiuro and Winchester Mountains were determined to be about 29 to 23 m.y. old (Creasey and Krieger, 1978). The distinctive "turkey track" andesite porphyries in various areas in southeastern Arizona yield age dates of between 39 and 24 m.y. (Drewes, 1980).

Older volcanic rocks, of Tertiary and Cretaceous age, also occur in the area, but they are of limited extent. These rocks consist mainly of andesitic lava flows with locally interbedded sedimentary rocks. The Precambrian rocks exposed throughout the Willow Spring Canyon area are characteristically medium- to coarse-grained, non- to weakly foliated granites similar to those widely distributed in the Stockton Pass area to the north (Swan, 1976).

Northeast- and north-trending felsic to intermediate dikes, sills, and plugs intrude all rock units described. These intrusives may be genetically related to the large Gillespie Quartz Monzonite stock, which is exposed less than 4 km to the north. Swan (1976) showed that intermediate to felsic dikes, occupying joints and faults of various orientations, intrude both the stock and, locally, adjacent Precambrian country rock. Moreover, additional evidence for a genetic relationship between the dikes and a regionally associated mid-Tertiary stock is provided by relationships observed in the Santa Teresa Mountains northwest of the Pinaleno range. There, fine-grained dikes, associated with the mid-Tertiary Santa Teresa granite, cut mid-Tertiary "turkey track" andesite (Rehig and Reynolds, 1980).

Although not itself in the Willow Spring Canyon area, the Gillespie Quartz Monzonite stock will be described here because of its presumed genetic association with the numerous intrusives in the area and because it is an inferred uranium source. The Gillespie Quartz Monzonite was emplaced in the Stockton Pass fault zone, which is north of the Willow Spring Canyon area, about 35 m.y.b.p. (Swan, 1976). The stock is, for the most part, a medium- to

coarse-grained equigranular quartz monzonite, containing approximately equal proportions of quartz, K-feldspar, and sodic (An 16-20) plagioclase. The major oxide composition of the quartz monzonite is about 71% SiO_2, 14.4% Al_2O_3, 4.2% Na_2O, and 5.2% K_2O. It has an agpaitic coefficient of 0.88. The stock, characterized by sharp contacts with the intruded country rock and commonly by an aphanitic texture near contacts, is considered to be an epizonal intrusive body.

Most of the rocks in the Willow Spring Canyon area are highly brecciated and strongly altered. Hematitic and limonitic staining are widespread, and evidence of argillization, chloritization, and silicification is commonly found.

Abundant faults, trending northwest, north, and northeast, transect the area. Northwesterly and perhaps northerly oriented faults may be elements of the Texas Lineament of the Basin and Range fault systems, but the origin and relative age of northeast-trending faults, some of which are normal faults, are not known. Regionally, the mid-Tertiary volcanic and associated clastic and pyroclastic rocks dip southwestward (Cooper, 1960); but, in the area of faults, dip directions commonly vary considerably from the regional trend.

Evidence of Uranium Favorability

Anomalous concentrations of uranium are found on the Golondrina Prospect (Occurrence 9, App. A; Pl. 2A), which is located at the head of Willow Spring Canyon in the southern Pinaleno Mountains. Uranium occurs as irregular, localized disseminations in a heavily limonite- and hematite-stained fault gouge. The gouge occurs along a northeast-trending, northwest-dipping fault that juxtaposes a highly fractured and strongly altered "turkey track" andesite porphyry and an equally brecciated and altered agglomeratic or possibly epiclastic volcanic conglomerate unit. The mineralized fault was interpreted by Cooper (1960) to be a north-trending thrust fault, with the andesite porphyry thrust over the agglomerate. Recent reconnaissance geologic mapping in the area, however, showed the fault to be a north-trending, somewhat curvilinear fault (Wynn, 1981). The fault, which is commonly marked by the positive relief of a silicified breccia, was traversed for a total distance of about 2.5 km. The maximum radioactivity encountered, outside the prospect area, was 1.5 times background (MLM 360, Table 4).

The richest concentrations of uranium (MLM 357, Table 4) are associated with bright-orange-yellow mimetite, $Pb_5(AsO_4)_3Cl$, which occurs as surface incrustations or as fracture or vug fillings. No uranium minerals were identified, but SEM/EDS studies showed that uranium is contained within the mimetite. Disseminated pyrite, chalcopyrite, and reportedly chalcocite (Granger and Raup, 1956) are commonly associated with the radioactive mimetite along the fault. Secondary minerals, including limonite, hematite, and minor malachite, commonly stain both the fault and adjacent wall rock. Elements enriched along with uranium include arsenic, cadmium, chromium, copper, iron, lithium, lead, and zinc (Table 4). Although anomalous concentrations of uranium are restricted to the fault, anomalous amounts of copper, lead, and zinc occur in both the fault and the adjacent wall rock.

TABLE 4. SELECTED ANALYTICAL AND PETROGRAPHIC DATA FOR WILLOW SPRING AREA ROCKS

Sample no.		Chemical U_3O_8 (ppm)	Radiometric eU (ppm)	cU_3O_8/eU_3O_8	Radiometric eTh (ppm)	Significant associated elements (ppm, unless otherwise noted)
MLM 357	fault gouge containing mimetite	580.00	510.00	0.97	24.00	As(1.7%), Cd(32000), Cr(40), Cu(350), Fe(4.3%), Li(570), Mo(11), Pb(4.3%), Zn(1.7%)
MLM 358	altered porphyritic andesite	5.00	7.00	0.60	17.00	Cu(187), Fe(4.2%), Pb (2160), Zn(6380)
MLM 359	agglomerate(?)	3 .00	3.00	0.90	7.00	Cu(369), Li(991), Pb(3510), Zn(1.7%)
MLM 360	altered vitric tuff	9 .00	12.00	0.60	32.00	
MLM 361	silicified vitrif tuff	8 .00	7.00	1.00	31.00	

The country rock exhibits pervasive limonitic and hematitic staining for distances as great as 20 to 30 m from the fault. The andesite porphyry unit adjacent to the fault exhibits moderate to strong argillization and chloritization and slight sericitization and silicification.

The source of uranium in the Willow Spring Canyon area is uncertain, but there is a spatial and possibly genetic relationship between the uraniferous, volcanic host rocks and the Gillespie Quartz Monzonite stock and other associated intrusives. Mineralizing hydrothermal solutions emanating from this leucocratic stock could have been widely disseminated via permeable fault and fracture zones, which are widespread throughout the area. Many of the area faults are of considerable lengths (Copper, 1960; Wynn, 1981) and, presumably, depths (many of the faults are thought to be related to deeply buried Precambrian basement flaws). Furthermore, there is evidence that many of the faults have been reactivated with movement occurring as late as the Quaternary recorded along some faults (Swan, 1976).

In addition to providing effective conduits for metalliferous solutions, fault and fracture zones may provide favorable sites for the localization of metal-bearing veins and vein systems. There, hexavalent uranium in ascending solutions may have been effectively reduced to a tetravalent form by either a chemical-reduction mechanism involving disseminated sulfides or by a mechanically induced decrease in oxygen fugacity of the system as the temperature, pressure, and pH of the hydrothermal fluids changed with upward migration through dilatant zones (Mathews, 1978a). Although there are no substantiating subsurface data, primary uranium and possibly lead-, zinc-, and copper-sulfide minerals may be preserved at depth along faults within reduced volcanic or volcaniclastic rock.

Favorable Area

The area favorable for magmatic-hydrothermal uranium deposits (Class 330) is defined as the combined surface and estimated subsurface extent of faulted Tertiary volcanic and associated rocks in the vicinity of Willow Spring Canyon (Pl. 1, area F). The favorable environment extends over an area of 22.5 km^2. Thickness of the favorable volcanic rocks is not known with certainty, but is estimated to be about 200 m. The subsurface extent of the favorable environment is estimated to be at depths no greater than 200 m. The entire favorable area is within the Coronado National Forest.

AREA G: TYRONE LACCOLITH

Area G is a roughly wedge-shaped area in the Laramide Tyrone laccolith, which intrudes the east-central side of the Burro Mountains batholith. It is favorable for uranium deposits of the allogenic type (Class 370) because there is a uranium source available (Burro Mountains granite), and there are transmissive zones (shear zones) between uranium sources and depositional sites (large area of disseminated sulfides in the Tyrone laccolith). The uranium occurrences lack veins, have a low thorium-to-uranium ratio, and lack the heavy-metal trace-element suite that nearby magmatic-hydrothermal uranium occurrences have (areas A, B, and D). These features indicate allogenic uranium deposits. The processes of uranium concentration and deposition

demonstrably occurred. A mechanism by which uranium was derived, transported, and deposited to form the occurrence is supported by the available evidence. The host rock is quartz monzonite and monzonite of the Tyrone laccolith that contain disseminated sulfides emplaced during the Laramide porphyry copper mineralization that formed the Tyrone porphyry copper deposit.

The uranium occurrences of area G (Pl. 2A and 11) are characterized by disseminated uranyl phosphate and unidentified uranium silicate minerals in intensely sheared zones, which lack evidence of hydrothermal activity. It is likely that uranium was derived by weathering from the Burro Mountains granite, which surrounds the Tyrone quartz monzonite laccolith. Uranium was probably transported by surficial waters to areas of intense shearing in the laccolith; uranium deposition occurred where the shear zones intersected areas of disseminated sulfides.

Geology of Favorable Area

Area G is part of the Tyrone-Burro Peak block of the Burro Mountains batholith (Gillerman, 1970). The Tyrone-Burro Peak block is a horst separated from the Willow Creek block to the north by the northeast-trending Austin-Amazon fault and separated from the White Signal block in the south by the similarly trending Neglected-Sprouse-Copeland fault (Pl. 11).

The Burro Mountains granite consists primarily of pinkish-gray, medium- to coarse-grained, leucocratic gneissic granite and granite. The granite has a hypidiomorphic- to xenomorphic-granular texture that is locally porphyritic. The rock commonly contains from 23% to 36% perthitic microcline, 22% to 70% oligoclase, 30% to 35% quartz, and as much as 4% biotite. Accessory minerals are sphene, zircon, tourmaline, apatite, magnetite, rutite, and ilmenite. Adjacent to the Tyrone laccolith the granite is moderately to strongly sericitized, kaolinized, and silicified. Further descriptions of the granite are provided in Hewitt (1959), Gillerman (1964, 1968, 1970), and Hedlund (1978a, 1978d, 1978e).

The Paleocene Tyrone laccolith (potassium-argon age of 56.2 m.y.; McDowell, 1971) is elongated in a northeasterly direction. It is approximately 6.5 km wide and 8 km long and occupies a topographic depression surrounded by Burro Mountains granite. The laccolith (Kolessar, 1970) consists of porphyritic and nonporphyritic quartz monzonite and monzonite, which is a light-gray, medium-grained, holocrystalline, hypidiomorphic-granular rock. The rock typically contains 14% to 16% anorthoclase, 55% to 65% oligoclase, 6% to 16% quartz, 1% to 4% biotite, and less than 1% hornblende. Accessory minerals are sphene, apatite, and iron oxides. In the eastern part of the Tyrone laccolith and adjacent Burro Mountains granite is the Tyrone porphyry copper deposit (Kolessar, 1970). Primary minerals are pyrite, chalcopyrite, sphalerite, molybdenite, and bornite. Chalcocite and minor covellite are the ore minerals in the supergene zone of the deposit. The area of the Tyrone laccolith that contains disseminated hypogene sulfide minerals is limited. The area is wedge shaped; the northeasterly Burro Chief fault forms the northern boundary. An east-to-west zone of faulting intersects the Burro Chief fault and forms the southern boundary of the area (Pl. 11). The mineralization that formed the Tyrone porphyry copper deposit

is believed to have occurred during Laramide time and was genetically associated with the Tyrone quartz monzonite laccolith (Gillerman, 1964; Kolessar, 1970).

Evidence of Favorability

The presence of a mechanism for the concentration and deposition of uranium within area G is evidenced by three uranium occurrences (Pl.2A; Pl. 11), all of which are described in Appendix C (uranium-occurrence reports 39, 40, 41). The uranium occurrences and potential uranium deposits in area G are classified as allogenic (Class 370) rather than magmatic-hydrothermal (Class 330) because data from the occurrences are more characteristic of allogenic-type uranium occurrences than of magmatic-hydrothermal occurrences. The occurrences are classified as allogenic rather than authigenic (Class 360) because of the proposed uranium source.

The known occurrences are in N. 20° E.- to N. 60° E.-trending, steeply dipping shear zones that are abundant (Hedlund, 1978a) in the quartz monzonite of area G. The intensity of shearing is illustrated by the thin-section report (App. E) of sample MLM 003, which shows that the host rock has undergone mylonitization along the shears. The host rock is intensely sericitized and variably iron stained, but it is unknown whether this alteration is a byproduct of the process by which uranium was deposited, a result of shearing and weathering, or part of the ubiquitous sericitization associated with the episode of porphyry copper mineralization that occurred nearby. The predominant uranium mineral in the occurrences is metatorbernite, but trace amounts of an unidentified uranium silicate mineral were also noted (MLM 003). The maximum uranium content measured was 940 ppm cU_3O_8 (Occurrence 41, MLM 002). However, a thin-section analysis of a sample (MLM 003) from Occurrence 41, which was not analyzed for U_3O_8, contained 9.5% metatorbernite. That percentage of metatorbernite in the rock is roughly equivalent to a uranium content of between 4% and 5%. The uranium contents of outcrop samples from the other two occurrences were much lower (Occurrence 39, MLM 145, 29 ppm cU_3O_8; Occurrence 40, MLM 146, 31 ppm cU_3O_8).

The allogenic nature of the uranium occurrences is indicated by the low thorium-to-uranium ratio (less than 0.1) and the low thorium contents of the deposits, which are not elevated over background levels of thorium in the Tyrone laccolith. Even weathered portions of magmatic-hydrothermal uranium occurrences often have thorium contents elevated over host-rock background levels. Morphology of the known occurrences is irregular within shear zones, and there is no trace of a hydrothermal-vein system; again, the characteristics are of allogenic rather than magmatic-hydrothermal deposits. The heavy-metal trace-element suite within the uranium occurrences is restricted to Cu, Mo, Pb, and Sb (Occurrence 41--MLM 002, 117 ppm Cu, 69 ppm Mo, 273 ppm Sb; Occurrence 40--MLM 146, 83 ppm Cu, 12 ppm Mo, 356 ppm Pb). Presence of these metals can be explained as being the result of the pervasive episode of porphyry copper mineralization in the area. This suite of trace elements is very different from the extensive suite of trace metals associated with the magmatic-hydrothermal uranium occurrences to the south (area A) and north (areas B and D). Recent or perhaps even ongoing uranium deposition of the allogenic type is indicated by a cU/eU ratio of greater than 1 (MLM 001, MLM 002).

Allogenic rather than authigenic classification of the uranium occurrences in area G is dependent on the choice of source rock for the uranium. The uranium source for authigenic occurrences is the host rock. The uranium source for allogenic occurrences is outside the host rock. A comparison of the quartz monzonite of the Tyrone laccolith and the Burro Mountains granite, which the laccolith intrudes, indicates that the Burro Mountains granite was the probable uranium source. The background levels of uranium in the Tyrone laccolith are low (less than 1 ppm cU_3O_8, MLM 023, MLM 024). The thorium-to-uranium ratios of the laccolith are also normal, which indicates there was little leaching of uranium from the rock during the weathering process. An extensive gamma-ray spectrometric survey of the laccolith showed that these uranium and thorium levels are typical of the laccolith outside area G. Conversely, samples of Burro Mountains granite adjacent to the laccolith contain 6 to 7 ppm cU_3O_8 (MLM 021, 022, 024) and have thorium-to-uranium ratios of between 6.2 and 12.8. The high thorium-to-uranium ratios and high uranium contents of the Burro Mountains granite indicate that it is a much better potential source for uranium derived during the weathering cycle than is the Tyrone laccolith. The thorium-to-uranium ratios of the granite suggest that removal of uranium from the granite during weathering did occur and is occurring. The HSSR anomaly surrounding the entire Burro Mountains granite (the principal rock type of the batholith) is capable of releasing significant amounts of uranium to the near-surface environment during the weathering cycle.

It is proposed that surficial weathering of the Burro Mountains granite has released and is releasing uranium to surficial and near-surface ground waters. Traces of apatite in the granite and lack of carbonates in the near-surface environment indicate that uranium is probably transported as $UO_2(HPO_4)_2^{-2}$ complexes (Langmuir, 1977). The uranium-bearing surficial waters moved from the Burro Mountains granite into the Tyrone laccolith and were concentrated in highly sheared and fractured areas. Langmuir (1977) indicated that uranium phosphate minerals become less soluble as pH decreases. A low pH environment would be provided where the shear zones transporting the uranium-bearing ground waters intersected oxidizing disseminated sulfides in the eastern Tyrone laccolith. In such an environment, uranyl phosphate minerals such as metatorbernite would precipitate. If the uranium-bearing solutions encountered unoxidized disseminated sulfides at depth in the shear zones, reduction would occur and uraninite or tetravalent uranium silicate minerals would precipitate. As weathering progressed and the oxidized zone descended in the mineralized shears, tetravalent uranium minerals would be oxidized and converted to hexavalent uranium phosphate minerals. A widespread area of disseminated sulfides in the host rock is critical for the deposition of sufficient uranium to meet the NURE tonnage and grade requirements for favorability. Because of the diffuse nature of solution transport in a near-surface environment, a fairly large depositional site is needed to ensure that sufficient amounts of uranium-bearing surficial waters intersect the depositional site and deposit a significant amount of uranium.

The potential size of the allogenic uranium deposits in area G is speculative. Because of ongoing surficial weathering processes, uranium is probably continually moving downward in the favorable environment. Therefore, except for some high-grade surficial remnants of uranium deposits such as at Occurrence 41, surficial contents of uranium should be low. Depending on the

local hydrogeology and the movement of uranium-bearing surficial waters, uranium could be present as low-grade disseminations, as higher grade deposits in shears, or both. As the known occurrences are located in shears, and at least some surface samples were high grade, there is a potential for high-grade uranium deposits in the shears. Surface indications are that the mineralized shears could be of considerable size. At Occurrence 39, anomalous radioactivity was detected continuously along a shear zone at least 600 m long and 60 m wide. Numerous shear zones in area G could host uranium in the subsurface. The minimum limit on depth of deposits is probably the depth where disseminated sulfides are unoxidized. In area G, this can range from near surface to 200 m below the surface.

Favorable Area

Area G was delineated on the basis of the coincidence of disseminated sulfides and pervasive, abundant shear zones. The area of disseminated sulfides (Pl. 11) was extrapolated from data in Kolessar (1970). Extensive shearing and faulting in the Tyrone laccolith are also shown on Plate 11.

Area G has a surface area of 13.3 km^2; the favorable environment is at the surface. Thickness of the favorable environment is estimated at somewhat in excess of the depth to the hypogene disseminated sulfide minerals (about 300 m). The land of area G is partly national forest and partly private.

ENVIRONMENTS UNFAVORABLE FOR URANIUM DEPOSITS

In the Silver City Quadrangle, all Precambrian metamorphic rocks are unfavorable for magmatic-hydrothermal and contact metasomatic (Classes 330 and 340, Mathews, 1978a) and unconformity-related and vein-type (Classes 710 and 720, Mathews, 1978b) deposits. Precambrian intrusive rocks and Laramide and mid-Tertiary intrusive rocks, except in favorable areas A, B, D, E, and G (Pl. 1), are unfavorable for all classes of uranium deposits associated with plutonic igneous rocks (Classes 310 through 380, Mathews, 1978a). All Paleozoic and Cretaceous sedimentary rocks, except in favorable area D (Pl. 1), are judged unfavorable for sandstone (Subclasses 241 through 244, Austin and D'Andrea, 1978) and marine black shale (Class 130, Jones, 1978) deposits. Where intruded by Laramide and mid-Tertiary igneous rocks, the Paleozoic and Cretaceous carbonate rocks are also unfavorable for magmatic-hydrothermal and contact metasomatic (Classes 330 and 340) deposits. Upper Cretaceous and Cenozoic volcanic rocks are unfavorable for all volcanogenic uranium deposits (Classes 510 through 540, Pilcher, 1978) and, except in area F, for magmatic-hydrothermal (Class 330) deposits. Upper Cenozoic basin-fill and Quaternary surficial deposits, except in area C, are unfavorable for uranium deposits in sandstone (Subclasses 241 through 244) and in volcaniclastic lacustrine environments of the hydroallogenic class (Class 540).

PRECAMBRIAN METAMORPHIC ROCKS

All Precambrian metamorphic rocks within the quadrangle are unfavorable for all classes of uranium deposits. In particular, the metamorphic rocks are

unfavorable depositional environments for magmatic-hydrothermal (Class 330), contact metasomatic (Class 340), and unconformity-related (Class 710) uranium deposits and also for vein-type uranium deposits in metamorphic rocks (Class 720).

Precambrian metasedimentary and metavolcanic rocks occur in the Pinaleno (Swan, 1976) and Dos Cabezas (Erickson, 1969) Mountains in the west and the Burro batholith (Hewitt, 1959; Gillerman, 1964) in the east (Pl. 8). In the west the rocks are generally assigned to the Pinal Schist, and in the east they are assigned to the Bullard Peak and Ash Creek series (Fig. 2). The age of Pinal sedimentation is 1,720 m.y. ago, and the age of Pinal metamorphism is pre-1,660 m.y. ago (Silver, 1978). Ages of the Bullard Peak and Ash Creek series are unknown, but general geologic similarity may indicate a correlation with the Pinal.

The Pinal originally consisted of eugeosynclinal sediments--quartz sands, conglomerates, dacitic to basaltic volcanic flows, and tuffaceous sediments. Postmetamorphic rocks are predominantly phyllites, feldspathic phyllites and argillites, quartzites, metaconglomerates, and amphibolites. Metamorphic rank is in the chlorite-albite-epidote-quartz or biotite-albite-epidote-quartz facies of the greenschist facies.

The Bullard Peak series consists of quartz-feldspar gneiss, biotite gneiss, biotite schist, muscovite schist, hornblende gneiss, sillimanite gneiss, granite gneiss, and amphibolite resulting from amphibolite facies regional metamorphism of argillaceous feldspathic sandstone, calcareous argillaceous siltstone, shale, dolomitic shale, diabase, and granite. After metamorphism of the Bullard Peak series, the sediments of the Ash Creek series were deposited--silty dolomite and limestone, feldspathic and argillaceous sandstone, and shale. Low-grade regional metamorphism (greenschist facies) and contact metamorphism of the Ash Creek produced sericite phyllite, andalusite hornfels, biotite hornfels, diopside quartzite, serpentine marble-ophicalcite rocks, calcite-serpentine-chlorite rocks, and talc and magnetite serpentine (Woodward, 1970).

The metamorphic rocks are unfavorable for magmatic-hydrothermal uranium deposits despite the presence of two magmatic-hydrothermal uranium occurrences (Occurrences 22 and 24, App. C) hosted by quartz muscovite schists (MLM 094, App. E) of the Bullard Peak series within favorable area D (Pl. 1). These two occurrences are the only uranium occurrences hosted by Precambrian metamorphic rocks within the quadrangle. The occurrences were formed by the same episode of mid-Tertiary uranium mineralization that formed the magmatic-hydrothermal uranium deposits hosted by Precambrian granite and Cretaceous Beartooth Quartzite in area D. The metamorphic rocks are not considered favorable in area D because their response to faulting and shearing is poor, resulting in few depositional sites, and the rocks are apparently not chemically favorable as host rocks for magmatic-hydrothermal uranium deposition. Chemical unfavorability is indicated by the general lack of wall-rock alteration (MLM 094; Occurrence 24) at the two known occurrences. The unsuitability of the metamorphic rocks as host rocks for magmatic-hydrothermal uranium deposits is further evidenced by Occurrence 23 (area D), where xenoliths of metamorphic rocks in granite have selectively not been mineralized, whereas the surrounding granite has been mineralized. In favorable area E (Pl. 1), an intrusive body produced uranium-bearing hydrothermal solutions that

mineralized adjacent granite but did not mineralize equally adjacent Pinal Schist. The evidence indicates that even when a source of uranium-bearing magmatic-hydrothermal solutions is present, the resulting uranium deposition in the metamorphic rocks is too sparse (two known occurrences in the quadrangle), too small in size (Occurrences 22 and 24), and too low grade (maximum 296 ppm cU_3O_8, MLM 117) to qualify as favorable under the NURE tonnage and grade requirements for favorability.

Precambrian metamorphic rocks are also unfavorable for contact metasomatic uranium deposits because of a general lack of altered shear or brecciated zones; a lack of fluorite, sulfides, or other indications of contact metasomatic mineralization; and the lack of anomalous radioactivity at any intrusive contact with the metamorphic rocks. The metamorphic rocks are unfavorable for unconformity-related uranium deposits and vein-type uranium deposits in metamorphic rocks because the metamorphic rocks of the quadrangle are in a mobile belt tectonic setting, whereas the known uranium deposits of these types are located in shield areas. The rocks are also unfavorable because of a general lack of shear zones and attendant silicification, chloritization, and hematitic alteration. The erosional surface of the metamorphic rocks is not overlain by a regional sandstone sequence, which indicates that the Precambrian metamorphic rocks are not favorable for unconformity-related uranium deposits.

The Precambrian metamorphic rocks of the quadrangle have a consistently low uranium content (4 to less than 1 ppm cU_3O_8; MLM 094, MLM 094, MLM 102). Except in the two uranium occurrences, the maximum level of uranium found in the Precambrian metamorphic rocks was 9 ppm eU (MLM 674). No anomalous radioactivity was detected on the ground or by airborne radiometric surveys.

PRECAMBRIAN INTRUSIVE ROCKS

All environments in Precambrian igneous rocks, except for those in favorable areas A, B, D, and E (Pl. 1) and those in the unevaluated Precambrian intrusive rocks in the southern Dos Cabezas Mountains, are unfavorable for uranium deposits associated with plutonic igneous rocks (Classes 310 through 380). The unfavorable rocks crop out in five areas of the quadrangle (Pl. 7). From east to west, the areas are the Silver City area, the Burro batholith, the Granite Gap area of the southern Peloncillo Mountains, the Dos Cabezas Mountains, and the Pinaleno Mountains. Although Precambrian intrusive rocks of the five areas are unfavorable for all the classes of uranium deposits associated with plutonic igneous rocks, some classes of potential uranium deposits are more probable than others. In the following discussion, specific evidence indicating unfavorability for each region will be listed only for the most probable of the possible classes in plutonic igenous rocks.

Silver City Region

Precambrian intrusive rocks of the Silver City region consist of porphyritic biotite granite, sodic muscovite granite, granite, pegmatites, and aplite (Jones and others, 1964; Woodward, 1970; Cunningham, 1974; Finnel,

1976b). The rocks are unfavorable for pegmatite-type uranium occurrences because no uranium-bearing pegmatites are known in the area; uranium-bearing pegmatites in other parts of the quadrangle are too small and too low grade to meet the NURE requirements. The area is unfavorable for magmatic-hydrothermal uranium deposits because there are no known sources for uranium-bearing hydrothermal solutions; faults and shear zones, potential depositional sites, are neither prevalent nor anomalously radioactive, nor do they have the hydrothermal-type wall-rock alteration common in areas favorable for such deposits. There are neither airborne radiometric nor HSSR anomalies in the area. There are no known uranium occurrences.

Burro Batholith

The unfavorable Precambrian intrusive rocks of the Burro batholith consist of anorthosite, diabase, monzonite and quartz monzonite, quartz diorite gneiss, biotite quartz diorite, diorite, syenite, granite, pegmatites, and aplite dikes (Hewitt, 1959; Ballman, 1960; Gillerman, 1964; Hedlund, 1978a, b, d, e, f). Further descriptions of the Precambrian intrusive rocks and the structural setting are provided in the discussions of favorable areas A, B, D, and G, which also occur in the Burro batholith.

The unfavorable Precambrian intrusive rocks of the Burro batholith contain scattered, small, uranium occurrences of three classes (Pl. 2A): magmatic-hydrothermal (Occurrences 49, 53, 54, 57, 60), pegmatitic (Occurrence 55), and authigenic (Occurrence 48). Despite the presence of some minor uranium occurrences, the Burro batholith is unfavorable for magmatic-hydrothermal uranium deposits outside favorable areas A, B, and D (Pl. 1) because of lack of sufficient uranium sources and structurally favorable depositional sites for the uranium. In essence, the magmatic-hydrothermal occurrences in the unfavorable Precambrian intrusive rocks of the Burro batholith are small, scattered outliers of the favorable areas. They are too small and scattered to contain sufficient uranium to meet the NURE tonnage and grade requirements. The area is also unfavorable for pegmatitic uranium occurrences. The rare-earth-bearing pegmatites are small, scattered, and low grade (maximum 105 ppm cU_3O_8, Occurrence 55). The area is unfavorable for authigenic and allogenic deposits because it lacks adequate depositional sites. The one authigenic occurrence (Occurrence 48) known in the unfavorable rocks is small and low grade (maximum 207 ppm cU_3O_8, MLM 020).

The discussion of the allogenic uranium deposits of area G emphasized the importance of two factors necessary for deposition--a high shear-zone density and a large area of disseminated sulfides. Although shear zones and veins containing base-metal sulfides are present in the unfavorable area, they are not sufficiently abundant to host allogenic or authigenic uranium deposits of sufficient size to meet the NURE tonnage and grade requirements. Weathering of the Precambrian rocks could have provided uranium for authigenic deposits. Despite that possibility however, the area is unfavorable because it lacks adequate depositional sites. Weathering of the granites and rare-earth-bearing pegmatites in the unfavorable areas and in the uraniferous favorable areas of the Burro batholith accounts for the HSSR anomaly located over the entire batholith, favorable and unfavorable areas alike (Pl. 4). There are no significant airborne radiometric anomalies in the unfavorable Precambrian intrusive rocks of the Burro batholith.

Granite Gap-Southern Peloncillo Mountains

Precambrian rocks of the Granite Gap area consist of amphibolite, granite porphyry, basalt dikes, and possibly pegmatites (Armstrong and others, 1978; Drewes and Thorman, 1980a, b). Although the area has undergone pervasive contact metamorphism, it is unfavorable for contact metasomatic uranium deposits primarily because a source of uranium appears to have been lacking. Samples MLM 611, 612, 613, 627, 628, and 635 did not contain anomalous amounts of uranium. Radiometric traverses of the area indicate that the samples are representative. There are no uranium occurrences and no airborne radiometric or HSSR uranium anomalies in the area.

Dos Cabezas Mountains

Except for the rocks in the unevaluated area (see discussion of unevaluated Precambrian silicic intrusive rocks, southern Dos Cabezas Mountains), the unfavorable Precambrian intrusive rocks of the Dos Cabezas Mountains consist of gneissic quartz monzonite, quartz monzonite, dacite porphyry, pegmatite, and alaskite dikes (Erickson, 1968a, 1969; Drewes, 1980). The unfavorable Precambrian intrusive rocks contain only one reported magmatic-hydrothermal uranium occurrence (Occurrence Y4, App. A). It is too small and low grade to meet NURE tonnage and grade requirements. The area is unfavorable for magmatic-hydrothermal uranium deposits because the rocks lack intense faulting and shearing and are thus structurally unfavorable. Moreover, there is no apparent source of uranium. The Precambrian rocks are intruded by numerous Laramide and post-Laramide stocks, but the stocks are mainly quartz dioritic, quartz monzonitic, and granodioritic in composition, and they commonly have low uranium contents. There are no significant airborne radiometric uranium anomalies in the area. An HSSR survey was not done on the Arizona half of the quadrangle.

Pinaleno Mountains

The unfavorable Precambrian intrusive rocks of this region are mapped as undivided granite; however, pegmatites are present. In favorable area E nearby, the Precambrian granitoid rocks range in composition from quartz monzonitic to granitic and contain Precambrian diabase dikes and sills. Outside area E, the unfavorable Precambrian intrusive rocks contain one reported uranium occurrence (Occurrence Y15; App. A) in a rare-earth-bearing pegmatite. The area is unfavorable for pegmatitic uranium deposits for the same reasons that the rest of the quadrangle is unfavorable for this class of deposit. When they are present, uranium-bearing pegmatites are too small and too low grade to meet NURE requirements. The rocks are unfavorable for magmatic-hydrothermal uranium deposits because they lack abundant fault and shear zones and a source of uranium. A source of uranium-bearing hydrothermal solutions, such as the mid-Tertiary Gillespie Quartz Monzonite, which was the source of uranium in area E, is lacking for the rest of the Precambrian intrusive rocks in the Pinaleno Mountains. No significant anomalous radioactivity was detected on the ground or by airborne radiometric surveys.

PALEOZOIC SEDIMENTARY ROCKS

All Paleozoic rocks are unfavorable for uranium deposits in sandstone (Subclasses 241 through 244) or marine black shale (Class 130). The rocks are marine and contain no apparent concentrations of carbonaceous material; the shale units in particular display no evidence of deposition under strongly reducing conditions. Except for one uranium occurrence in Bliss Sandstone (Occurrence 60, App. A), the Paleozoic rocks lack any evidence of uranium enrichment.

The Permian and Pennsylvanian Naco Group consists of an interstratified sequence of limestone, dolomite, sandstone, and siltstone. The Pennsylvanian Magdalena Group, which is restricted to the New Mexico portion of the quadrangle, consists of limestone, siltstone, and minor sandstone and conglomerate.

The Black Prince Limestone, restricted to the Arizona portion of the quadrangle, straddles the Mississippian-Pennsylvanian boundary. It consists predominantly of limestone with minor mudstone at its base. The Mississippian Paradise Formation comprises interstratified limestone, calcareous siltstone and shale, thinly bedded quartzitic sandstone, and locally conglomerate (Gillerman, 1958). The Mississippian Escabrosa Group (Escabrosa Limestone, in Arizona) consists predominantly of limestone and minor interbeds of shale.

The Devonian period is represented by the Percha Shale and the Martin Formation. The Percha consists of dark-colored shales and nodular limestone; the Martin comprises limestone and calcareous shale.

The Lower Silurian Fusselman Dolomite, present only in the eastern part of the quadrangle, is a massive cherty dolomite. It overlies the Middle to Upper Ordovician Montoya Group, which is also restricted to the eastern portion of the quadrangle. The Montoya consists of dolomite and alternating chert beds (Hayes and Cone, 1975). The El Paso Limestone trangresses the Cambrian-Ordovician boundary. It is mostly a cherty limestone or dolomite, but locally consists of sandy dolomite.

The Middle to Upper Cambrian Abrigo Formation, which is restricted to the southwest corner of the quadrangle, consists of interstratified sandstone, siltstone, shale, limestone, and sandy dolomite. Other Cambrian units, which include the Bolsa Quartzite, Coronado Sandstone, and Bliss Sandstone, consist mainly of sandstone with minor beds of siltstone, shale, and dolomite (Hayes and Cone, 1975).

In summary, the entire Paleozoic sedimentary assemblage was deposited under marine conditions varying from open-marine to beach environments. Adequate amounts of carbonaceous material are not likely to have been concentrated or preserved in those depositional environments. Moreover, effective stratigraphic controls, important in localizing sandstone-type uranium deposits, are lacking. Although dark-colored shales are common in the Paleozoic sequence, these shales are not known to be highly pyritic or bituminous; therefore, they do not reflect deposition in strongly reducing environments, which is characteristic of the uraniferous black shales.

Overall, evidence of uranium enrichment throughout the Paleozoic section is lacking. The one uranium occurrence in the Cambrian Bliss Sandstone is found within an erosional remnant of Bliss that unconformably overlies Precambrian granite. Both the granite and overlying sandstone are highly fractured along a shear zone, which provides a local depositional site for uranium and fluorine minerals. The presence of a localized concentration of uranium is the only favorable characteristic exhibited by the Bliss Sandstone. Moreover, except where locally fractured along the above-mentioned shear zone, the Bliss Sandstone exhibits no chemical, stratigraphic, or structural characteristics that would favor uranium precipitation and concentration.

CRETACEOUS SEDIMENTARY ROCKS

All Cretaceous rocks, except for the Beartooth Quartzite in area D (Pl. 1) and the unevaluated Virden Formation, are unfavorable for uranium deposits in sandstone (Subclasses 241 through 244) and in marine black shale (Class 130). The rocks are predominantly marine, but exceedingly coarse-grained, continental deposits occur locally. Sufficient amounts of carbonaceous material are not likely to have been concentrated or preserved within these marine and continental units. Moreover, there is no substantiating evidence that the shale units accumulated under strongly reducing conditions. Furthermore, there are no reported uranium occurrences or other indications, such as HSSR or ARMS anomalies, of uranium enrichment in these rocks.

The Upper Cretaceous Colorado Shale is restricted to the New Mexico portion of the quadrangle (Morrison, 1965). It comprises shale, sandstone, and minor limestone beds deposited within a shallow-marine environment.

The Lower Cretaceous Bisbee Group, which is largely restricted to the south-central and southwestern parts of the quadrangle, consists of alternating beds of limestone, sandstone, and shale that were deposited within shallow-marine environments (Gillerman, 1958). Locally, a nonmarine facies, the Glance Conglomerate, is found at the base of the Bisbee Group. The conglomerate is a poorly sorted, alluvial-fan deposit that records extensive erosion related to middle Mesozoic tectonism (Bilodeau, 1978).

CRETACEOUS BEARTOOTH QUARTZITE

The Beartooth Quartzite is unfavorable throughout the quadrangle for uranium deposits hosted by sandstones (Subclasses 241 through 244). Except for favorable area D, the Beartooth is unfavorable for magmatic-hydrothermal uranium deposits (Class 330).

The Beartooth is restricted to the northeastern quarter ot the quadrangle (Pl. 7) and consists largely of medium- to coarse-grained sandstone, commonly orthoquartzitic; pebble conglomerate interbeds are present locally. The upper part of the unit contains both sandstone and interbedded gray to black shale; the lower part locally contains a basal arkose or arkosic conglomerate. The sandstones are typically well stratified and locally have small-scale cross-bedding; they are commonly well indurated. The Beartooth reaches a maximum thickness of 47 m in the Silver City region (Cunningham, 1974) and was deposited in a transgressive epicontinental sea. Although tentatively

assigned to the Late Cretaceous, it may be equivalent to the Lower Cretaceous Dakota Sandstone (Morrison, 1965). The Beartooth unconformably overlies Precambrian to Permian rocks and is conformably overlain by the Colorado Shale. For a further description of the Beartooth Quartzite, see the discussion of area D (northern Big Burro and Little Burro Mountains).

The Beartooth in unfavorable for sandstone-type uranium deposits because it lacks internal and external sources of uranium and the internal permeability controls on solution movement that are present in fluvial sandstones. The Beartooth is also unfavorable because it is generally an oxidizing environment and lacks the widespread reducing zones necessary for sandstone-type uranium deposition. Outside area D, the Beartooth is unfavorable for magmatic-hydrothermal uranium deposits because a source of uranium-bearing hydrothermal solutions was lacking. There is usually a sequence of Paleozoic rocks present between the Precambrian rocks and the Beartooth Quartzite, except in area D. Area D is the only part of the quadrangle where both Beartooth Quartzite and a source of uranium-bearing hydrothermal solutions are present.

INTRUDED PALEOZOIC AND CRETACEOUS CARBONATE ROCKS

Paleozoic and Cretaceous carbonate rocks, which are widely intruded by Laramide and mid-Tertiary dikes and plugs, are unfavorable for magmatic-hydrothermal (Class 330) and contact metasomatic (Class 340) uranium deposits. The intrusive rocks apparently did not progress far enough in the magmatic differentiation process to have concentrated sufficient uranium to form deposits in the intruded carbonates. The carbonates are hosts for copper, lead, zinc, silver, gold, and tungsten in contact metasomatic replacement and hydrothermal-vein deposits. However, no evidence of uranium enrichment and little evidence of fluorite has been found during geologic and radiometric reconnaissance of 22 of the base- and precious-metal deposits. HSSR and ARMS studies indicate no uranium enrichment in the intruded carbonate environment.

Intruded Paleozoic and Cretaceous carbonate units, which occur in the central Peloncillo (Gillerman, 1958; Armstong and others, 1978), Dos Cabezas (Erickson, 1969), and Victorio (Thorman and Drewes, 1980) Mountains and near Santa Rita (Gillerman, 1964), were evaluated because of a possible analogy with uraniferous Paleozoic carbonates in the Bisbee area, about 60 km south of the quadrangle. There, uranium-bearing and base- and precious-metal-bearing solutions, associated with the emplacement of Jurassic-age granite stocks, mineralized highly fractured and chemically reactive Paleozoic carbonate rocks (Bryant and Metz, 1966).

Two important differences between the Bisbee and Silver City Quadrangle areas are readily apparent. The uraniferous Paleozoic carbonates near Bisbee were intruded by highly differentiated stocks of Jurassic age. Rocks intruding Paleozoic and Cretaceous carbonates in the Silver City Quadrangle are of Laramide and mid-Tertiary ages. They consist of intermediate to silicic compositions and do not represent a highly differentiated assemblage of rocks. Even the more silicic phases, which include granitic, quartz monzonitic, and rhyolitic rocks, are characterized by agpaitic coefficients ($K_2O + Na_2O/Al_2O$) of less than 1 (Armstrong and others, 1978; sample MLM 374, App. B); they lack sodic plagioclase and sodic amphiboles or pyroxenes.

LARAMIDE AND MID-TERTIARY INTRUSIVE ROCKS

All environments in the Laramide and mid-Tertiary intrusive rocks of the quadrangle, except in areas G and B and in intrusive bodies genetically associated with mid-Tertiary volcanic rocks (discussed under unfavorable mid-Tertiary rhyolitic volcanic and associated intrusive rocks), are unfavorable for uranium deposits associated with plutonic igneous rocks (Classes 310 through 380).

Laramide and mid-Tertiary intrusive bodies occur throughout the quadrangle (Pl. 7), but are especially prevalent in the Santa Rita-Silver City area (Hernon and others, 1964; Jones and others, 1964, 1970; Davis and Guilbert, 1973; Cunningham, 1974), the Burro batholith (Gillerman and Whitebread, 1956; Gillerman, 1964; Kolessar, 1970; Hedlund, 1978a, d, e, f), the southern Peloncillo Mountains (Gillerman, 1958; Armstrong and others, 1978; Drewes and Thorman, 1980a, b), the Dos Cabezas Mountains (Cooper, 1960; Erickson, 1969), and the southern Pinaleno Mountains (Swan, 1976).

Laramide intrusives range from intermediate to silicic in composition. They include andesite, andesite porphyry, diabase, quartz diorite, large amounts of monzonite and quartz monzonite porphyry, granite, and intrusive rhyolite. Age dating indicates that the Laramide-age rocks are generally between 62 and 48 m.y. old. Mid-Tertiary intrusives include hornblende andesite porphyry, plagioclase andesite porphyry, dacite porphyry, quartz latite porphyry, pegmatite granodiorite granite, and granite porphyry with rhyolite and felsite dikes. The mid-Tertiary intrusives are generally between 35 and 29 m.y. old.

Laramide intrusive plutons within the quadrangle provide mineralizing solutions that have produced a large number of metallic deposits, some of which are very large. The most important deposits are the copper porphyries, which commonly consist of copper and subsidiary molydenum disseminated throughout intrusive plutons of porphyritic granodiorite, quartz monzonite, or quartz latite. Supergene enrichment of copper porphyry deposits is common. Evidence of this type of mineralization within the quadrangle is found in the Santa Rita, Tyrone, and Lordsburg areas. Ore solutions from Laramide intrusives also formed a large number of contact-metamorphic and magmatic-hydrothermal metallic deposits in rocks, often sedimentary carbonates, adjacent to the intrusives. Ore metals include iron, copper, lead, zinc, silver, gold, and tungsten. Fluorite is also common. Mineralization associated with mid-Tertiary intrusives was similar to that associated with the Laramide intrusives, but generally resulted in smaller deposits.

In general, the Laramide to mid-Tertiary intrusive bodies are unfavorable for orthomagmatic (Class 310), pegmatitic (Class 320), autometasomatic (Class 350), authigenic (Class 360), and anatectic (Class 380) uranium occurrences because the intrusive bodies do not meet criteria (Mathews, 1978a) that would indicate that the process of silicic igneous differentiation has progressed far enough to concentrate uranium sufficient for uranium deposits. They lack pegmatitic development, have an index of igneous differentiation that is low to moderate ($K_2O + Na_2O/Al_2O_3$ of less than 1), and lack sodic amphiboles. The intrusive bodies are unfavorable for magmatic-hydrothermal (Class 370) uranium deposits because they lack uranium sources, are structurally unfavorable, or lack depositional sites for uranium. Except for

the favorable areas mentioned above, Laramide to mid-Tertiary intrusive rocks do not host any uranium occurrences (Pl. 2A, 2B; App. A), have low uranium and thorium contents (App. B and D), and have no significant airborne radiometric anomalies. An HSSR survey did not reveal any uranium anomalies that could be genetically related to Laramide and mid-Tertiary intrusive bodies.

Two classes of potential uranium deposits (magmatic-hydrothermal and allogenic) require further discussion. Although most of the Laramide and mid-Tertiary intrusive bodies in the quadrangle provide no indication that they have ever generated uranium-bearing hydrothermal solutions, a few intrusive bodies are thought to have been sources of uraniferous hydrothermal solutions (see discussions of favorable areas A, B, E, and F). Nevertheless, they are considered unfavorable. The unfavorable designation in these cases is supported by the one instance where the intrusive body postulated as a uranium source is exposed on the surface. The mid-Tertiary Gillespie Quartz Monzonite is proposed as the source of uranium-bearing hydrothermal solutions for areas E and F (Pl. 1). The stock lacks anomalous uranium concentrations and has a high thorium-to-uranium ratio (5.5, MLM 124). Unmineralized shear zones in the stock and similarly trending mineralized shears outside the stock, as well as the inferred shallow depth of intrusion of the stock (epizonal), indicate that uranium-bearing hydrothermal solutions generated by the Gillespie Quartz Monzonite left the stock. Therefore, although the stock is proposed as the uranium source for the surrounding country rocks, the stock itself is unfavorable for uranium deposits associated with plutonic igneous rocks.

With the exception of favorable area G (Pl. 1) in the Laramide quartz monzonite Tyrone laccolith, all Laramide and mid-Tertiary intrusive bodies in the quadrangle are unfavorable for allogenic deposits. In the discussion of area G, it was emphasized that three factors were necessary for deposition: country rocks adjacent to the intrusive body that could provide uranium to surficial and ground waters during the weathering cycle; faults and shear zones to permit transport of uranium-bearing solutions from the source rocks to the depositional sites within the intrusive body; and a widespread area of reductant-producing disseminated sulfides within the intrusive body. Lack of any one of the factors would result in nondeposition and unfavorability. Given these criteria, it is evident that only those Laramide to mid-Tertiary intrusive bodies within the quadrangle that contain disseminated sulfides of the porphyry copper type provide suitable depositional sites for uranium. Although all the stocks that contain disseminated sulfides are intensely sheared and faulted, none, except the Tyrone stock, are adjacent to suitable sources of uranium. The Laramide Santa Rita stock is adjacent to the Tertiary Kneeling Nun rhyolite tuff, but the tuff contains low levels of uranium (3 to 4 ppm cU_3O_8; MLM 372, MLM 373). In addition, a detailed radiometric and geochemical survey of the Santa Rita stock (Davis and Guilbert, 1973) revealed only low levels of uranium.

UPPER CRETACEOUS AND CENOZOIC INTERMEDIATE TO MAFIC VOLCANIC ROCKS

Intermediate to mafic volcanic and associated volcaniclastic rocks in the Pyramid, central Peloncillo, Summit, and Pinos Altos Mountains are unfavorable for volcanogenic uranium deposits (Classes 510, 520, 530, 540). Except for area F (Pl. 1), they are also unfavorable for magmatic-hydrothermal (Class 330) uranium deposits.

Silica-deficient magmas, from which the intermediate to mafic suite of volcanics is derived, do not generate or concentrate appreciable amounts of lithophile elements, including uranium. This inability to concentrate uranium is sufficient reason to designate the intermediate to mafic suite unfavorable for volcanogenic uranium deposits. Although the intermediate to mafic volcanic rocks may qualify as potential host rocks for magmatic-hydrothermal deposits as in area F (Pl. 1), they are not known, outside of this area, to be intruded by large leucocratic plutons and, therefore, have no demonstrated source for uranium.

Except for one uranium occurrence (Occurrence 9, App. A, Pl. 2A) in area F (Pl. 1), there are no known uranium occurrences in the intermediate to mafic volcanic rocks. Moreover, there is no indication from HSSR or ARMS surveys of any uranium enrichment in these rocks.

MID-TERTIARY RHYOLITIC VOLCANIC AND ASSOCIATED INTRUSIVE ROCKS

Mid-Tertiary rhyolitic volcanic and intrusive rocks in the Pyramid, central Peloncillo, northern Chiricahua, Winchester, and Summit Mountains and in the Santa Rita area have been judged unfavorable for volcanogenic uranium deposits (Classes 510 through 540), as well as for magmatic-hydrothermal (Class 330) uranium deposits associated with plutonic rocks. There is no evidence, either from the literature or from field studies, for the occurrence of highly differentiated peralkaline or high-silica, topaz-bearing, rhyolitic rocks within the quadrangle. Moreover, the rhyolitic rocks in the quadrangle show little evidence of being regionally enriched in uranium and apparently lack abundant lithophysae or miarolites, which commonly indicate that appreciable amounts of volatiles, and thus possibly uranium, were retained in the tuff sheets.

Although the volcanics have been largely exposed to prolonged subaerial erosional processes and resultant deep weathering, they do not appear to have been depleted of much of their original uranium, and, therefore, do not qualify as good sources of uranium for secondary uranium deposits. Moreover, suitable host rocks for such deposits are lacking.

Intrusive rocks associated with the mid-Tertiary volcanics do not appear to be highly evolved magmatic differentiates and consequently are not good source rocks for magmatic-hydrothermal uranium deposits. These intrusive rocks may have been emplaced at shallow depths, and they may have lost substantial amounts of volatiles and contained metals. Although green and clear fluorite are associated with some of the intrusives, the fluorine-bearing veins are barren in uranium and other lithophile elements, which commonly form stable complexes with fluorine.

Uranium in the Volcanogenic Environment

Geologic studies of volcanogenic uranium deposits (Pilcher, 1978) have shown that such deposits are characteristically associated with late-stage, highly differentiated volcanic rocks or their cogenetic intrusives. The magmatic differentiation that engenders such highly evolved rocks is also capable of generating and concentrating uranium-rich volatiles and solutions.

Moreover, postemplacement high-temperature devitrification and vapor-phase crystallization may liberate uranium from the glasses, redistribute it, and further concentrate it, commonly in lithophysal or miarolitic cavities.

Ore-grade deposits of uranium and commonly other lithophile elements are associated with voluminous, highly evolved peralkaline volcanic and associated rocks (Goodell, 1978; Wallace and Roper, 1980) that originated from large cauldron complexes within taphrogenes. In the western United States, such taphrogenes are commonly Basin and Range relaxation features. Anomalously uraniferous rocks are also associated with much smaller, silica- and fluorine-rich, topaz-bearing, rhyolitic dome-and-flow complexes (Burt and Sheridan, 1980) that are commonly found within the same tectonic setting as the larger peralkaline cauldron complexes.

The mid-Tertiary volcanic environments of the Silver City Quadrangle were evaluated for four types of volcanogenic uranium deposits, as well as for magmatic-hydrothermal deposits associated with comagmatic intrusives. Uranium, concentrated by both magmatic and high-temperature crystallization processes, may occur in the highly differentiated volcanic and intrusive rocks as initial magmatic (Class 510), pneumatogenic (Class 520), or hydroauthigenic (Class 530) uranium deposits. Furthermore, uranium may have been leached from these rocks and redistributed by meteoric waters and further concentrated in secondary hydroallogenic (Class 540) deposits within host rocks associated with the volcanic complex. Finally, hydrothermal solutions from intrusive phases may produce magmatic-hydrothermal uranium vein or replacement deposits (Class 330).

Uranium Favorability for Volcanogenic Uranium Deposits

The predominantly rhyolitic to quartz latitic ash-flow tuffs and lavas that compose the Pyramid Mountain Volcanic Complex and Rimrock Mountain Group in the Pyramid Mountains (Deal and Elston, in preparation); the Weatherby Canyon Ignimbrite, Steins Mountain Quartz Latite Porphyry, and Quarry Peak Rhyolite in the central Peloncillo Mountains (Gillerman, 1958); the Faraway Ranch Formation in the northern Chiricahua Mountains (Fernandez and Enlows, 1966); unnamed rhyolitic rocks in the Winchester Mountains (Creasey and Krieger, 1978); the Noah Mesa tuff and other unnamed tuffs in the Summit Mountains (Wahl, 1980); and the Kneeling Nun Tuff in the Santa Rita area (Elston and others, 1975; Giles, 1968) represent, for the most part, a calc-alkaline suite of rocks. These rocks are all peraluminous, having agpaitic coefficients less than 1 (Table 5). Mineralogically, they consist of varying amounts of plagioclase, sanidine, quartz, and biotite. The composition of the plagioclase is characteristically in the andesine- oligoclase range; no sodic-rich amphibole or pyroxene minerals have been reported. Two units, the Weatherby Canyon Ignimbrite and the Rimrock Mountain Group, have comparatively high silica (SiO_2) and alkali contents (MLM 309, 320, 321, 377, 380; Table 5) relative to the other rhyolitic rocks evaluated. These apparently more highly differentiated rocks are more alkaline than the typical calc-alkalic suite of rhyolitic volcanics, but they, like the calc-alkalic rocks, have agpaitic coefficients less than 1 and lack sodic-rich plagioclase, amphiboles, or pyroxenes. However, there are no high-silica, topaz-bearing rhyolites known to be associated with these higher silica suites of rocks.

TABLE 5. SELECTED ANALYTICAL AND PETROGRAPHIC DATA FOR MIDDLE TERTIARY RHYOLITIC VOLCANIC AND ASSOCIATED SEDIMENTARY AND INTRUSIVE ROCKS

Area	Sample no.	Rock name (description)	SiO_2	K_2O	Na_2O[1]	Agpaitic coefficient	Chemical U_3O_8 cU_3O_8 (ppm)	Radiometric eU (ppm)	Radiometric eTh (ppm)	Fluorine (ppm)
Pyramid Mountains (Muir Cauldron Rocks)	MLM 316	Flow-banded latite	78.02	3.97	3.40	0.73	1	3	22	<200
	MLM 311	Quartz monzonite	66.07	3.59	3.80	0.67	2	4	17	284
	MLM 304	Fresh water limestone	---	--	--	--	4	2	4	---
	MLM 317	Dacite	76.40	4.16	4.04	0.76	2	3	21	353
	W76-27[2]	Rhyolite	72.59	5.10	4.08	0.84	-	-	--	---
Pyramid Mountains (Post Cauldron Rocks)	MLM 320	Latitic crystal-vitric tuff	77.73	4.76	3.55	0.92	5	5	33	964
	MLM 309	Rhyolitic to quartz latitic crystal-vitric tuff	81.02	4.69	3.51	0.89	3	4	20	<200
	MLM 321	Rhyolitic crystal-vitric tuff	77.91	4.46	3.35	0.86	6	6	30	2094
Central Peloncillo Mountains	MLM 377	Silicified (quartz?) latitic crystal-vitric tuff	79.74	9.86	0.77	--	9	9	31	351
	MLM 380	Silicified Rhyolitic? vitric-crystal tuff	78.12	9.50	1.54	--	9	9	53	3240
	MLM 388	Quartz latite porphyry (field name)	76.40	4.45	3.30	0.77	5	4	25	330
	MLM 389	Rhyolitic vitric-crystal tuff (field name)	78.08	3.90	3.22	0.73	1	3	17	259

TABLE 5. SELECTED ANALYTICAL AND PETROGRAPHIC DATA FOR MIDDLE TERTIARY RHYOLITIC VOLCANIC AND ASSOCIATED SEDIMENTARY AND INTRUSIVE ROCKS (Continued)

Area	Sample no.	Rock name (description)	SiO_2	K_2O	Na_2O[1]	Agpaitic coefficient	Chemical U_3O_8 cU_3O_8 (ppm)	Radiometric eU (ppm)	Radiometric eTh (ppm)	Fluorine (ppm)
Winchester Mountains	MLM 356	Silicified, flow-banded rhyolite(?)	76.10	5.68	0.39	---	11	9	26	208
Summit Mountains	A67[3]	Rhyolitic ash-flow tuff	75.87	5.39	3.68	0.89	--	-	--	---
	TUR[3]	Rhyolitic ash-flow tuff	74.90	5.57	3.18	0.88	--	-	--	---
	MLM 394	Rhyolitic vitric-crystal tuff (vitrophyre)	75.82	4.52	2.45	0.68	8	7	35	330
	MLM 390[4]	Porphyritic rhyolite	78.95	7.86	0.54	---	5	4	31	---
	MLM 391[5]	Flow-banded rhyolite	74.33	5.76	2.39	0.73	3	3	17	---
Northern Chiricahua Mountains	MLM 341	Quartz monzonite(?)	---	---	---	---	25	36	54	---
	MLM 344	Fresh-water limestone	---	---	---	---	16	12	2	---
	MLM 345	Trachytic vitric tuff	75.81	5.25	2.67	0.79	3	4	16	559
	MLM 347	Lithic arenite	---	---	---	---	2	4	8	---
	MLM 349	Silicified vitric tuff	74.11	3.54	3.62	0.78	2	5	22	406
	MLM 350	Altered quartz monzonite	55.76	4.64	4.17	0.67	<1	3	9	1167
	MLM 353	Quartz monzonite granophyre(?)	73.98	4.46	4.10	0.86	2	4	13	500

TABLE 5. SELECTED ANALYTICAL AND PETROGRAPHIC DATA FOR MIDDLE TERTIARY RHYOLITIC VOLCANIC AND ASSOCIATED SEDIMENTARY AND INTRUSIVE ROCKS (Continued)

Area	Sample no.	Rock name (description)	SiO_2	K_2O	Na_2O[1]	Agpaitic coefficient	Chemical U_3O_8 (U_3O_8 (ppm)	Radiometric eU (ppm)	Radiometric eTh (ppm)	Fluorine (ppm)
Santa Rita	Spec. 413	Rhyolitic tuff	71.23	4.81	3.50	0.86	--	-	--	---
	MLM 372	Crystal-vitric tuff	70.60	6.21	5.93	1.10	4	4	20	549
	MLM 375	Quartz-latitic crystal-vitric tuff	73.72	5.66	3.68	0.95	4	4	20	442
	MLM 374	Silicified flow-banded latite	73.32	5.30	3.30	0.85	2	2	4	397

[1] Refer to Appendix B or cited references for complete chemical analyses.

[2] Deal and Elston (in preparation)

[3] Wahl (1980)

[4] Major oxide determination of sample TP-6 (Wahl, 1980)

[5] Major oxide determination of sample V-23 (Wahl, 1980)

[6] Elston (1957)

The ash-flow tuffs, which vary from nonwelded to densely welded, commonly show evidence of spherulitic or axiolitic devitrification within the groundmass. However, the apparent lack of lithophysae or miarolitic cavities in any of the tuffs studied is interpreted to mean that substantial amounts of volatiles, and thus possibly uranium, were not retained after crystallization of the tuffs.

The results of rock sampling and HSSR and ARMS surveys indicate that the mid-Tertiary volcanic and associated rocks are not regionally enriched in either uranium or other lithophilic elements. Furthermore, a comparison of chemical-uranium and equivalent-uranium contents of the volcanic rocks (Table 5) reveals that uranium has not been appreciably depleted from these rocks as a result of chemical weathering, thus decreasing the likelihood of forming concentrations of secondary uranium in hydroallogenic (Class 340) deposits in rocks associated with the rhyolitic volcanic assemblage. Walton and others (1980) arrived at this same conclusion as a result of their studies of volcanic rocks in southwestern New Mexico.

Not only potential uranium-source rocks, but also possible host rocks for hydroallogenic deposits are lacking. Field studies throughout the mid-Tertiary volcanic complexes indicate that possible host rocks for hydroallogenic uranium deposits occur only within the Pyramid Mountains, and these rocks, it was determined, lack favorable characteristics. In the Pyramids, a 30-m-thick sequence of interbedded pumiceous conglomerate, laminated fine-grained clastics, fresh-water limestone, and chert occurs locally. These sediments, which are interbedded with rhyolitic ash-flow tuffs and lavas of the Muir Cauldron, have been interpreted as moat deposits by Deal and Elston (in preparation). These moat sediments do not contain carbonaceous material or any other apparent means of reducing or concentrating uranium. Moreover, these sediments, which contain little uranium (MLM 304, Table 5), appear highly oxidized and are relatively steeply dipping (15° to 25°).

In summary, the rhyolitic volcanic and associated rocks are judged unfavorable for all types of volcanogenic uranium deposits because of the absence of peralkaline or high-silica, topaz-bearing rhyolites, the apparent scarcity of lithophysae or miarolites in the tuffs or lavas, lack of evidence for regional enrichment of uranium or other lithophile elements in these volcanic rocks, and lack of suitable sedimentary host rocks associated with the volcanic assemblage.

Uranium Favorability for Magmatic-Hydrothermal Deposits

Intrusive rocks associated with the mid-Tertiary rhyolitic volcanic complexes consist primarily of dikes, small domes, and plugs. A composite stock, possibly associated with a resurgent stage of the Muir Cauldron, occurs in the Pyramid Mountains (Deal and Elston, in preparation).

The dikes, domes, and plugs are similar in terms of mineralogy and chemistry to the associated volcanic suite. The intrusives range from latite to rhyolite. The more felsic rocks are characterized by phenocrysts of plagioclase (ranging from andesine to oligoclase), sanidine, quartz, and biotite. The plagioclase is not soda rich, and no soda-rich pyroxenes or amphiboles occur. Agpaitic coefficients of the more felsic units are

significantly lower than 1 (MLM 316, 376, 390, 391; Table 5). The composite stock consists of granodioritic and monzonite porphyry (MLM 311, Table 5) phases and thus does not represent a highly differentiated intrusive body.

Although the intrusive rocks commonly show evidence of minor to strong argillic alteration, there is generally little evidence in the country rock for extensive hydrothermal alteration, quartz veins, or metal deposits associated with the emplacement of these intrusives. An important exception to this, however, is found in the Steeple Rock area where rhyolitic dikes, intruded along northwest-trending faults, are associated with strong hydrothermal alteration and base- and precious-metal deposits (Powers, 1976; Biggerstaff, 1974). Green to clear fluorite is commonly found in these veins also. Rock sampling and ground radiometric traverses in the Steeple Rock area and in other areas of mid-Tertiary intrusives revealed no evidence for enrichment of uranium or other lithophile elements, such as Be, Li, Mg, Mo, W, that are commonly associated with uranium. Lack of evidence of extensive hydrothermal alteration and metal deposits (except in the Steeple Rock area) associated with exposed mid-Tertiary intrusive rocks may indicate that the rocks were emplaced at relatively shallow depths with a resultant, substantial loss of mineralizing volatiles and, thus, loss of metals.

In summary, the intrusive rocks do not represent a highly differentiated suite of rocks and, therefore, are not likely to have generated enough uranium to form magmatic-hydrothermal deposits. Moreover, these granodioritic to peraluminous rhyolitic rocks, for the most part, are not known to be associated with extensive hydrothermal alteration, quartz veins, or metal deposition. In those rare cases where green to clear fluorite was found to be associated with intrusive bodies, there was absolutely no evidence of uranium enrichment.

UPPER CENOZOIC BASIN-FILL SEDIMENTS

Areas of exposed Late Cenozoic basin-fill sediments in the upper Safford Basin (Harbour, 1966), the Duncan basin (Morrison, 1965), and the Mangas Valley (Leopoldt, in preparation) are, except for area C (Pl. 1), unfavorable for uranium deposits associated with either sandstone (Subclasses 241 through 244) or volcaniclastic lacustrine environments of the hydroallogenic class (Class 540). These locally derived, basin-fill deposits lack a demonstrated source of uranium; they are flanked by ranges or fault blocks consisting largely of uranium-poor, intermediate to mafic volcanic rocks. Furthermore, the sediments accumulated either as alluvial-fan deposits or within shallow, ephemeral lakes and associated oxidizing flood plains--environments that commonly do not favor the development of any chemical, stratigraphic, or structural means of concentrating or preserving uranium. These basin-fill sediments have been deeply dissected and widely oxidized as a result of predominantly degradational processes active since the early Pleistocene.

Although one localized area of anomalous radioactivity was found in the Mangas Valley (MLM 365, Table 6), ground radiometric traverses and rock sampling revealed little additional evidence of uranium enrichment in the basin-fill sediments (Table 6). There is no indication from ARMS and HSSR surveys of regional enrichment in uranium.

TABLE 6. SELECTED ANALYTICAL DATA FOR UPPER CENOZOIC BASIN-FILL ROCKS

Area	Sample no.	Rock name	Chemical U_3O_8 cU_3O_8 (ppm)	Radiometric eU (ppm)	Radiometric eTh (ppm)
Upper Safford Basin	MLM 337	vitric tuff	15	4	9
	MLM 338	mudstone	8	3	13
	MLM 339	mudstone	8	6	9
Duncan Basin	MLM 368	marl	2	5	8
	MLM 369	mudstone	2	6	10
Mangas Valley	MLM 365	mudstone	60	46	23
	MLM 366	mudstone	4	8	9
	MLM 367	vitric tuff	3	6	3
	MLM 376	chert	11	10	4

QUATERNARY SEDIMENTARY DEPOSITS

Quaternary sedimentary deposits, which consist largely of unconsolidated to poorly consolidated gravel, sand, silt, and clay, are unfavorable for uranium deposits in sandstone (Subclasses 241 through 244) and volcaniclastic lacustrine environments of the hydroallogenic class (Class 540). These widely oxidized sedimentary units, which represent pediment and terrace deposits, alluvial-fan aprons, valley alluvium, and minor playa and eolian sediments, lack any apparent reductants or stratigraphic or structural characteristics that would enhance the concentration and preservation of uranium.

UNEVALUATED ENVIRONMENTS

PRECAMBRIAN SILICIC INTRUSIVE ROCKS, SOUTHERN DOS CABEZAS MOUNTAINS

Precambrian silicic intrusive rocks in the southern flank of the Dos Cabezas Mountains (Pl. 7) are unevaluated because of conflicting data. The unevaluated environment consists primarily of Dos Cabezas rapakivi quartz monzonite (1380 m.y.; Erikson, 1969) and includes the Eaton and Cienega gneisses (Erickson, 1968a). Although all three rock units are quartz monzonites, there is considerable textural variation. The Eaton gneiss is a coarse-grained granitoid gneiss whose foliation is marked by subparallel clots of biotite. The Cienega gneiss is a medium-grained, weakly porphyritic gneiss whose foliation is marked by alignment of feldspar phenocrysts. The Dos Cabezas rapakivi quartz monzonite contains mixed rimmed and unrimmed euhedral plagioclase and subhedral potash feldspar phenocrysts up to 6 cm across in a coarse-grained groundmass. The Precambrian quartz monzonite intrudes Pinal Schist. There are Laramide and mid-Tertiary silicic intrusive bodies within the Dos Cabezas Mountains less than 20 km away.

The unevaluated environment contains three uranium occurrences (Pl. 2a) hosted by faults and shear zones, two of which are described in uranium-occurrence reports (Occurrences 1 and 2, App. C). Occurrence 1 is a minor occurrence (16 pp cU_3O_8, 31 ppm eU, 525 ppm eTh; MLM 138), but Occurrence 2 contains at least 198 ppm cU_3O_8, 152 ppm eU, 1,586 ppm Th, and 4,600 ppm F (MLM 134). Furthermore, a U.S Atomic Energy Commission Preliminary Reconnaissance Report (Miller, 1955) listed high uranium contents in drill core from Occurrence 2. These values are 0.53% eU_3O_8 and 0.32% cU_3O_8 in 1.0 ft of core from a depth of 150 ft, and 1.27% eU_3O_8 and 1.09% cU_3O_8 in 1.5 ft of core from a vein intercept at a depth of 190 ft. These grades of uranium would approach NURE tonnage and grade requirements. They certainly indicate favorability for this environment.

However, Texasgulf, Inc., cleaned out the drill holes at the Uranium Hills Claim that were reported to contain high uranium values. Texasgulf found less than 0.01% uranium in the mineralized zones and also drilled two nearby offsets that failed to penetrate any uranium mineralization whatsoever. Texasgulf concluded that the reported subsurface uranium values from the Uranium Hill Claims are false (W. Glenn Culver, written comm., 1980). More data are needed for evaluation of this environment.

VIRDEN FORMATION

The Upper Cretaceous Virden Formation (Elston, 1960) and equivalent unnamed strata (Morrison, 1965) comprise nonmarine shale, sandstone, and conglomerate that are restricted to a relatively small area in the north-central part of the quadrangle. Although the Virden reportedly contains carbonaceous material and some tuffaceous sandstone beds, it is widely faulted and commonly dips at angles of 30° or more. Because of its areal restriction and excessively high dips, the Virden Formation was originally assigned a low priority for field study. The unit remains unevaluated because of time constraints.

PELONCILLO, WHITLOCK, AND PINALENO MOUNTAINS

The north-central and northern Peloncillo and adjacent Whitlock Mountains and the southern Pinaleno Mountains consist primarily of Tertiary volcanic rocks. Although the rocks in these areas are currently being studied by the U.S. Geological Survey, there is no information presently available about them other than they have been divided into felsic and intermediate to mafic volcanic suites (Wynn, 1981). Because of lack of data these areas remain unevaluated.

NORTHERN CHIRICAHUA MOUNTAINS

Rhyolite Canyon Formation

Parts of the mid-Tertiary Rhyolite Canyon Formation in the Douglas Quadrangle are favorable for hydroauthigenic (Class 530) and hydroallogenic (Class 540) uranium deposits. The Rhyolite Canyon in the Silver City Quadrangle is restricted almost entirely to the Chiricahua National Monument (Marjaniemi, 1970; Sabins, 1957), however, and was not evaluated because geologic studies in lands administered by the National Park Service were prohibited (Pl. 13). The unit remains unevaluated in the Silver City Quadrangle because of lack of data.

Faraway Ranch Formation

A sequence of well-sorted, thin-bedded, olive-green to brown sandstones and fetid, cherty limestones is exposed in Keating Canyon (Pl. 15) in the northern Chiricahua Mountains. Sabins (1957) placed this sedimentary sequence in the Faraway Ranch Formation, but its exact stratigraphic position within the formation was not determined. The sequence probably does not exceed 30 m in thickness. No carbonaceous material was seen in the sedimentary units but 0.05% to 0.11% organic carbon (MLM 344, 345, 347, App. B) was detected chemically.

A relatively thick, organic-carbon-bearing sedimentary sequence that is interlayered with rhyolitic to rhyodacitic rocks of the Faraway Ranch Formation could be favorable for hydroallogenic (Class 540) uranium deposits. Inadequacy of the data precludes evaluation of this sequence at this time.

SCHOOLHOUSE MOUNTAIN REGION

The Schoolhouse Mountain region encompasses an area of about 180 km (Wahl, 1980). The area contains a thick sequence of Oligocene rhyolitic ash-flow tuffs, moat deposits, and minor intrusive phases that may have been derived from the proposed Schoolhouse Mountain Cauldron (Wahl, 1980). The area was not evaluated because time constraints precluded the gathering of enough data. However, a uranium occurrence (Occurrence 25, App. A, Pl. 2) was found during this project.

The uranium occurrence is in a highly altered tuff of the Schoolhouse Mountain Formation(?) adjacent to a northwest-trending, strongly limonite- and manganese-stained, intermediate porphyritic dike. Moderate to strong alteration was observed throughout the area of the uranium occurrence. This alteration may be related to the hydrothermal activity that causes numerous hot springs and wells in the Cliff-Gila area as shown by Summers (1979).

TERTIARY BASINS

Tertiary rocks and sediments in basins underlying such prominent valleys as San Simon, Sulfur Springs, Animas, Mangas, and Mimbres-Palomas Valleys were not evaluated because of extensive alluvial cover and lack of subsurface data. Theoretically, enormous amounts of uranium may have been leached from adjacent mid-Tertiary felsic volcanic and Precambrian granitic ranges and transported into the hydrologic regime of these basins. It is possible that uranium deposits similar to those of the Artillery Mountains-Date Creek Basin region (Sherborne and others, 1979) are present in the basins. However, inadequate knowledge about the nature of the basin fill precludes evaluation.

QUATERNARY CALCRETE ENVIRONMENTS

Calcrete deposits in the San Simon Valley and in the Mimbres-Palomas basin near the eastern boundary of the quadrangle were studied as part of a favorability evaluation of calcretes in the southwestern United States (Carlisle, 1978). Therefore, the calcretes were not evaluated during this study.

Carlisle (1978) found thin, surficial calcrete exposed in the axial parts of San Simon Valley and calcrete associated with soils in parts of the Mimbres-Palomas basin. He concluded that all calcretes examined were pedogenic and that they do not compare favorably with the carnotite-bearing valley calcretes of western Australia and southwest Africa.

INTERPRETATION OF RADIOMETRIC AND HYDROGEOCHEMICAL AND STREAM-SEDIMENT DATA

RADIOMETRIC DATA

The analysis of ARMS data by Texas Instruments Corporation (1978b) resulted in the identification of 226 anomalies of high statistical

significance. These "first-priority" anomalies are characterized by having simultaneous, statistically valid equivalent-uranium, equivalent-uranium/equivalent-thorium, and equivalent-uranium/equivalent-potassium anomalies and therefore represent the most probable targets for uranium enrichment.

This information, interpreted within the context of the regional geology, formed the basis for the delineation of 19 areas of possible uranium enrichment in the quadrangle (Pl. 3). Selected radiometric anomalies within those areas were field evaluated by means of outcrop examination and radiometric traverses to gather information about the validity and significance of these apparent anomalies. Of the 19 areas depicted, three (areas 2, 5, and 8) are associated with clusters of known uranium occurrences, two (areas 6 and 12) are associated with slightly uranium-enriched mid-Tertiary intrusive (MLM 341, App. B; 25 ppm cU_3O_8) and volcanic (MLM 380, App. B; 9 ppm cU_3O_8) rocks, and two (areas 11 and 13) are invalid anomalies related to cultural features not shown on our base map. The remainder of the apparently anomalously radioactive areas were determined to represent nothing more than the normal uranium contents of contrasting rock types, or surficial deposits derived therefrom, which are not adequately differentiated on the generalized geologic base map used in analysis and interpretation of radiometric data.

GEOCHEMICAL DATA

One area, which encompasses much of the southern Big Burro Mountains, was determined to be favorable (Pl. 4) on the basis of HSSR data. This area is characterized by high uranium values in both stream sediments and ground waters, by high uranium-to-conductivity ratios, and by high uranium-versus-conductivity residuals. The last parameter indicates that uranium contents of ground waters are higher than can be predicted by their conductivities.

Geologic and geochemical evaluation during this study of the anomalies and surrounding areas in the Big Burro Mountains indicates that the anomaly is a result of two factors. The first is the multiple sources of uranium available to the near-surface weathering environment, and the second is the lack of any geologic environment in the area that would impede the movement of uranium transported by near-surface and surface waters. Surficial weathering processes derive uranium from several sources in the area. One source is the uranium deposits of favorable area A (Pl. 1). Outside favorable area A, the major source of mobile uranium to the near-surface environment is the weathering of the Precambrian Burro Mountains granite. As mentioned in the discussion of favorable area G, the Burro Mountains granite has a high uranium content (6 to 7 ppm cU_3O_8; MLM 021, 022, 025), and has thorium-to-uranium ratios of between 6.2 and 12.8. The high uranium content indicates that the Burro Mountains granite could have been a good source of uranium. The high thorium-to-uranium ratios indicate that uranium has been removed from the granite by weathering processes. The weathering processes and the liberation of uranium from the granite would be especially effective in an area of high topographic relief, such as that on the southwestern side of the Burro Mountains. Additional sources of uranium are the scattered uranium occurrences of the region outside area A. They include vein-type (Occurrences 49, 53, 54, 57, Pl. 2A) and pegmatitic occurrences (Occurrence 55).

Weathering of the granite and the pegmatites would provide substantial amounts of radioactive heavy-mineral resistates. The discussions of areas A and G have pointed out that once uranium is liberated, there is no geologic environment in the Precambrian rocks of the southern Burro Mountains that would immobilize the uranium transported in the surficial and near-surface oxidizing environments. Given the trace content of apatite in the granite and the lack of carbonates in the near-surface environment, uranium is probably transported as $UO_2(HPO_4)_2^{-2}$ complexes (Langmuir, 1978).

The numerous ground-water anomalies detected in the Animas Valley (Sharp and others, 1978) are not, however, so important as indicators of uranium enrichment as those in the favorable area. A comparative analysis of uranium values and corresponding conductivity values for ground waters show that all ground-water samples with high uranium contents in the Animas Valley also have high conductivity values. This indicates that the elevated uranium values are related to high amounts of dissolved solids in the water. Hence, elevated uranium values in ground waters do not necessarily indicate significant uranium enrichment in the aquifer (Wenrich-Verbeeck and others, 1980).

RECOMMENDATIONS TO IMPROVE EVALUATION

DRILLING PROGRAMS

Drilling is recommended to improve the evaluation of all seven favorable areas (Pl. 1), as well as to evaluate the Precambrian silicic intrusive rocks in the southern Dos Cabezas Mountains and the basin-fill deposits in the Tertiary basins. In area A, the depth to which the uranium-bearing veins extend is unknown. The primary ore-mineral suite of the veins is also uncertain. Knowledge of the primary ore-mineral suite and ore paragenesis of the veins would result in more accurate determinations of hypogene ore grade, sequence of ore deposition, and ultimately age and origin of the episode of uranium mineralization which formed the veins.

Drilling in area B would provide subsurface information on uranium grades in the hydrothermal veins at depth. Present information of uranium content is limited to mine-dump samples and a few shallow subsurface samples. At present, it appears that uranium ore grade may increase with depth. Drilling would determine if this increase of grade with depth is true and would also give indications of the vertical extent of the uranium-bearing veins.

Subsurface extent of favorable tuffaceous rocks in area C is not known. The oxidized surface rocks, which locally contain substantial uranium concentrations, may extend basinward at depth. Evidence for a redox boundary in the deeper parts of the basin should be sought by way of a wide-spaced drilling program in the eastern halves of T. 8 S., R. 28 E., T. 9 S., R. 28 E., and T. 10 S., R. 28 E.

Shallow drilling (less than 100 m) is recommended in the Beartooth Quartzite of area D near mineralized shear zones to determine the lateral extent and grade of uranium present in the Beartooth away from the shear zones. Such drilling is recommended in the Wild Horse Mesa region (Pl. 8) of area D1.

Secondary uranium minerals or unidentified uranium compounds occur in shear and fault zones in Precambrian granite and overlying Tertiary volcanic rocks in areas E and F. Drilling of one or more of the mineralized shear or fault zones would determine the hypogene ore-mineral suite, grade of the hypogene uranium at depth, and vertical extent of the uranium mineralization in the shear zones.

The vertical extent, ore-mineral suite, and grade of the allogenic uranium occurrences of area G are unknown. Theoretical considerations indicate that ore grade may increase at depth where primary sulfides deposited by the episode of porphyry copper mineralization in the area are present. Drilling (probably to a depth of less than 300 m) would determine if this is true or if the allogenic occurrences of area G are noneconomical surficial occurrences.

The Precambrian silicic intrusive rocks of the southern Dos Cabezas Mountains were unevaluated because of conflicting subsurface information. A drilling program in the area of Occurrence 2 would resolve this conflict.

Stratigraphic test-hole drilling is recommended for the largely unevaluated Tertiary basins. Felsic volcanic and Precambrian granitic detritus, which theoretically are good sources of uranium, are a major constituent of the basin-fill sediments. Rocks containing carbonaceous material may be present at depth. Subsurface data gathered through drilling would be used in the evaluation of the basins.

ARMS STUDY

Interpretation of ARMS data may be significantly improved if a more detailed geologic map were used in the statistical analysis of data. The U.S. Geological Survey has been involved in extensive geologic mapping throughout the Silver City Quadrangle in preparation for publication of a 1:250,000-scale map of the quadrangle. Although much of this information is not yet available, a reinterpretation of the ARMS data should be made after the information is published.

HSSR SAMPLING

Stream-sediment and ground-water samples should be collected in the Arizona portion of the quadrangle. Only the New Mexico portion was sampled during the HSSR survey. The sample-site density in Arizona should be approximately the same as that used in the New Mexico part of the quadrangle (Sharp and others, 1978).

SELECTED BIBLIOGRAPHY

Aiken, C. L. V., 1978, Gravity and aeromagnetic anomalies of southeastern Arizona, in Callender, J. F., Wilt, J. C., and Clemons, R. E., eds., Land of Cochise): New Mexico Geological Society Guidebook, 29th Field Conference, p. 301-313.

Aldrich, M. J., Jr., 1972, Tracing a subsurface structure by joint analysis, Santa Rita-Hanover axis, southwestern New Mexico: Albuquerque, University of New Mexico, Ph.D. dissertation, 106 p.

Armstrong, A. K., and Mamet, B. L., 1978, The Mississippian system of southwestern New Mexico and southeastern Arizona, in Callender, J. F., Wilt, J. C., and Clemons, R. E., eds., Land of Cochise: New Mexico Geological Society Guidebook, 29th Field Conference, p. 183-192.

Armstrong, A. K., Silberman, M. L., Todd, V. R., Hoggatt, W. C., and Carten, R. B., 1978, Geology of central Peloncillo Mountains, Hidalgo County, New Mexico: New Mexico State Bureau of Mines and Mineral Resources Circular 158, 19 p.

Austin, S. R., and D'Andrea, R. F., Jr., 1978, Sandstone-type uranium deposits, in Mickle, D. G., and Mathews, G. W., eds., Geologic characteristics of environments favorable for uranium deposits: U.S. Department of Energy Open-File Report GJBX-67(78), p. 87-120.

Bain, G. W., 1950, Geology of the fissionable material: Economic Geology, v. 45, p. 273-323.

Ballman, D. L., 1960, Geology of the Knight Peak area, Grant County, New Mexico: New Mexico Bureau of Mines and Mineral Resources Bulletin 70, 39 p.

Biggerstaff, B. P., 1974, Geology and ore deposits of the Steeple Rock-Twin Peaks area, Grant County, New Mexico: El Paso, University of Texas, M.S. thesis, 102 p.

Bilodeau, W. L., 1978, The Glance Conglomerate, a lower Cretaceous syntectonic deposit in southeastern Arizona, in Callender, J. R., Wilt, J. C., and Clemons, R. E., eds., Land of Cochise: New Mexico Geological Society Guidebook, 29th Field Conference, p. 209-214.

Bornhurst, T. J., Elston, W. E., Della Valle, R. S., and Balagna, J. P., 1980, Distribution of uranium in mid-Tertiary volcanic rocks, Mogollon-Datil volcanic field New Mexico [abs.]: Southwest Section, American Association of Petroleum Geologists Annual Meeting, El Paso, Texas, Proceedings, p. 17.

Bryant, D. G., and Metz, H. E., 1966, Geology and ore deposits of the Warren mining district, in Titley, S. R., and Hicks, C. L., eds., Geology of the porphyry copper deposits, southwestern North America: University of Arizona Press, Tucson, p. 189-203.

Burt, D. M., and Sheridan, M. F., 1980, Uranium mineralization in fluorine-enriched volcanic rocks: U.S. Department of Energy Open-File Report GJBX-225(80), 494 p.

Carlisle, D., 1978, The distribution of calcretes and gypcretes in southwestern United States and their uranium favorability: U.S. Department of Energy Open-File Report GJBX-29(78), 274 p.

Clay, D. W., 1960, Late Cenozoic stratigraphy in the Dry Mountain area, Graham County, Arizona: Tucson, University of Arizona, M.S. thesis, 68 p.

Condie, K. C., and Budding, A. J., 1979, Geology and geochemistry of Precambrian rocks, central and south-central New Mexico: New Mexico Bureau of Mines and Mineral Resources Memoir 35, 56 p.

Coney, P. J., and Reynolds, S. J., 1980, Cordilleran metamorphic core complexes and their uranium favorability: U.S. Department of Energy Open-File Report GJBX-258(80), 627 p.

Cooper, J. R., 1960, Reconnaissance map of the Willcox, Fisher Hills, Cochise, and Dos Cabezas Quadrangles, Cochise and Graham Counties, Arizona: U.S. Geological Survey Mineral Investigations Field Studies Map MF-231, scale 1:62,500.

Creasey, S. E., and Krieger, M. H., 1978, Galiuro Volcanics, Pinal, Cochise, and Graham Counties, Arizona: U.S. Geological Survey Journal of Research, v. 6, no. 1, p. 115-131.

Crittenden, M. D., Coney, P. J., Davis, G. H., eds., 1980, Cordilleran metamorphic core complexes: Geological Society of America Memoir 153, 490 p.

Cunningham, J. E., 1974, Geologic map and sections of Silver City Quadrangle, New Mexico: New Mexico Bureau of Mines and Mineral Resources Geologic Map 30, scale 1:24,000.

Davidson, E. S., 1962, Origin of sediments in the intermontane Safford Basin, Graham County, Arizona: Geological Society of America Special Paper 68, 18 p.

Davis, J. D., and Guilbert, J. M., 1973, Distribution of the radioelements potassium, uranium, and thorium in selected porphyry copper deposits: Economic Geology, v. 68, no. 2, p. 145-160.

Deal, E. G., and Elston, W. E., in preparation, Geology of the Lightning Dock KGRA and vicinity, Pyramid Mountains and Animas Valley, Hidalgo County, New Mexico: New Mexico Bureau of Mines and Mineral Resources Circular 177.

Deal, E. G., Elston, W. E., Erb, E. E., Peterson, S. L., Reiter, D. E., and Damon, P. E., 1978, Cenozoic volcanic geology of the Basin and Range Province in Hidalgo County, southwestern New Mexico, in Callender, J. F., Wilt, J. C., and Clemons, R. E., eds., Land of Cochise: New Mexico Geological Society Guidebook, 29th Field Conference, p. 219-229.

DeVoto, R. H., 1978, Uranium geology and exploration: Golden, Colorado School of Mines, 396 p.

Drewes, Harald, 1978, The Cordilleran orogenic belt between Nevada and Chihuahua: Geological Society of America Bulletin, v. 89, p. 641-657.

-----1980, Tectonic map of southeast Arizona: U.S. Geological Survey Miscellaneous Investigations Series Map I-1109, scale 1:125,000.

Drewes, H., and Thorman, C. H., 1978, Major geologic structures between Lordsburg, New Mexico, and Douglas and Tucson, Arizona, in Callender, J. F., Wilt, J. E., and Clemons, R. E., eds., Land of Cochise: New Mexico Geological Society Guidebook, 29th Field Conference, p. 291-295.

-----1980a, Geologic map of the Steins Quadrangle and the adjacent part of the Vanar Quadrangle, New Mexico: U.S. Geological Survey Miscellaneous Geologic Investigations Map I-1220 (in preparation).

-----1980b, Geologic map of the Cotton City Quadrangle and the adjacent part of the Vanar Quadrangle, New Mexico: U.S. Geological Survey Miscellaneous Geologic Investigations Map I-1221 (in preparation).

Elston, W. E., 1957, Geology and mineral resources of Dwyer Quadrangle, Grant, Luna, and Sierra Counties, New Mexico: New Mexico Institute of Mining and Technology, State Bureau of Mines and Mineral Resources Bulletin 38, 86 p.

-----1960, Reconnaissance geologic map of Virden 30-minute quadrangle: New Mexico Bureau of Mines and Mineral Resources Geologic Map 15, scale 1:126,720.

-----1968, Terminology and distribution of ash flows of the Mogollon-Silver City-Lordsburg region, New Mexico, in Titley, S. R., ed., Southern Arizona Guidebook III: Tucson, Arizona Geological Society, p. 231-240.

-----1976, Tectonic significance of the mid-Tertiary volcanism in the Basin and Range Province, critical review with special reference to New Mexico, in Elston, W. E., and Northrop, S. A., eds., Cenozoic volcanism in southwestern New Mexico: New Mexico Geological Society Special Publication 5, p. 93-102.

-----1978, Mid-Tertiary cauldrons and their relationship to mineral resources, southwestern New Mexico; brief review: New Mexico Geological Society Special Publication 7, p. 107-113.

Elston, W. E., Damon, P. E., Coney, P. J., Rhodes, R. L., Smith, E. I., and Bickerman, M., 1973, Tertiary volcanic rocks, Mogollon-Datil province, New Mexico and surrounding region; K-Ar dates, patterns of eruption, and periods of mineralization: Geological Society of America Bulletin, v. 84, p. 2259-2274.

Elston, W. E., Erb, E. E., and Deal, E. G., 1979, Tertiary geology of Hidalgo County, New Mexico: New Mexico Geology, v. 1, no. 1, p. 1, 3-6.

Elston, W. E., and Northrop, S. A., eds., 1976, Cenozoic volcanism in southwestern New Mexico: New Mexico Geological Society Special Publication 5, 151 p.

Elston, W. E., Rhodes, R. C., Coney, P. J., and Deal, E. G., 1976a, Progress report on the Mogollon Plateau volcanic field southwestern New Mexico, III--Surface expression of a pluton, in Elston, W. E., and Northrop, S. A., eds., Cenozoic volcanism in southwestern New Mexico: New Mexico Geological Society Special Publication 5, p. 3-28.

Elston, W. E., Rhodes, R. C., and Erb, E. E., 1976b, Control of mineralization by mid-Tertiary volcanic centers, southwestern New Mexico, in Elston, W. E., and Northrop, S. A., eds., Cenozoic volcanism in southwestern New Mexico: New Mexico Geological Society Special Publication 5, p. 125-130.

Elston, W. E., Seager, W. R., and Clemons, R. E., 1975, Emory cauldron, Black Range, New Mexico, source of the Kneeling Nun Tuff, in Seager, W. R., Clemons, R. E., Callender, J. F., eds., Las Cruces County: New Mexico Geological Society, 26th Field Conference, p. 283-294.

Enlows, H. E., 1955, Welded tuffs of Chiricahua National Monument, Arizona: Geological Society of America Bulletin, v. 66, p. 1215-1246.

Erickson, R. C., 1968a, Geology and geochronology of the Dos Cabezas Mountains, Cochise County, Arizona, in Southern Arizona Guidebook III: Arizona Geological Society, p. 193-197.

-----1968b, Welded intrusive volcanic breccias in the Dos Cabezas Mountains, Arizona: U.S. Atomic Energy Commission, Geochron Annual Report, Tucson, University of Arizona, cont. 164 (600-689-106), 41 p.

-----1969, Petrology and geochemistry of the Dos Cabezas Mountains, Cochise County, Arizona: Tucson, University of Arizona, Ph.D. dissertation, 441 p.

Ettinger, L. J., 1962, Geology of the Pat Hills, Cochise County, Arizona: Tucson, University of Arizona, M.S. thesis, 47 p.

Eyde, T. H., 1978, Arizona zeolites: State of Arizona Department of Mineral Resources Mineral Report 1, 40 p.

Fernandez, L. A., Jr., and Enlows, H. E., 1966, Petrography of the Faraway Ranch Formation, Chiricahua National Monument, Arizona: Geological Society of America Bulletin, v. 77, p. 1017-1030.

Feth, J. H., and Hem, J. D., 1963, Reconnaissance of headwater springs in the Gila River drainage basin: U.S. Geological Survey Water-Supply Paper 1619-H, 54 p.

Finnell, T. L., 1976a, Geologic map of the Reading Mountain Quadrangle, Grant County, New Mexico: U.S. Geological Survey Miscellaneous Field Studies Map MF-800, scale 1:24,000.

-----1976b, Geologic map of the Twin Sisters Quadrangle, Grant County, New Mexico: U.S. Geological Survey Miscellaneous Field Studies Map MF-779, scale 1:24,000.

Flege, R. F., 1959, Geology of the Lordsburg Quadrangle, Hidalgo County, New Mexico: New Mexico Institute of Mining and Technology, State Bureau of Mines and Mineral Resources Bulletin 62, 31 p.

Fleischhauer, H. L., Jr., 1977, Quaternary geology of Lake Animas, Hidalgo County, New Mexico: Socorro, New Mexico Institute of Mining and Technology, M.S. thesis, 149 p.

Flower, R. H., 1953, Paleozoic sedimentary rocks of southwestern New Mexico, in Kottlowski, F. E., Callaghan, E., and Jones, W. R., eds., Guidebook of southwestern New Mexico: New Mexico Geological Society Guidebook, 4th Field Conference, p. 106-112.

Giles, D. L., 1968, Ash-flow tuffs of the Cobre Mountains, in Titley, S. R., ed., Southern Arizona Guidebook III: Arizona Geological Society, p. 289-291.

Gillerman, Elliot, 1951, Fluorspar deposits of Burro Mountains and vicinity, New Mexico: U.S. Geological Survey Bulletin 973-F, p. 261-288.

-----1953a, Search for and geology of uranium in sandstone-type deposits--White Signal-Black Hawk districts, New Mexico, in Search for and geology of radioactive deposits, semiannual progress report: U.S. Geological Survey Report TEI-330, p. 111-113.

-----1953b, White Signal uranium deposits, in Kottlowski, F. E., Callaghan, E., and Jones, W. E., eds., Guidebook of Southwestern New Mexico: New Mexico Geological Society Guidebook, 4th Field Conference, p. 133-137.

-----1958, Geology of the central Peloncillo Mountains, Hidalgo County, New Mexico, and Cochise County, Arizona: New Mexico Institute of Mining and Technology, State Bureau of Mines and Mineral Resources Bulletin 57, 152 p.

-----1964, Mineral deposits of western Grant County, New Mexico: New Mexico Institute of Mining and Technology, State Bureau of Mines and Mineral Resources Bulletin 83, 213 p.

-----1967, Structural framework and character of mineralization, Burro Mountains, New Mexico: Economic Geology, v. 62, p. 370-375.

-----1968, Uranium mineralization in the Burro Mountains, New Mexico: Economic Geology, v. 63, p. 239-246.

-----1970, Mineral deposits and structural pattern of the Big Burro Mountains, New Mexico, in Guidebook of the Tyrone-Big Hatchet Mountains-Florida Mountains region: New Mexico Geological Society Guidebook, 4th Field Conference, p. 115-121.

Gillerman, E. G., and Whitebread, D. H., 1956, Uranium-bearing nickel-cobalt-native silver deposits, Black Hawk district, Grant County, New Mexico: U.S. Geological Survey Bulletin 1009K, p. 283-311.

Gilluly, J., Copper, J. R., and Williams, J. S., 1954, Late Paleozoic stratigraphy of central Cochise County, Arizona: U.S. Geological Survey Professional Paper 266, 49 p.

Goodell, P. C., 1978, Geologic setting of the Pena Blanca uranium deposits, Chihuahua, Mexico, in Henry, C. D., and Walton, A. W., eds., Formation of uranium ores by diagenesis of volcanic sediments: U.S. Department of Energy Open-File Report GJBX-22(79), section IX, p. 1-38.

Granger, H. C., and Bauer, H. L., Jr., 1950, Results of diamond drilling, Merry Widow claim, White Signal, Grant County, New Mexico: U.S. Geological Survey Report TEM-146, 9 p.

-----1951, Uranium occurrence on the Blue Jay claim, White Signal district, New Mexico: U.S. Geological Survey Report TEM-117, 21 p.

-----1952, Uranium occurrences on Merry Widow claim, White Signal district, Grant County, New Mexico: U.S. Geological Survey Circular 189, 16 p.

Granger, H. C., Bauer, H. L., Jr., Lovering, T. G., and Gillerman, Elliot, 1952, Uranium deposits in Grant County, New Mexico: U.S. Geological Survey Report TEI-156, 65 p.

Granger, H. C., and Raup, R. B., 1956, Some uranium deposits in Arizona: U.S. Geological Survey Bulletin 1147-A, 54 p.

Griggs, R. L., and Wagner, H. C., 1966, Geology and ore deposits of the Steeple Rock mining district, Grant County, New Mexico: U.S. Geological Survey Bulletin 1222-E, p. E1-E29.

Gruner, J. W., 1956, Concentration of uranium in sediments by multiple migration-accretion: Economic Geology, v. 51, p. 495-520.

Hahman, W. R., Sr., Stone, C., and Witcher, J. C., 1978, Preliminary map, geothermal energy resources of Arizona: Bureau of Geology and Mineral Technology Geothermal Map 1, scale 1:1,000,000.

Harbour, 1966, Stratigraphy and sedimentology of the upper Safford Basin sediments: Tucson, University of Arizona, Ph.D. dissertation, 242 p.

Hayes, P. T., 1978, Cambrian and Ordovician rocks of southwestern Arizona and southwestern New Mexico, in Callender, J. F., Wilt, J. C., and Clemons, R. E., eds., Land of Cochise: New Mexico Geological Society Guidebook, 29th Field Conference, p. 165-173.

Hayes, P. T., and Cone, G. E., 1975, Cambrian and Ordovician rocks of southern Arizona and New Mexico and westernmost Texas: U.S. Geological Survey Professional Paper 873, 98 p.

Hayes, P. T., and Drewes, Harald, 1978, Mesozoic depositional history of southwestern Arizona, in Callender, J. F., Wilt, J. C., and Clemons, R. E., eds., Land of Cochise: New Mexico Geological Society Guidebook, 29th Field Conference, p. 201-207.

Hedlund, D. C., 1978a, Geologic map of the Wind Mountain Quadrangle, Grant County, New Mexico: U.S. Geological Survey Miscellaneous Field Studies Map MF-1031, scale 1:24,000.

-----1978b, Geologic map of Gold Hill Quadrangle, Hidalgo and Grant Counties, New Mexico: U.S. Geological Survey Miscellaneous Field Studies Map MF-1035, scale 1:24,000.

-----1978c, Geologic map of the Hurley East Quadrangle, Grant County, New Mexico: U.S. Geological Survey Miscellaneous Field Studies Map MF-1036, scale 1:24,000.

-----1978d, Geologic map of the Tyrone Quadrangle, Grant County, New Mexico: U.S. Geological Survey Miscellaneous Field Studies Map MF-1037, scale 1:24,000.

-----1978e, Geologic map of the Burro Peak Quadrangle, Grant County, New Mexico: U.S. Geological Survey Miscellaneous Field Studies Map MF-1040, scale 1:24,000.

-----1978f, Geologic map of the White Signal Quadrangle, Grant County, New Mexico: U.S. Geological Survey Miscellaneous Field Studies Map MF-1041, scale 1:24,000.

Heindl, L. A., 1958, Cenozoic alluvial deposits of the upper Gila River area, New Mexico and Arizona: Tucson, University of Arizona, Ph.D. dissertation, 249 p.

Hernon, R. M., Jones, W. R., and Moore, S. L., 1964, Geology of the Santa Rita Quadrangle, New Mexico: U.S. Geological Survey Geologic Quadrangle Map GQ-306, scale 1:24,000.

Hewitt, C. H., 1959, Geology and mineral deposits of the northern Big Burro Mountains-Redrock area, Grant County, New Mexico: New Mexico Bureau of Mines and Mineral Resources Bulletin 60, 151 p.

Jones, C. A., 1978, Uranium occurrences in sedimentary rocks exclusive of sandstone, in Mickle, D. G., and Mathews, G. W., eds., Geologic characteristics of environments favorable for uranium deposits: U.S. Department of Energy Open-File Report GJBX-67(78), p. 1-86.

Jones, W. R., Case, J. E., and Pratt, W. P., 1964, Aeromagnetic and geologic map of part of the Silver City mining region, Grant County, New Mexico: U.S. Geological Survey Geophysical Investigations Map GP-424, scale 1:63,360.

Jones, W. R., Moore, S. L., and Pratt, W. P., 1970, Geologic map of the Fort Bayard Quadrangle, Grant County, New Mexico: U.S. Geological Survey Geologic Quadrangle Map GQ-865, scale 1:24,000.

Kolessar, J., 1970, Geology and copper deposits of the Tyrone district, in Woodward, L. A., ed., Guidebook of the Tyrone-Big Hatchett Mountains-Florida Mountains region: New Mexico Geological Society Guidebook, 21st Field Conference, p. 127-132.

Kottlowski, F. E., 1960, Summary of Pennsylvanian sections in southwestern New Mexico and southeastern Arizona: New Mexico Bureau Mines and Mineral Resources Bulletin 66, 187 p.

-----1963, Paleozoic and Mesozoic strata of southwestern and south-central New Mexico: New Mexico Institute of Mining and Technology, State Bureau of Mines and Mineral Resources Bulletin 79, 100 p.

Knechtel, M. M., 1938, Geology and ground-water resources of the valley of Gila River and San Simon Creek: U.S. Geological Survey Water-Supply Paper 796-F, p. 181-222.

Langmuir, Donald, 1977, Uranium solution-mineral equilibria at low temperatures with applications to sedimentary ore deposits: U.S. Department of Energy Open-File Report GJO-1659-3, 39 p.

Leopoldt, Winfried, in preparation, Neogene geology of the central Mangas graben, Cliff-Gila area, Grant County, New Mexico: Albuquerque, University of New Mexico, M.S. thesis.

Lindsay, Everett, 1978, Late Cenozoic vertebrate faunas, southeastern Arizona, in Callender, J. F., Wilt, J. E., and Clemons, R. E., eds., Land of Cochise: New Mexico Geological Society Guidebook, 29th Field Conference, p. 269-275.

Lovering, T. G., 1956, Radioactive deposits in New Mexico: U.S. Geological Survey Bulletin 1009-B, p. 315-390.

Luedke, R. G., and Smith, R. L., 1978, Map showing distribution, composition, and age of Late Cenozoic volcanic centers in Arizona and New Mexico: U.S. Geological Survey Miscellaneous Investigations Map I-1091-A, scale 1:1,000,000.

Luning, R. H., Thiede, D. S., O'Neill, A. J., Nystrom, R. J., and White, D. L., 1980, Uranium resource evaluation, Mesa Quadrangle, Arizona: U.S. Department of Energy Preliminary Open-File Report PGJ-032(80), 123 p.

Marjaniemi, D. K., 1968, Tertiary volcanism in the northern Chiricahua Mountains, Cochise County, Arizona, in Southern Arizona Guidebook III: Arizona Geological Society, p. 209-214.

-----1970, Geologic history of an ash-flow sequence and its source area in the Basin and Range Province of southeastern Arizona: Tucson, University of Arizona, Ph.D. dissertation, 176 p.

Mathews, G. W., 1978a, Uranium occurrences in and related to plutonic igneous rocks, in Mickle, D. G., and Mathews, G. W., eds., Geologic characteristics of environments favorable for uranium deposits: U.S. Department of Energy Open-File Report GJBX-67(78), p. 121-180.

-----1978b, Uranium occurrences of uncertain genesis, in Mickle, D. G., and Mathews, G. W., eds., Geologic characteristics of environments favorable for uranium deposits: U.S. Department of Energy Open-File Report GJBX-67(78), p. 221-250.

McDowell, F. W., 1971, K-Ar ages of igneous rock from the western United States: Isochron/West 2, p. 12.

Mickle, D. G., and Mathews, G. W., eds., 1978, Geologic characteristics of environments favorable for uranium deposits: U.S. Department of Energy Open-File Report GJBX-67(78), 250 p.

Miller, R. H., 1955, Uranium Hill Claims: U.S. Atomic Energy Commission Preliminary Reconnaissance Report A-59, Open-File Report, 1 p.

Miyashiro, A., 1978, Nature of alkali volcanic rock series: Contributions to Mineralogy and Petrology, v. 66, p. 91-104.

Morrison, R. B., 1965, Geologic map of the Duncan and Canador Peak Quadrangles, Arizona and New Mexico: U.S. Geological Survey Miscellaneous Geologic Investigations Map I-442, scale 1:48,000.

Pilcher, R. C., 1978, Volcanogenic uranium occurrences, in Mickle, D. G., and Mathews, G. W., eds., Geologic characteristics of environments favorable for uranium deposits: U.S. Department of Energy Open-File Report GJBX-67(78), p. 181-220.

Powers, R. S., 1976, Geology of the Summit Mountains and vicinity, Grant County, New Mexico, and Greenlee County, Arizona: Houston, University of Houston, M.S. thesis, 107 p.

Pye, W. D., 1959, Silurian and Devonian stratigraphy, southeastern Arizona and southwestern New Mexico, in Heindl, L. A., ed., Guidebook II, Southern Arizona: Arizona Geological Society, p. 25-30.

Rehrig, W. A., and Reynolds, S. J., 1980, Geologic and geochronologic reconnaissance of a northwest-trending zone of metamorphic core complexes in southern and western Arizona: Geological Society of America Memoir 153, p. 131-157.

Rogers, J. J. W., and Adams, J. S. S., 1969, Uranium (Chapter 92), in Wedepohl, K. H., ed., Handbook of geochemistry: New York, Springer-Verlag.

Ross, C. A., 1973, Pennsylvanian and Early Permian depositional history, southeastern Arizona: American Association of Petroleum Geologists Bulletin, v. 57, p. 887-912.

Rytuba, J. J., Glanzman, R. K., and Conrad, W. K., 1979, Uranium, thorium, and mercury distribution through the evolution of the McDermitt caldera complex: Rocky Mountain Association of Geologists and Utah Geological Association, Basin and Range Symposium and Great Basin Field Conference, p. 405-412.

Sabins, F. F., Jr., 1957, Geology of the Cochise Head and western part of the Vanar Quadrangles, Arizona: Geological Society of America Bulletin, v. 68, p. 1315-1342.

-----1957, Stratigraphic relations in Chiricahua and Dos Cabezas Mountains: American Association of Petroleum Geologists Bulletin, v. 41, no. 3, p. 466-510.

Scarborough, R. B., and Peirce, H. W., 1978, Late Cenozoic basins of Arizona, in Callender, J. R., Wilt, J. C., and Clemons, R. E., eds., Land of Cochise: New Mexico Geological Society Guidebook, 29th Field Conference, p. 253-259.

Scarborough, R. B., and Wilt, J. C., 1979, Uranium favorability of Cenozoic sedimentary rocks: U.S. Geological Survey Open-File Report 79-1429, 101 p.

Schreiber, J. F., Jr., 1978, Geology of the Willcox Playa, Cochise County, Arizona, in Callender, J. F., Wilt, J. C., and Clemons, R. E., eds., Land of Cochise: New Mexico Geological Society Guidebook, 29th Field Conference, p. 277-282.

Seff, Phillip, 1962, Stratigraphic geology and depositional environment of the 111 Ranch area, Graham County, Arizona: Tucson, University of Arizona, Ph.D. dissertation, 171 p.

Sharp, R. R., Jr., Morris, W. A., and Aamodt, P. L., 1978, Uranium hydrogeochemical and stream-sediment reconnaissance data release for the New Mexico portions of the Douglas, Silver City, Clifton and St. Johns NTMS Quadrangles, New Mexico-Arizona: U.S. Department of Energy Open-File Report GJBX-69(78), 123 p.

Sherborne, J. E., Jr., Buckovic, W. A., Dewitt, D. B., Hellinger, T. S., and Pavlak, S. J., 1979, Major uranium discovery in volcaniclastic sediments, Basin and Range Province, Yavapai County, Arizona: American Association of Petroleum Geologists Bulletin, v. 63, no. 4, p. 621-646.

Silver, L. T., 1978, Precambrian formations and Precambrian history in Cochise County, in Callender, J. R., Wilt, J. C., and Clemons, R. E., eds., Land of Cochise: New Mexico Geological Society Guidebook, 29th Field Conference, p. 157-163.

Smith, R. L., and Bailey, R. A., 1968, Resurgent cauldrons, in Coats, R. R., Hay, R. G., and Anderson, C. A., eds., Studies in volcanology: Geological Society of America Memoir 116, p. 613-662.

Steven, T. A., Cunningham, C. G., and Machette, M. N., 1980, Integrated uranium system in the Marysvale volcanic field, west-central Utah: U.S. Geological Survey Open-File Report 80-524, 42 p.

Steven, T. A., Luedke, R. G., and Lipman, P. W., 1974, Relation of mineralization to calderas in the San Juan volcanic field, southwestern Colorado: U.S. Geological Survey Journal of Research, v. 2. no. 4, p. 405-409.

Summers, W. K., 1979, Hydrothermal anomalies in New Mexico: New Mexico Bureau of Mines and Mineral Resources Resource Map 1, scale 1:1,000,000.

Swan, M. M., 1976, The Stockton Pass fault, an element of the Texas Lineament: Tucson, University of Arizona, M.S. thesis, 119 p.

Texas Instruments, Inc., 1978a, Aerial radiometric and magnetic reconnaissance survey of portions of Arizona-New Mexico: U.S. Department of Energy Open-File Report GJBX-23(79), v. 1, 41 p.

-----1978b, Aerial radiometric and magnetic reconnaissance survey of portions of Arizona-New Mexico, Silver City Quadrangle: U.S. Department of Energy Open-File Report GJBX-23(79), v. 2, 80 p.

Thorman, C. H., 1977, Geologic map of parts of the Coyote Peak and Brockman Quadrangles, Hidalgo and Grant Counties, New Mexico: U.S. Geological Survey Miscellaneous Field Studies Map MF-924, scale 1:24,000.

Thorman, C. H., and Drewes, Harald, 1978, Cretaceous-early Tertiary history of the northern Pyramid Mountains, southwestern New Mexico, in Callender, J. F., Wilt, J. C., and Clemons, R. E., eds., Land of Cochise: New Mexico Geological Society Guidebook, 29th Field Conference, p. 215-218.

-----1980, Geologic map of the Victoria Mountains, New Mexico: U.S. Geological Survey Miscellaneous Field Studies Map MF-1175, scale 1:24,000.

Trauger, F. C., 1972, Water resources and general geology of Grant County, New Mexico: New Mexico State Bureau of Mines and Mineral Resources Hydrologic Report 2, 211 p.

U.S. Geological Survey, 1980, Aeromagnetic map of the southern part of the Silver City 1° by 2° Quadrangle, Arizona and New Mexico: U.S. Geological Survey Open-File Report 80-1128, scale 1:62,500.

Vine, J. D., Asher-Bolinder, Sigrid, Morgan, J. D., and Higgins, Brenda, 1979, Lithologic log and lithium content of sediments penetrated in a test boring drilled in Willcox Playa, Cochise County, Arizona: U.S. Geological Survey Open-File Report 79-397, 16 p.

Wahl, D. E., 1980, Mid-Tertiary volcanic geology in parts of Greenlee County, Arizona, Grant and Hidalgo Counties, New Mexico: Tempe, Arizona State University, Ph.D. dissertation, 148 p.

Wallace, A. B., and Roper, M. W., 1980, Geology and uranium deposits along the northeastern margin of the McDermitt caldera complex, southern Malheur County, Oregon [abs.]: American Association of Petroleum Geologists, Southwest Section Annual Meeting, Technical Program and Abstracts, p. 49.

Waller, M. R., 1952, Lake beds in the Chiricahua National Monument: Tulsa, Oklahoma, University of Tulsa, M.S. thesis, 96 p.

Walton, A. W., Salter, T. L., and Zetterland, Dale, 1980, Uranium potential of southwestern New Mexico (southern Hidalgo County), including observations of crystallization history of lavas and ash-flow tuffs and the release of uranium from them: U.S. Department of Energy Open-File Report GJBX-169(80), 114 p.

Wargo, J. G., 1959, The geology of the Schoolhouse Mountain Quadrangle, Grant County, New Mexico: Tucson, University of Arizona, Ph.D. dissertation, 187 p.

Wenrich-Verbeek, K. J., Spirakis, C. S., Billingsley, G. H., Hereford, Richard, Nealey, L. D., Ulrich, G. E., Verbeek, E. R., and Wolfe, E. W., 1980, Uranium resource evaluation, Flagstaff Quadrangle, Arizona: U.S. Department of Energy Preliminary Open-File Report PGJ-014(80), 103 p.

Wilson, E. D., and Moore, R. T., 1958, Geologic map of Graham and Greenlee Counties, Arizona: Arizona Bureau of Mines County Geologic Map Series 3-4, scale 1:375,000.

Woodward, L. A., 1970, Precambrian rocks of southwestern New Mexico, in Woodward, L. A., ed., Guidebook of the Tyrone-Big Hatchet Mountains-Florida Mountains region: New Mexico Geological Society Guidebook, 21st Field Conference, p. 27-32.

Wynn, J. C., 1981, Complete Bouguer gravity anomaly map of Silver City 1° by 2° Quadrangle, New Mexico, Arizona: U.S. Geological Survey Miscellaneous Investigations Series Map I-1310A, scale 1:250,000.

SILVER CITY, NEW MEXICO/ AZ

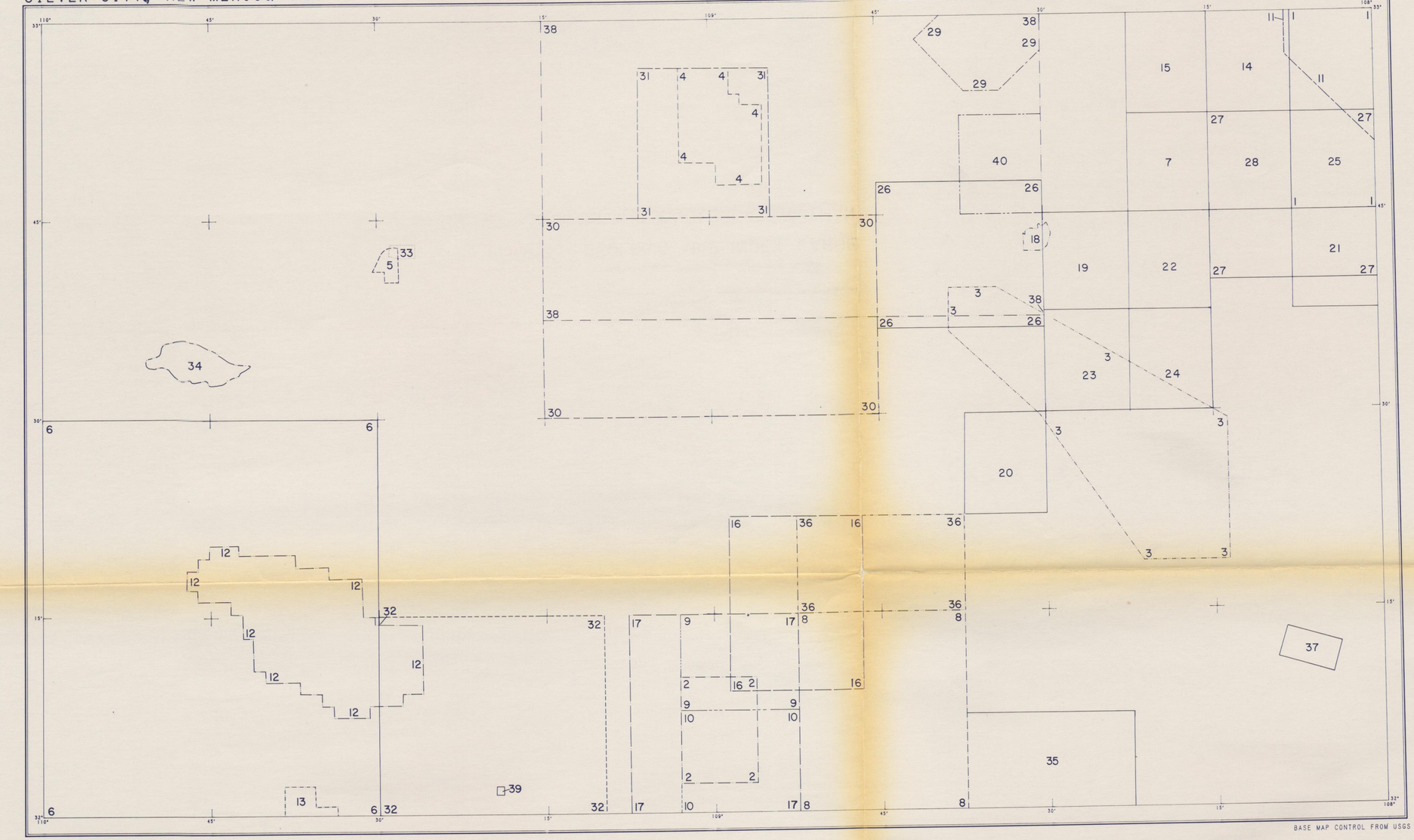

URANIUM RESOURCE EVALUATION
ISSUED BY THE U.S. DEPARTMENT OF ENERGY

BASE MAP CONTROL FROM USGS

5 0 5 10 15 20 25 MILES

5 0 5 10 15 20 25 KILOMETERS

INDEX

1. Aldrich, 1972, pl. 2, scale 1:32,000.
2. Armstrong and others, 1978, scale 1:24,000.
3. Ballmann, 1960, pl. 1, scale 1:63,360.
4. Biggerstaff, 1974, pl. 1, scale 1:20,000.
5. Clay, 1960, pl. 1, scale 1:7,920.
6. Cooper, 1960, scale 1:62,500.
7. Cunningham, 1974, scale 1:24,000.
8. Deal and Elston, (in preparation), scale 1:24,000.
9. Drewes and Thorman, 1980a, scale 1:24,000.
10. Drewes and Thorman, 1980b, scale 1:24,000.
11. Elston and others, 1979, scale 1:63,360.
12. Erickson, 1969, fig. 1, scale 1:31,680.
13. Ettinger, 1962, pl. 1, scale 1:12,288.
14. Finnell, 1976a, scale 1:24,000.
15. Finnell, 1976b, scale 1:24,000.
16. Fleichhauer, 1977, pl. 1, scale 1:48,000.
17. Gillerman, 1958, pl. 1, scale 1:48,000.
18. Gillerman and Whitebread, 1956, pl. 14, scale 1:8,000.
19. Hedlund, 1978a, scale 1:24,000.
20. Hedlund, 1978b, scale 1:24,000.
21. Hedlund, 1978c, scale 1:24,000.
22. Hedlund, 1978d, scale 1:24,000.
23. Hedlund, 1978e, scale 1:24,000.
24. Hedlund, 1978f, scale 1:24,000.
25. Hernon and others, 1964, scale 1:24,000.
26. Hewitt, 1959, pl. 1, scale 1:48,000.
27. Jones and others, 1964, scale 1:63,360.
28. Jones and others, 1970, scale 1:24,000.
29. Leopoldt, (in preparation), scale 1:24,000.
30. Morrison, 1965, scale 1:48,000.
31. Powers, 1976, pl. 1, scale 1:24,000.
32. Sabins, 1957, pl. 1, scale 1:62,500.
33. Seff, 1962, pl. 3, scale 1:7,920.
34. Swan, 1976, fig. 4, scale 1:24,000.
35. Thorman, 1977, scale 1:24,000.
36. Thorman and Drewes, 1978, scale 1:24,000.
37. Thorman and Drewes, 1980, scale 1:24,000.
38. Wahl, 1980, pl. 1, scale 1:48,000.
39. Waller, 1951, pl. 2, scale 1:7,920.
40. Wargo, 1959, scale 1:15,940.

Plate 13a. GEOLOGIC MAP INDEX, LARGE-SCALE MAPS
(SCALES OF AND GREATER THAN 1:63,360)

March 1981
Plate 13a.

SILVER CITY, NEW MEXICO/ AZ

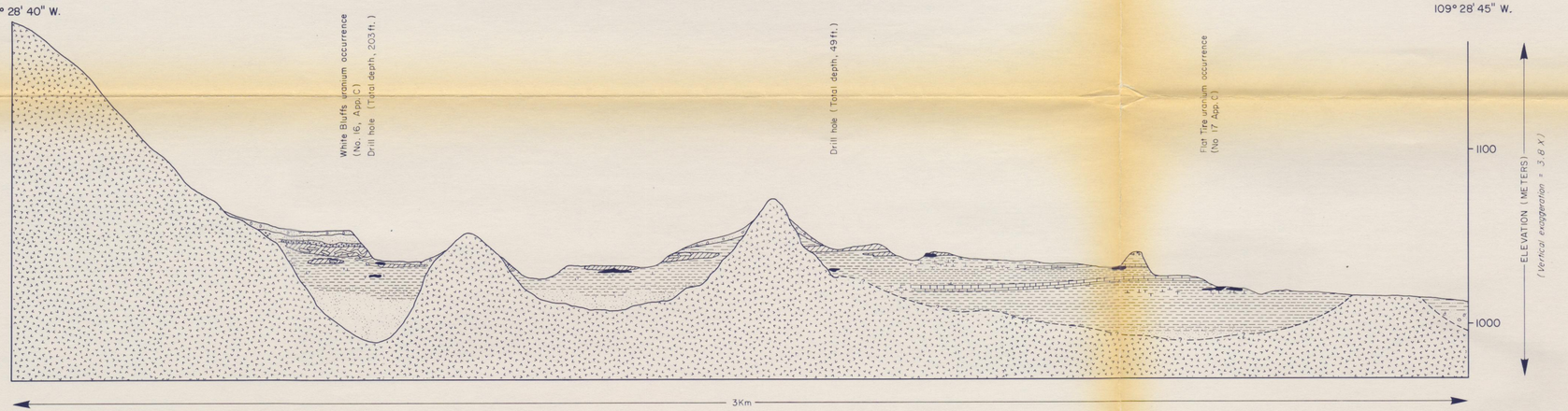

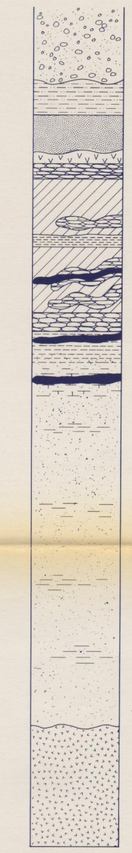

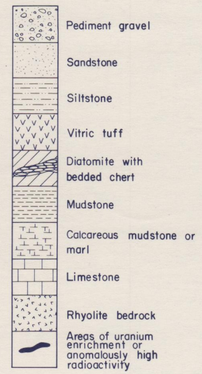

Plate 12. GENERALIZED GEOLOGIC CROSS SECTION OF THE DRY MOUNTAIN – III RANCH AREA AND ACCOMPANYING STRATIGRAPHIC SECTIONS

March 1981
Plate 12.

SILVER CITY, NEW MEXICO/ AZ

GEOLOGY MODIFIED FROM TRAUGER (1972)

LEGEND

- QTu — Quaternary-Tertiary basin fill, undivided.
- Tvu — Tertiary volcanic rocks, undivided.
- TKri — Eocene-Paleocene intrusive rhyolitic rocks.
- TKqm — Paleocene quartz monzonite Tyrone laccolith.
- TKi — Tertiary-Cretaceous intrusive rocks.
- €b — Cambrian Bliss sandstone.
- pCgr — Precambrian granitic rocks.
- pCbp — Precambrian Bullard Peak Series, metamorphic rocks.
- Geologic Contact
- Fault showing upthrown (U) and downthrown (D) sides. Dashed where approximate.
- Limits of sulfide mineralization in Tyrone laccolith area. Extrapolated from Kolessar (1970) and Hedlund (1978 a,c,d,e).
- Area of very numerous rhyolitic dikes, plugs, and sills. Extrapolated from Hedlund (1978 a,c,d,e).
- Areas favorable for uranium deposition.
- Area covered by Plate 2b (Detailed map of uranium occurrences in the White Signal area).
- •38Y — Uranium occurrences outside of area covered by Plate 2b.

Plate II. DISTRIBUTION OF FACTORS INFLUENCING URANIUM DEPOSITION IN THE BIG BURRO MOUNTAIN BLOCK OF THE BURRO MOUNTAIN BATHOLITH – SOUTH HALF

March 1981
Plate II.

SILVER CITY, NEW MEXICO/ AZ

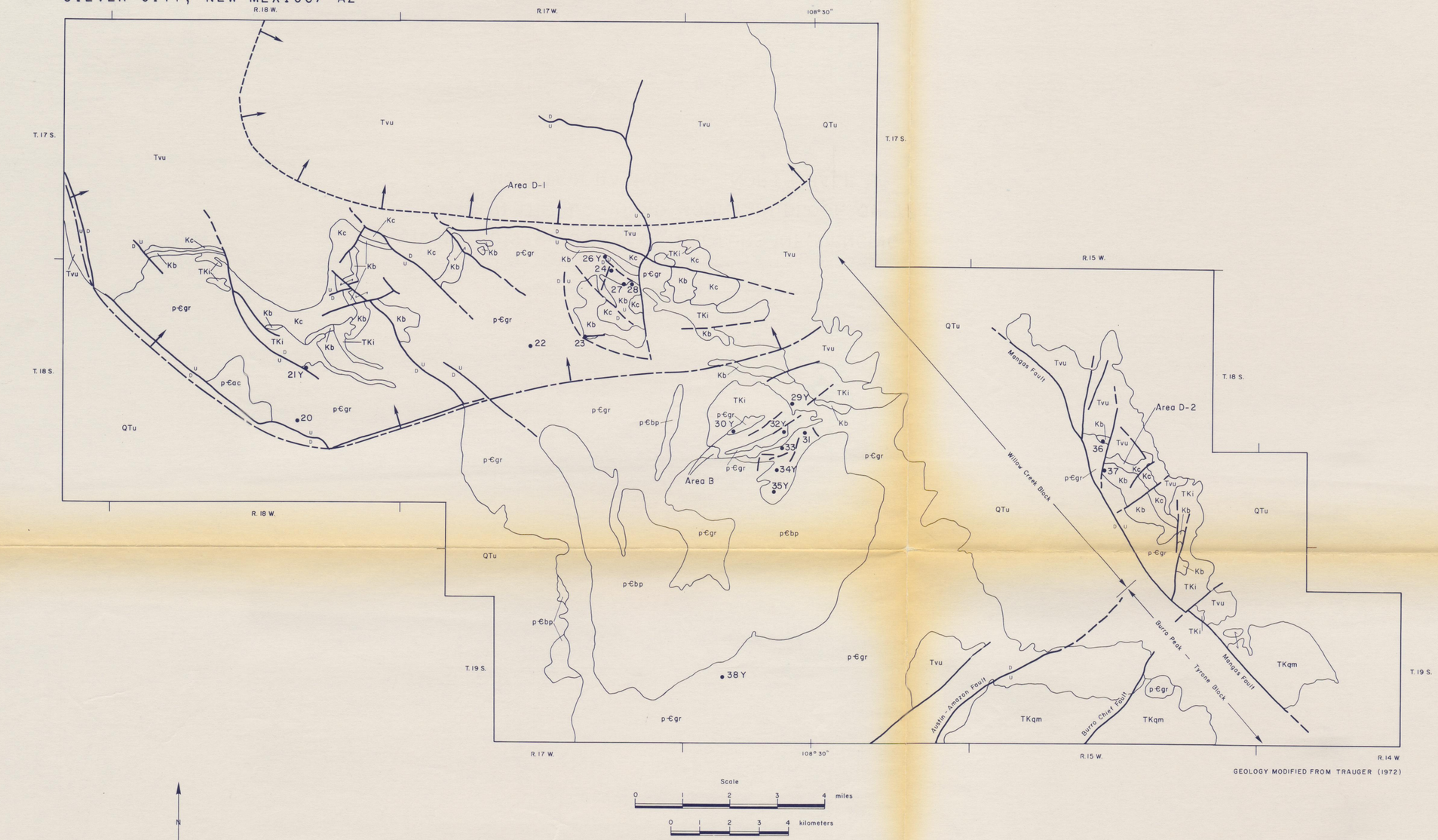

LEGEND

QTu	Quaternary - Tertiary basin fill, undivided
Tvu	Tertiary volcanic rocks, undivided
Kc	Cretaceous Colorado Shale
Kb	Cretaceous Beartooth Quartzite
TKqm	Paleocene quartz monzonite Tyrone laccolith
TKi	Tertiary - Cretaceous intrusive rocks
p-€gr	Precambrian granite rocks
p-€ac	Precambrian Ash Creek Series, metamorphic rocks
p-€bp	Precambrian Bullard Peak Series, metamorphic rocks
	Geologic contact
	Fault showing upthrown ( ) and downthrown ( ) sides. Dashed where approximate.
	Boundary of Schoolhouse Mountain Caldera. Arrows indicate interior of caldera (Wahl, 1980).
	Boundary of Schoolhouse Mountain Caldera ring fracture zone. Extrapolated from Wahl (1980).
•34Y	Uranium occurrences
	Areas favorable for uranium deposition

Scale
0 1 2 3 4 miles
0 1 2 3 4 kilometers

N

GEOLOGY MODIFIED FROM TRAUGER (1972)

Plate 10. DISTRIBUTION OF FACTORS INFLUENCING URANIUM DEPOSITION IN THE BIG BURRO MOUNTAIN BLOCK OF THE BURRO MOUNTAIN BATHOLITH - NORTH HALF

March 1981
Plate 10.

SILVER CITY, NEW MEXICO/ AZ

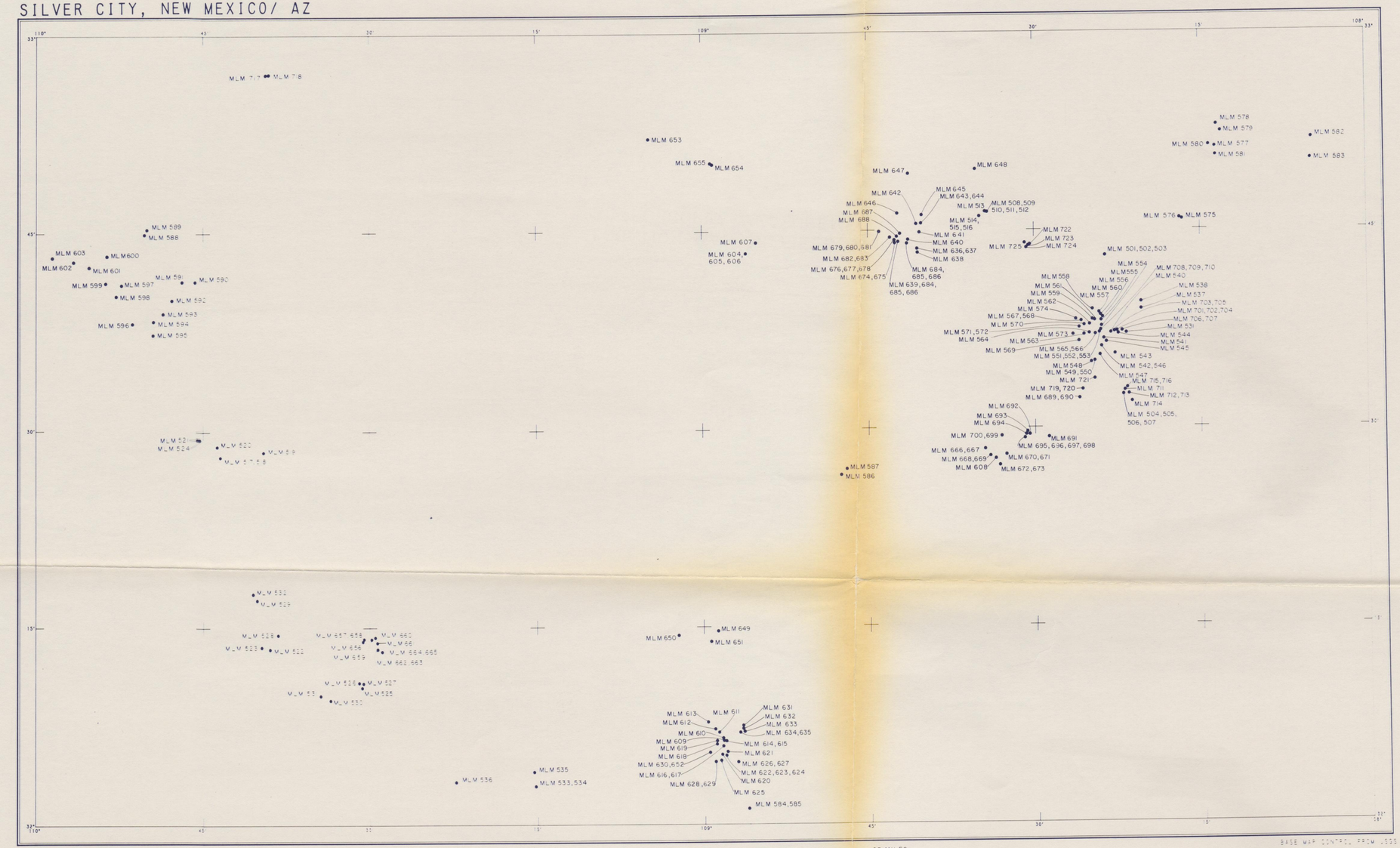

URANIUM RESOURCE EVALUATION
ISSUED BY THE U.S. DEPARTMENT OF ENERGY

BASE MAP CONTROL FROM USGS

5 0 5 10 15 20 25 MILES

5 0 5 10 15 20 25 KILOMETERS

Plate 9. LOCATION MAP OF FIELD GAMMA-RAY SPECTROSCOPIC MEASUREMENTS

March 1981
Plate 9.

SILVER CITY, NEW MEXICO/ AZ

White Signal Area

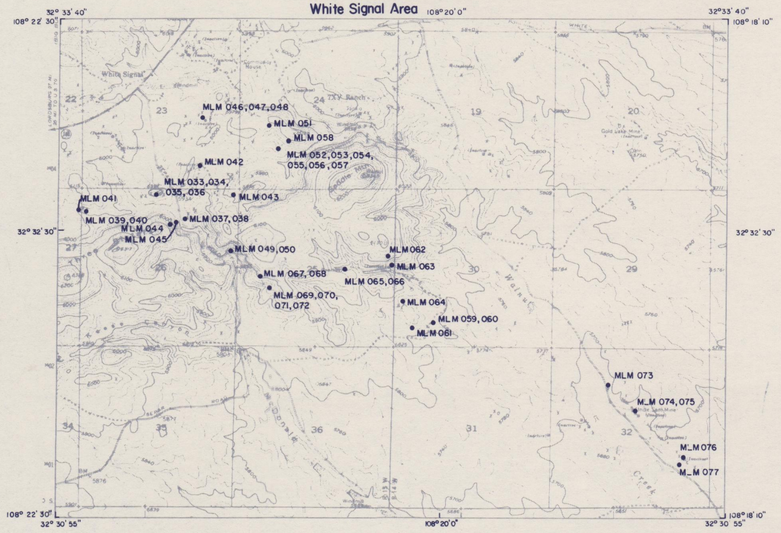

N

SCALE 1:24,000.

1 0 1 MILE

1/2 0

1 5 0 1 KILOMETER

CONTOUR INTERVAL 20 FT.

Base Map: White Signal Quadrangle
7.5' Series (topographic)

Dry Mountain-III Ranch Area

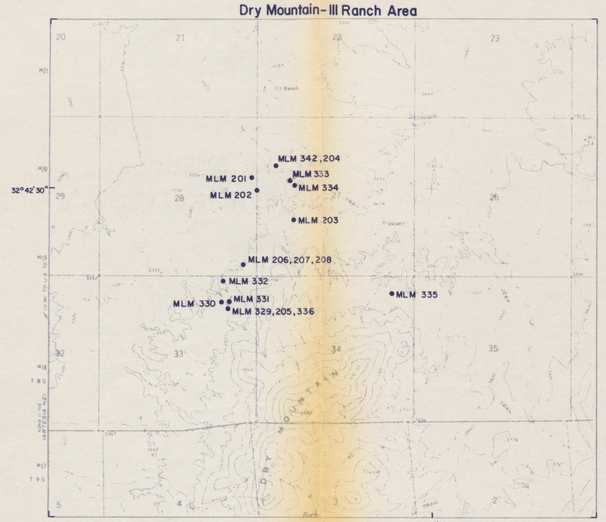

N

SCALE 1:24,000.

1 0 1 MILE

1/2 0

1 5 0 1 KILOMETER

CONTOUR INTERVAL 20 FT.

Base Map: Dry Mountain Quadrangle
7.5' Series (topographic)

Wild Horse Mesa Area

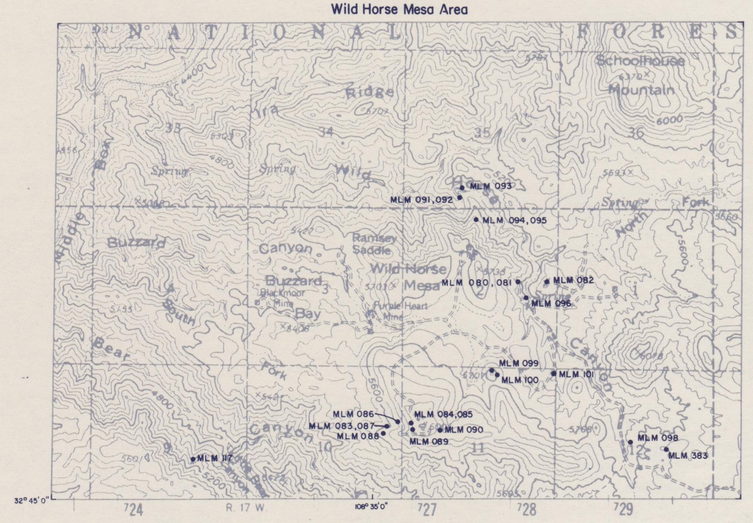

N

SCALE 1:24,000.

1 0 1 MILE

1 5 0 1 KILOMETER

CONTOUR INTERVAL 80 FT.

Base Map: Cliff Quadrangle
15' Series (topographic)

Plate 8. LOCATION MAP OF GEOCHEMICAL SAMPLES IN AREAS OF DETAILED STUDY

March, 1981
Plate 8.

SILVER CITY, NEW MEXICO/ AZ

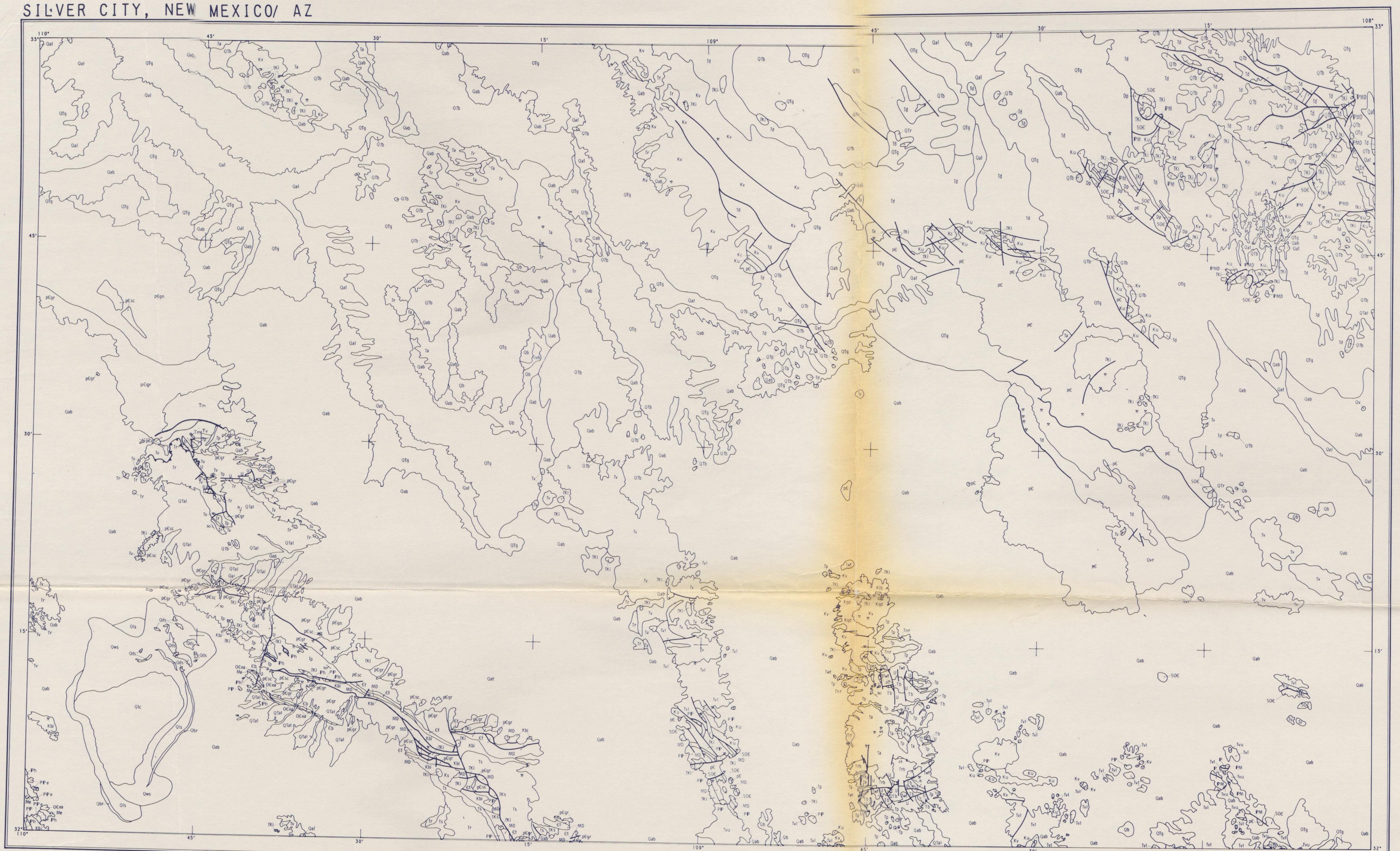

URANIUM RESOURCE EVALUATION
ISSUED BY THE U.S. DEPARTMENT OF ENERGY

BASE MAP CONTROL FROM USGS
DATA SOURCE: TEXAS INSTRUMENTS INC.

5 0 5 10 15 20 25 MILES

5 0 5 10 15 20 25 KILOMETERS

Plate 7. GEOLOGIC MAP

SYMBOLS

- Contact
- Fault, dotted where concealed; U on upthrown side
- Thrust fault, triangle on upper plate
- Strike and dip of beds
- Volcanic vent
- mine

N

EXPLANATION

SEDIMENTARY ROCKS — IGNEOUS ROCKS (EXTRUSIVE, INTRUSIVE) — METAMORPHIC

CENOZOIC

QUATERNARY

- Qab — Alluvium, boulders, gravel, sand and silt as bolson and valley fill deposits
- Qal — Alluvium, gravel, sand, silt and clay on flood plains and alluvial fans
- Qlc — Lake deposited clay
- Qls — Lake deposited sand and silt
- Qws — Wind blown sand and silt
- Qds — Dune sand
- Qbr — Beach ridges, gravel and sand
- Qvr — Rhyolite flows
- Qv — Products of Diatremic explosions
- Qb — Basalt flows

QUATERNARY TERTIARY

- QTg — Gila Conglomerate
- QTal — Gravel, sand, and silt of older valley fill, includes pediment gravel
- QTr — Rhyolite flows and tuff
- QTb — Basalt and basaltic-andesitic flows, upper part interlayered with Gila Conglomerate

TERTIARY

- Ts — Undivided conglomerate, gravel and sand
- Tr — Rhyolite
- Tv — Undivided rhyolite to andesite, locally interbedded with gravel, sand and silt
- Tm — Monzonite
- Td
  - Tvu
    - Trb — South Pyramid Rhyolite Breccia
    - Tnr — North Pyramid Rhyolite
    - Tper — Perlite, with stony rhyolite
  - Tvl
    - Twt — Rhyolitic welded tuff
    - Tb — Augite and olivine-augite basalt
    - Tp — Breccia, tuff and rhyolite
    - Ta — Pyroxene andesite
- Td — Datil Formation, includes rhyolite and andesite flows, tuffs, breccias and pyroclastic rocks, flows and intrusions
- Tvu — Rhyolite, latite and andesite, includes Cretaceous and Early Tertiary andesite
- Tvl — Quartz latite and rhyolite

TERTIARY CRETACEOUS

- TKs — Undivided conglomerate
- TKi — Stocks, laccoliths and sills, intermediate to silicic composition

MESOZOIC

CRETACEOUS

- Ku — Undivided Colorado Shale, Sarten Sandstone and Beartooth Quartzite
- Kv — Undivided volcanic rocks of chiefly andesitic composition, includes basalt, dacite and rhyolite
- Kgd — Granodiorite
- Kc — Carlile Shale
- Kib — Basaltic intrusive breccia
- Kbi — Bisbee Group, includes sandstone, shale, some infaulted lenses of volcanic rocks, and basal conglomerate
- Klp — Hornblende quartz diorite

PALEOZOIC

PERMIAN-PENNSYLVANIAN

- PP — Undivided rocks of Pennsylvanian and Permian ages, includes upper part of Chiricahua Limestone, Sherrer Formation, Colina Limestone, Earp Formation and Horquilla Limestone
- PPe — Earp Formation, includes limestone and shale

PENNSYLVANIAN

- P — Undivided rocks of Pennsylvanian age, includes the Madera Limestone and Sandia Formation and undivided rocks of Pennsylvanian and Mississippian ages
- Ph — Horquilla Limestone, includes thin shale beds

PENNSYLVANIAN MISSISSIPPIAN

- PM — Undivided rocks, includes the Syrena and Oswaldo Formations of Pennsylvanian age and the Lake Valley and Kelly Limestones of Mississippian age

PENNSYLVANIAN-MISSISSIPPIAN-DEVONIAN

- PMD — Undivided rocks of Pennsylvanian, Mississippian, and Devonian ages, includes the Madera Limestone and Sandia Formation of Pennsylvanian age; Helms Formation, Las Cruces Formation, Kelly Limestone, Lake Valley Limestone and Cabellero Formation of Mississippian age, and the Percha Shale of Devonian age

MISSISSIPPIAN DEVONIAN

- MD — Undivided rocks of Mississippian and Devonian ages, includes the Paradise Formation and Escabrosa Limestone of Mississipian age and the Percha Shale of Devonian age

MISSISSIPPIAN

- Me — Escabrosa Limestone and Martin Formation, including shale, dolomite, limestone and sandstone

DEVONIAN

- DP — Percha Shale

SILURIAN-ORDOVICIAN-CAMBRIAN

- SO€ — Undivided rocks of Silurian, Ordovician, and Cambrian ages, includes the Fusselman Dolomite of Silurian age, the Valmont Dolomite, Montoya Dolomite, Cutter Formation, Aleman Formation, Upham Dolomite, Cable Canyon Sandstone, El Paso Limestone, Bat Cave Limestone and Sierrite Limestone of Ordovician age, and the Bliss Sandstone of Ordovician and Cambrian age

ORDOVICIAN CAMBRIAN

- O€ea — Undivided rocks of Ordovician and Cambrian age, includes El Paso and Abrigo Formations consisting of limestone, sandstone and siltstone

CAMBRIAN

- €t — Undivided rocks of Cambrian age, includes Bolsa and Troy Quartzites and Abrigo and related limestones
- €b — Bolsa Quartzite, includes basal conglomerate

PRECAMBRIAN

PRECAMBRIAN

- p€ — Precambrian, undivided
- p€sc — Schist, includes Pinal Schist (p€p) composed of metagraywacke and quartzite
- p€gr — Granite
- p€gn — Granitic gneiss

March 1981
Plate 7.

SILVER CITY, NEW MEXICO / AZ

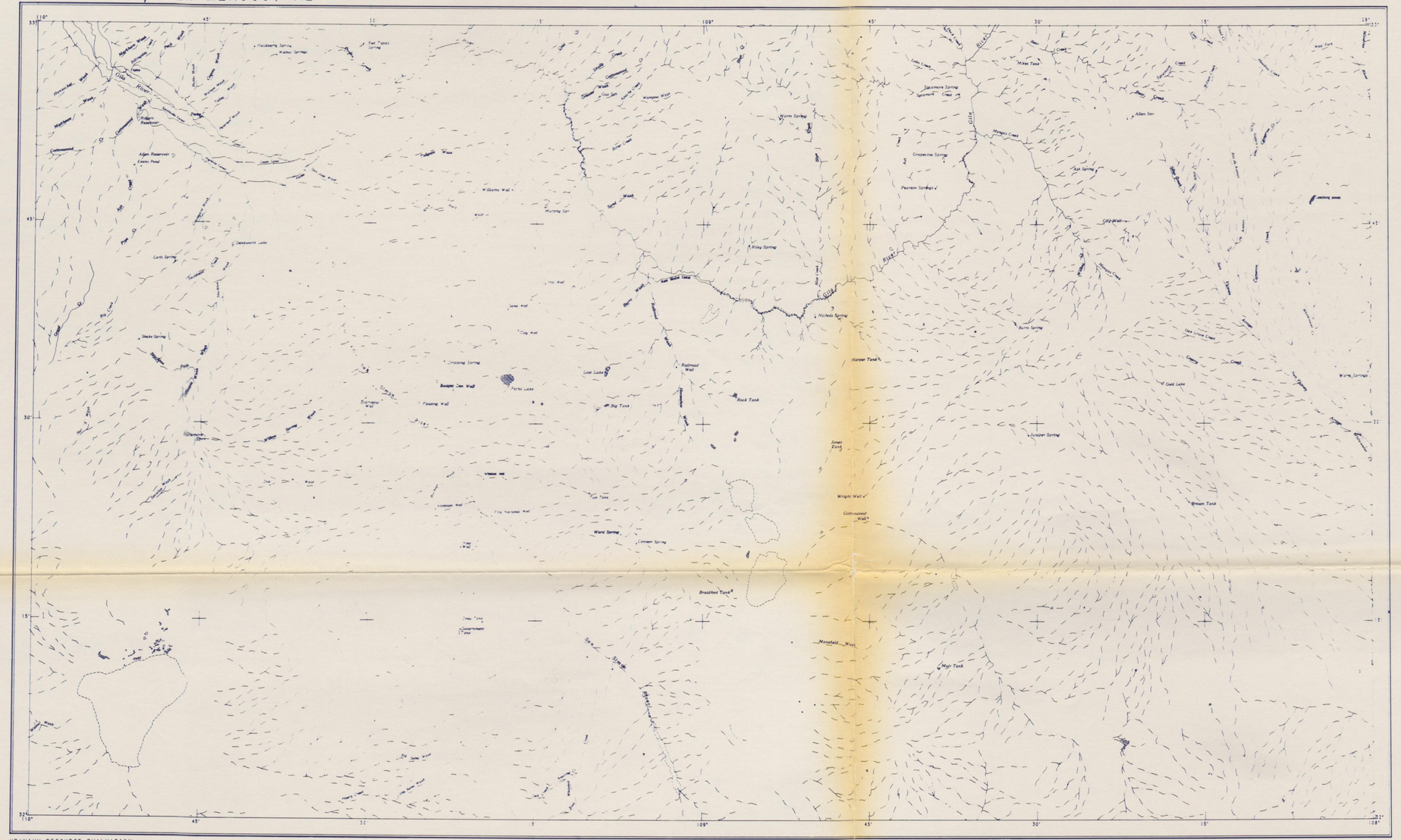

URANIUM RESOURCE EVALUATION
ISSUED BY THE U.S. DEPARTMENT OF ENERGY

5 0 5 10 15 20 25 MILES

5 0 5 10 15 20 25 KILOMETERS

BASE MAP CONTROL FROM USGS

Plate 6. DRAINAGE

March 1981
Plate 6.

SILVER CITY, NEW MEXICO/ AZ

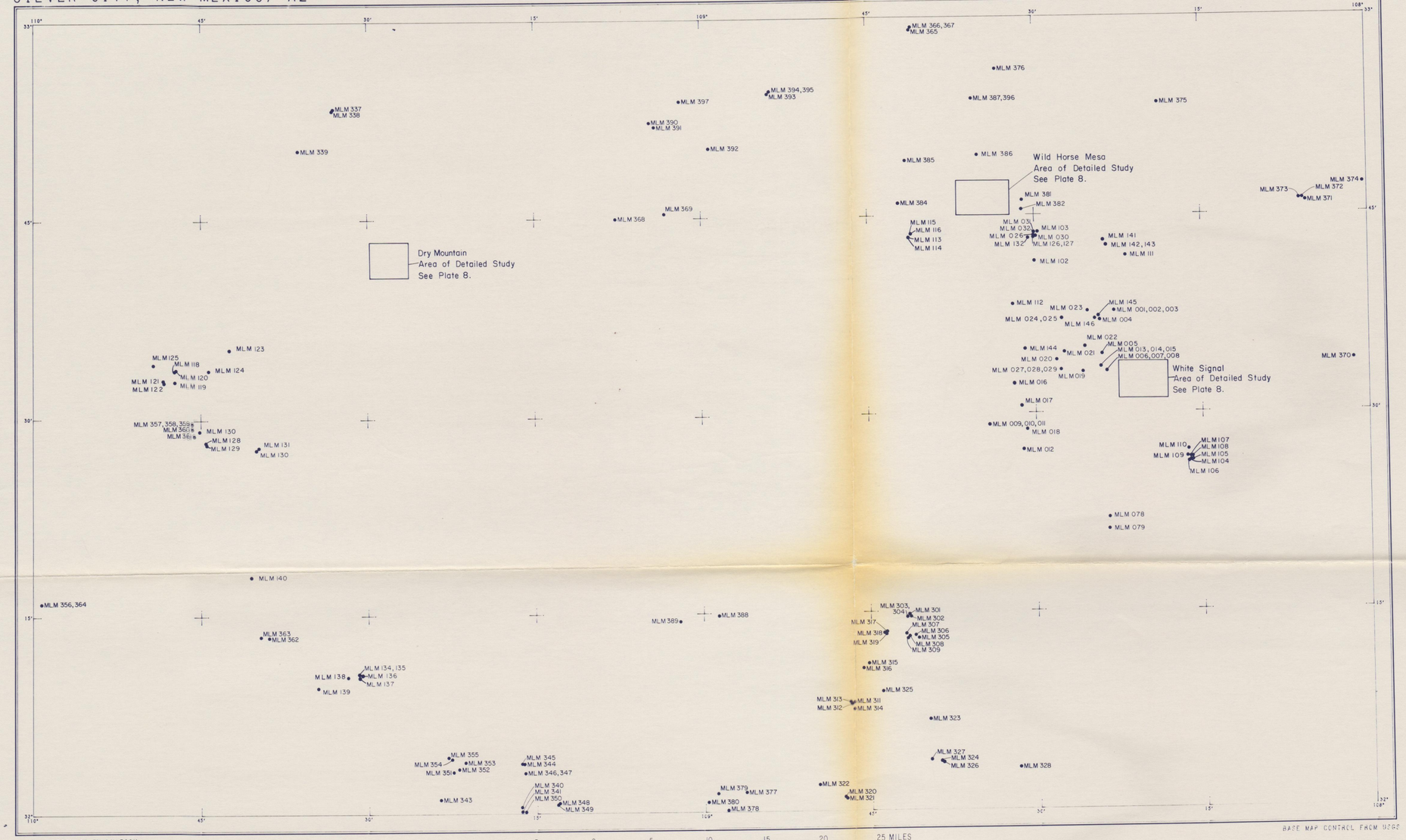

5 0 5 10 15 20 25 MILES

5 0 5 10 15 20 25 KILOMETERS

URANIUM RESOURCE EVALUATION
ISSUED BY THE U.S. DEPARTMENT OF ENERGY

BASE MAP CONTROL FROM USGS

Plate 5. LOCATIONS OF GEOCHEMICAL SAMPLES

March 1981
Plate 5.

SILVER CITY, NEW MEXICO/ AZ

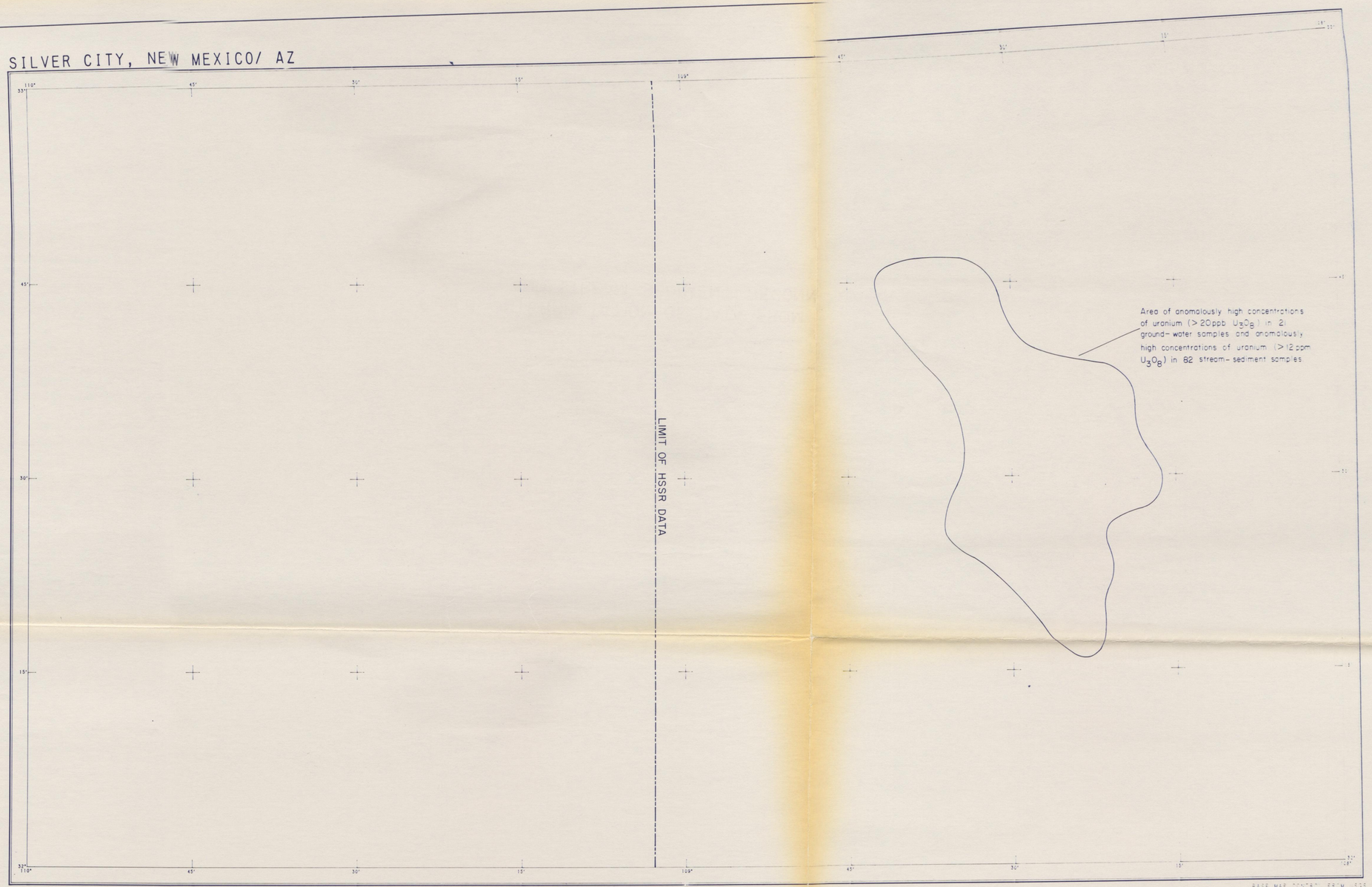

URANIUM RESOURCE EVALUATION
ISSUED BY THE U.S. DEPARTMENT OF ENERGY

5 0 5 10 15 20 25 MILES

5 0 5 10 15 20 25 KILOMETERS

BASE MAP CONTROL FROM USGS

HSSR DATA FROM SHARP AND OTHERS, 1978

Plate 4. INTERPRETATION OF DATA FROM HYDROGEOCHEMICAL AND STREAM-SEDIMENT RECONNAISSANCE

March 1981
Plate 4.

SILVER CITY, NEW MEXICO/ AZ

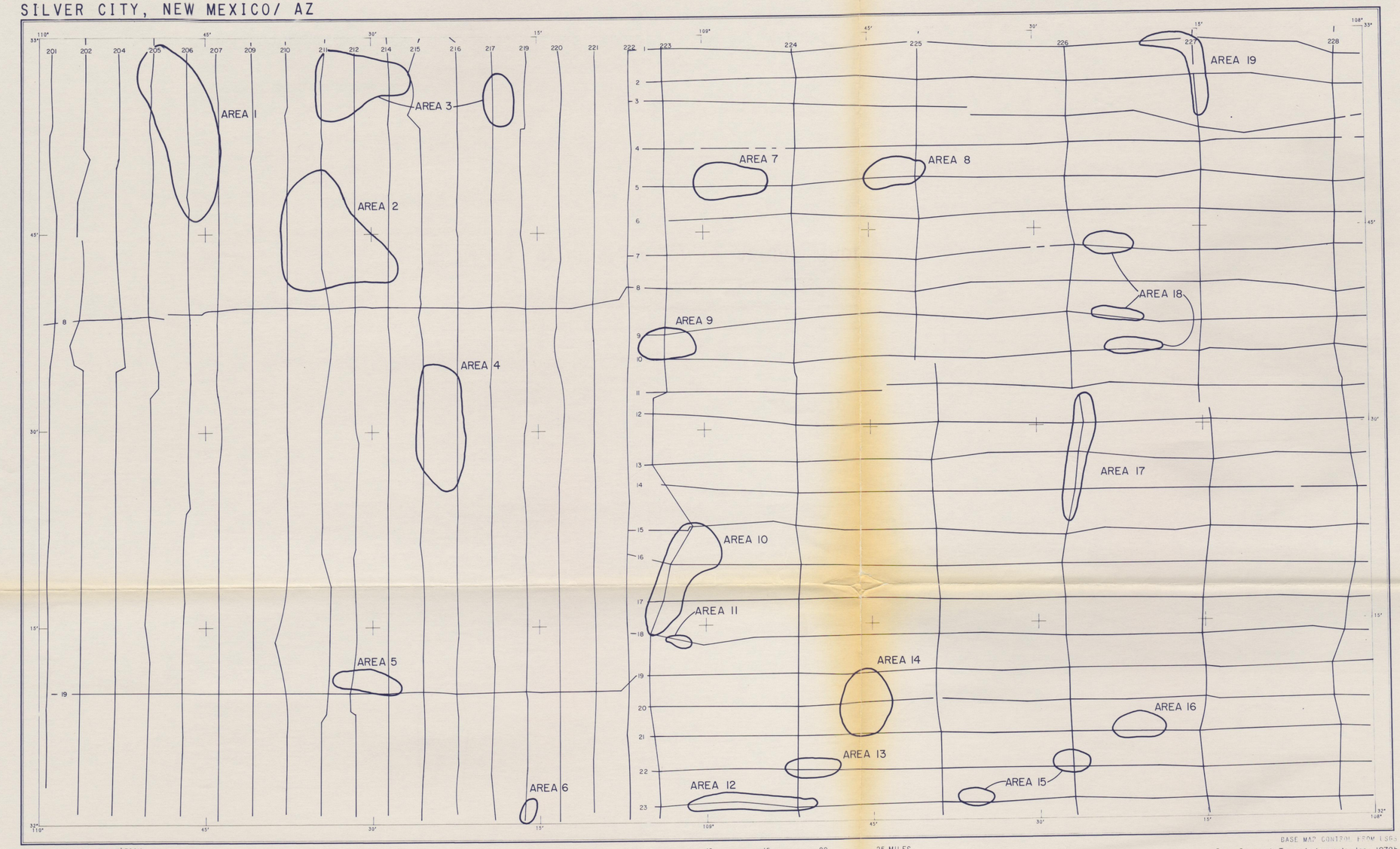

EXPLANATION

AERIAL RADIOMETRIC DATA

8 — 202 — Flightline and number

Area of apparent uranium enrichment based on the occurrence of one or more anomalies defined by anomalously high eU, eU/eTh and eU/eK values.

URANIUM RESOURCE EVALUATION
ISSUED BY THE U.S. DEPARTMENT OF ENERGY

5 0 5 10 15 20 25 MILES

5 0 5 10 15 20 25 KILOMETERS

BASE MAP CONTROL FROM USGS
Data Source : Texas Instruments, Inc., 1978b

Plate 3. INTERPRETATION OF AERIAL RADIOMETRIC DATA

March 1981
Plate 3.

SILVER CITY, NEW MEXICO/ AZ

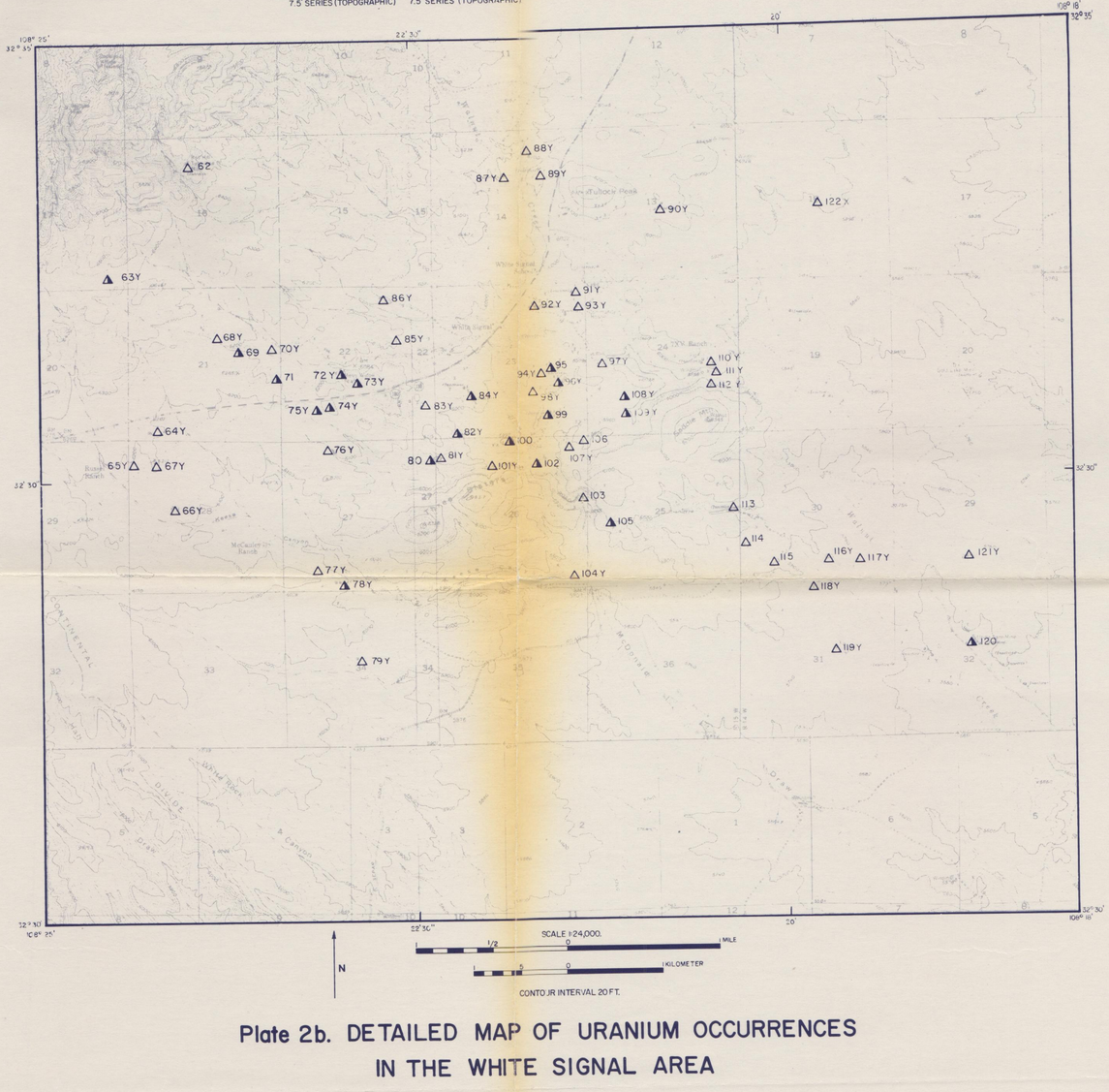

EXPLANATION

URANIUM OCCURRENCES

	CLASSIFICATION			
	Sedimentary	Plutonic	Volcanic	Other
Minor prospect or mineral occurrence	□	△	⬠	☼
Significant prospect or mine reporting minor production	◪	▲	◑	✹
Mine having production over 200,000 pounds U_3O_8	■	▲	⬟	✹
Not visited	□Y	△Y	⬠Y	☼Y
Not found	□X	△X	⬠X	☼X
Mining District	(dashed outline)			

Plate 2b. DETAILED MAP OF URANIUM OCCURRENCES
IN THE WHITE SIGNAL AREA

March 198
Plate 2b

SILVER CITY, NEW MEXICO/ AZ

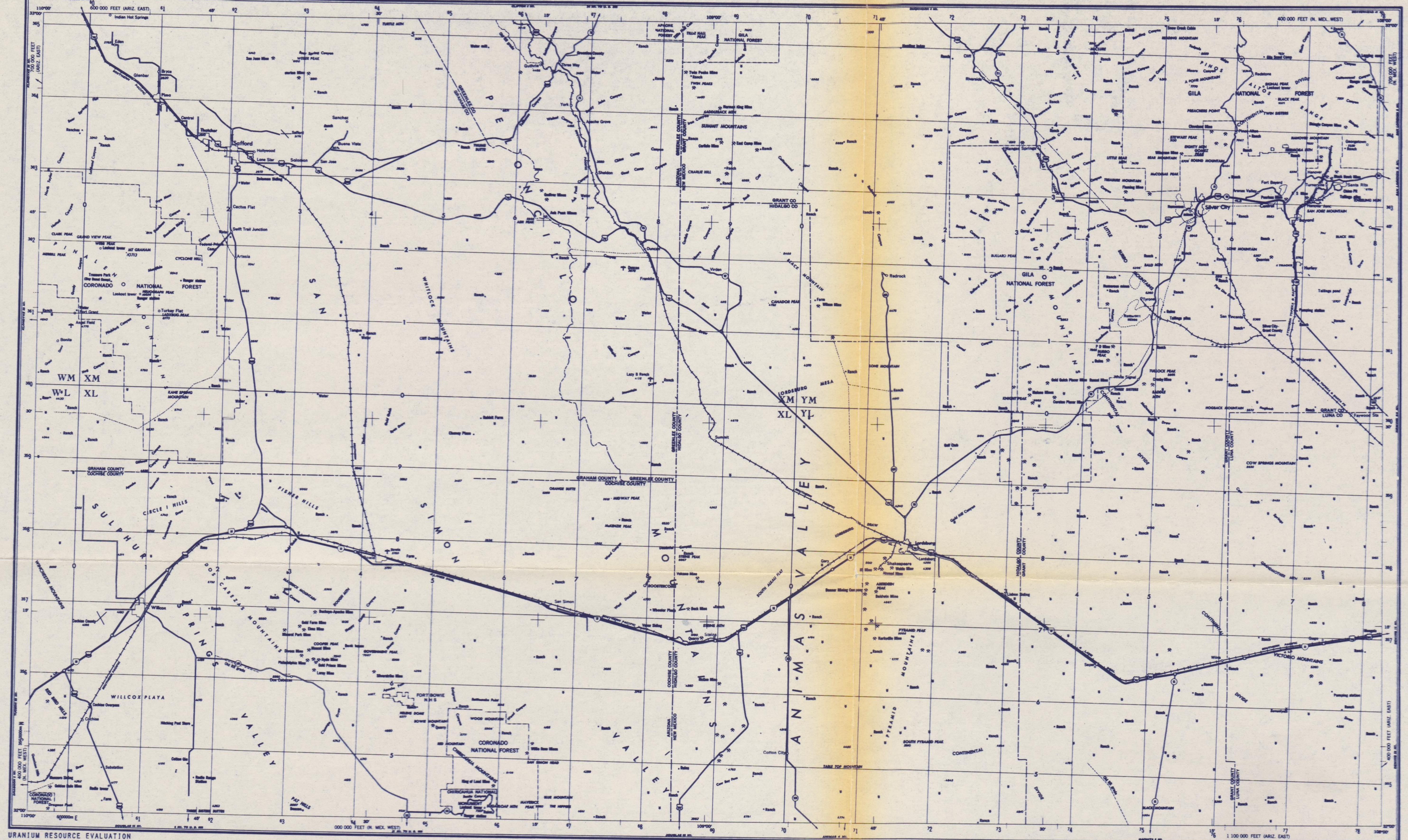

URANIUM RESOURCE EVALUATION
ISSUED BY THE U.S. DEPARTMENT OF ENERGY

BASE MAP CONTROL FROM USGS

5 0 5 10 15 20 25 MILES

5 0 5 10 15 20 25 KILOMETERS

Plate 15. CULTURE

March 1981
Plate 15.

SILVER CITY, NEW MEXICO/ AZ

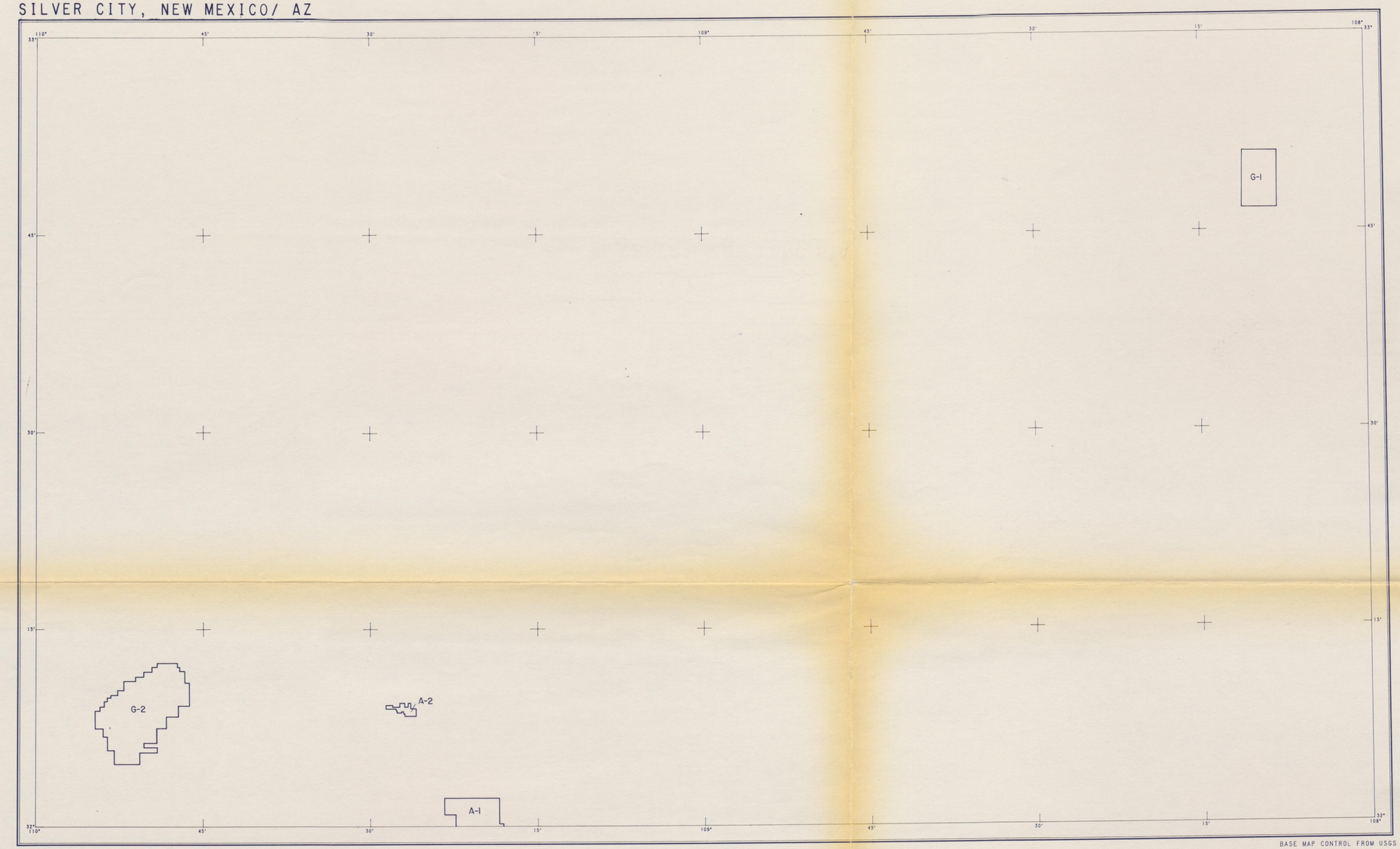

URANIUM RESOURCE EVALUATION
ISSUED BY THE U.S. DEPARTMENT OF ENERGY

5 0 5 10 15 20 25 MILES

5 0 5 10 15 20 25 KILOMETERS

BASE MAP CONTROL FROM USGS

INDEX

A. **Areas Managed by National Park Service**
- A-1 Chiricahua National Monument
- A-2 Fort Bowie National Historic Site

G. **Government Installations**
- G-1 Fort Bayard Military Reservation (Administered By U.S. Forest Service)
- G-2 Willcox Bombing Range

Plate 14. GENERALIZED LAND STATUS

March 1981
Plate 14.

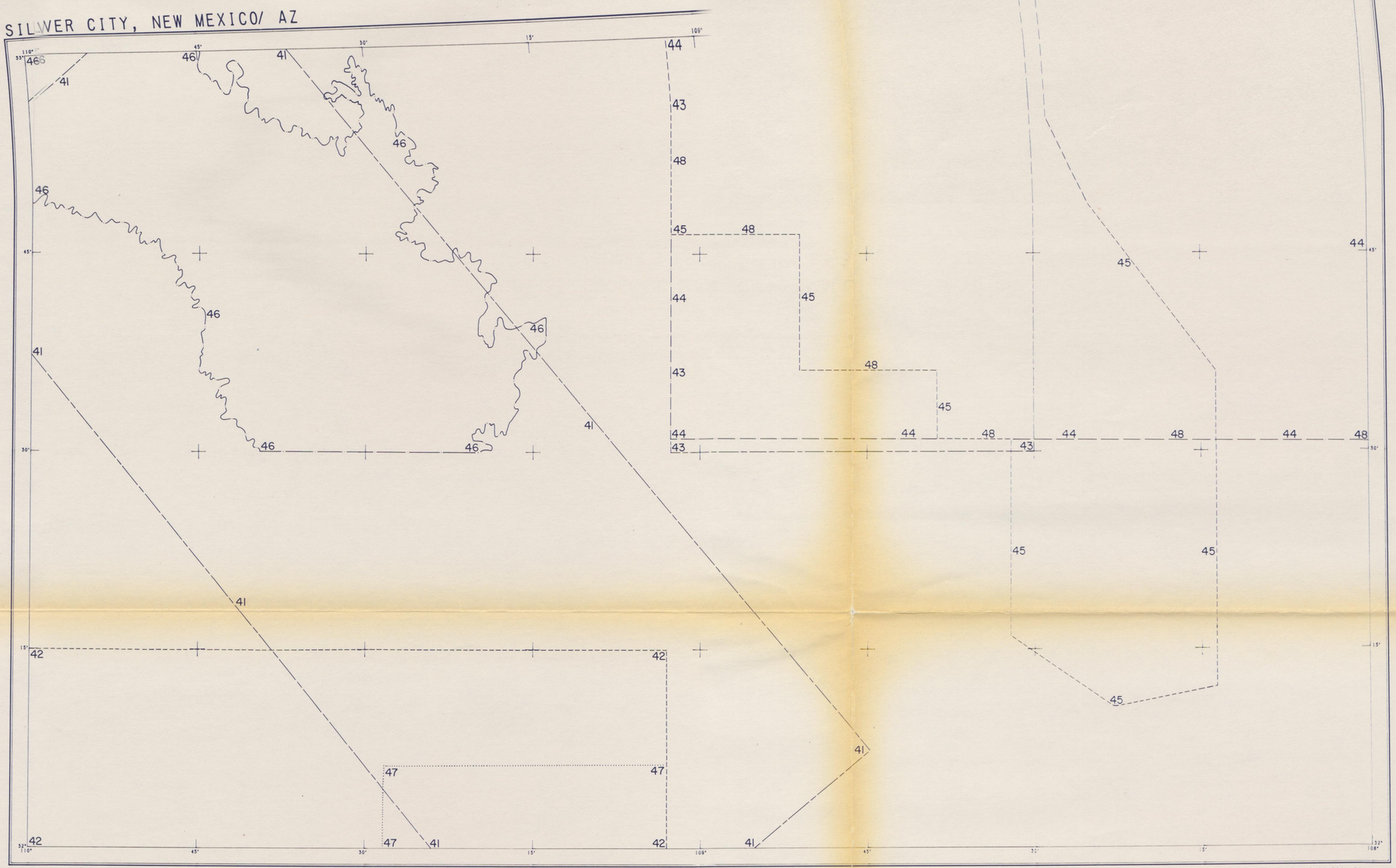

41. Carlisle, 1978, fig. 7.14, scale 1:000,...

42. Drewes, 1980, pl. 1, scale 1:125,000.

43. Elston, 1960, scale 1:126,720.

44. Elston and others, 1976, fig. 2, scale 1:250,000.

45. Gillerman, 1964, pl. 1, scale 1:126,720.

46. Harbour, 1966, fig. 4, scale 1:250,000.

47. Marjaniemi, 1970, pl. 1, scale 1:125,000.

48. Trauger, 1972, fig. 2, scale 1:175,500.

URANIUM RESOURCE EVALUATION
ISSUED BY THE U.S. DEPARTMENT OF ENERGY

5 0 5 10 15 20 25 MILES

5 0 5 10 15 20 25 KILOMETERS

BASE MAP CONTROL FROM USGS

Plate 13b. GEOLOGIC MAP INDEX, SMALL SCALE MAPS
(SCALES LESS THAN 1:63,360)

March 1981
Plate 13b.